

**Characterization of Redoximorphic Features in
Mine Waste–contaminated Wetland Soils**

A Thesis

Presented in Partial Fulfillment of the Requirements for the Degree of

Master of Science

with a

Major in Soil and Land Resources

In the College of Graduate Studies

University of Idaho

By

Patrick Hickey

April 2006

Major Professor: Daniel G. Strawn, Ph.D.

TD
428
MS6
MS3
2006

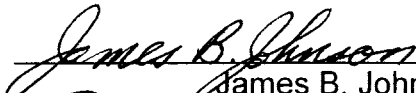
AUTHORIZATION TO SUBMIT THESIS

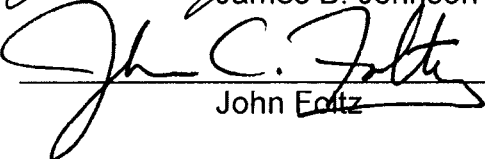
This thesis of Patrick Hickey submitted for the degree of Master of Science with a major in Soil and Land Resources and titled "Characterization of Redoximorphic Features in Mine Waste-contaminated Wetland Soils", has been reviewed in final form. Permission, as indicated by the signatures and dates given below, is now granted to submit final copies to the College of Graduate Studies for approval.

Major Professor  Date 5-10-2006
Daniel G. Strawn

Committee Members  Date 10 May 2006
Paul McDaniel

 Date May 11, 2006
James Harsh

Department Administrator  Date 11 May 2006
James B. Johnson

Discipline's College Dean  Date 5/11/06
John Eoltz

Final Approval and Acceptance by the College of Graduate Studies

 Date 5/25/06
Margrit von Braun

Abstract

Metal contamination from Northern Idaho mining operations has impacted wetlands along the Coeur d'Alene River floodplains resulting in a potentially hazardous environment for humans and animals. Contamination in these areas is often reported as total contaminant concentration per mass of soil, and assumes that the contaminants are homogeneously distributed throughout the soil. However, pedogenesis causes distinct secondary mineral redistribution within soil profiles, and leads to selective partitioning of contaminants within the profile at macro (cm) to sub-micron scales. This study examined the variability of redoximorphic features within a wetland, and contaminant enrichment in redoximorphic features relative to landscape position and water table height.

Six distinct categories of Fe and Fe/Mn-rich cemented redoximorphic features were identified. The Fe and Fe/Mn-cemented redox features were found to have Cd and Pb concentrations up to four and six times greater in magnitude than soil averages. Iron and Fe/Mn-cemented redox features also had elevated levels of As and Zn. The Fe/Mn-cemented aggregates had the highest Mn concentrations (approximately 3.4%), were most common in the 1-2 mm size fraction, and contained the highest concentration of Pb (approximately 2.6%). Iron-cemented root channel linings and Fe-cemented aggregates had comparable concentrations of As, Cd, Mn, Pb, and S. Coarse sand aggregates and Fe/Mn-cemented aggregates had similar concentrations of Cd, Mn, P, and Zn. Iron-cemented aggregates and cemented root channel linings had physical similarities, while coarse sand aggregates and Fe/Mn-cemented aggregates also

appeared similar. The Fe and Fe/Mn-cemented redox features were found primarily in the top 15 cm of soil and decreased with soil depth.

Results from this study show that pedogenesis in Coeur d'Alene wetland soils results in distinct redoximorphic features and non-homogeneous metal concentrations. Among these features are Fe and Mn – cemented aggregates that range in size from 1 to 2 mm in diameter. These aggregates have unique mineralogy and concentrate metals within the soils. Understanding contaminant partitioning and speciation in soils will allow for improved management and risk assessment of the contaminated soils.

Acknowledgements

This thesis represents a major milestone in my educational career; a career that would not have been possible without the help of many people. First and foremost I want to thank my parents and family whose support and love were paramount. They provided an environment that instilled a wonderful love of learning. Thanks Mom and Dad, Richard, and Steven!

Ms. Avena Jones, 5th and 6th grade teacher. You are perhaps the greatest inspiration that I had the honor of meeting during my educational path. Hopefully one day you'll know how far I progressed from the days of being the class clown.

My professors at both North Carolina State University and the University of Idaho not only provided education but humor, humility, and valuable friendship. Joe Kleiss, Aziz Amoozegar, Matt Morra, and so many others; thanks for guiding me along the path.

Without the profound wisdom and guidance of my committee members, Dan Strawn, Paul McDaniel, and Jim Harsh, my research would've been a mess. You all gave me a sense of direction and most importantly, accomplishment.

Anita Falen was a one in a million find here at the University of Idaho. She gave more of her time, energy, and heartfelt support than I could have ever expected of anyone. I would've never gotten it done without you. Thanks Anita.

And finally, my closest of friends were always there for me with laughs, love, and support from day one of college. Thanks Ryan, Darren, Brian, Ron, and the rest of you.

Table of Contents

Acknowledgements	v
List of Figures	viii
List of Tables	xiii
Chapter 1: Research Setting and Problem: Mine Waste - Contaminated Soils in the Coeur d'Alene River Basin	1
1.1 Introduction.....	1
1.2 History of Mining in the Silver Valley.....	2
1.3 Geological Composition of the Silver Valley.....	3
1.4 Superfund (CERCLA) Site Designation.....	4
1.5 Coeur d'Alene River Basin.....	4
1.6 Pedologic Features in Chemically Reactive Wetland Environments.....	6
1.7 Research Hypotheses.....	9
1.8 Research Objectives.....	11
Chapter 2: Pedogenic Cycling of Contaminants in a Mine Waste-impacted Wetland	12
2.1 Introduction.....	12
2.2 Materials and Methods.....	14
2.2.1 Site Description.....	14
2.2.2 Soil Collection.....	15
2.2.3 Soil pH Measurement.....	15
2.2.4 Soil Profile Determination.....	16
2.2.5 Particle-Size Analysis.....	16
2.2.6 Collection and Analysis of Mottled Soil.....	16
2.2.7 Visual Examination of Na-hexametaphosphate Collected Particles.....	17
2.2.8 Fe/Mn-Cemented Redoximorphic Feature Collection Sieving Method.....	19
2.2.8.1 Separation and Selection Method.....	20
2.2.8.2 Digestion and Analysis Method.....	21
2.2.9 Matrix Soil Elemental Analyses.....	22
2.3. Results.....	24
2.3.1 Results of Fe Concentrated and Fe Depleted Soil Elemental Analysis.....	32
2.3.2 Results of Aggregated Redoximorphic Feature Characterization.....	36
2.3.2.1 Fe and Mn-Rich Cemented Aggregates (F/M) (Figure 10):.....	36
2.3.2.2 Fe-cemented Aggregates (Fe) (Figure 12):.....	37
2.3.2.3 Fine Sand Aggregates (S) (Figure 13):.....	38
2.3.2.4 Coarse Sand Aggregates (A) (Figure 14):.....	39

2.3.2.5 Fe Root Channel Linings (RC) (Figure 15):	39
2.3.2.6 Other Particulates (O) (Figure 16):	40
2.3.3 Distribution and Concentration of Cemented Redoximorphic Aggregates	41
2.4 Cemented Redoximorphic Aggregate Distribution and Elemental Concentration Results	45
2.5 Discussion	48
2.5.1 Black Rock Slough Study Site	48
2.5.2 Soils Containing Fe and Mn Concentrations and Depletions	49
2.5.3 Fe and Fe/Mn-Cemented Redoximorphic Features	50
2.5.3.1 Feature Development	50
2.5.3.2 Feature Location	54
2.5.3.3 Aggregated Redoximorphic Features < 1mm	58
2.5.3.4 Feature Elemental Composition	58
2.5.3.5 Iron and Manganese Enrichment	61
2.6 Conclusions	64
Chapter 3: Summary	66
References	69
Appendix A: Cemented Redoximorphic Feature Data Tables	76
A-1.1 Description of Enrichment Calculation	95
Appendix B: Digital Photographs of Cemented Redoximorphic Features	97
Appendix C: Na-Hexametaphosphate-Wash Chelation Experiment	98
Appendix D: X-Ray Diffraction Analysis	104
Introduction:	104
Methods and Materials:	104
References	116
Appendix E. Fe/Mn-Cemented Aggregate Element Concentration Comparison	117

List of Figures

- Figure 1.** General Map of the Coeur d'Alene (CDA) mining district, CDA River, and Lake CDA. Also shown is the Bunker Hill Superfund site and lateral lakes associated with the CDA River. Map modified from Bookstrom (2001). 1
- Figure 2.** Map of the Black Rock Slough sampling site, location of sampling points, and illustration of the topographical slope change. 13
- Figure 3.** Aggregated redoximorphic features photographed before (top two photos) and after (bottom two photos) washing with 5% Na-hexametaphosphate solution. 19
- Figure 4.** Coeur d'Alene River averaged monthly heights as recorded by USGS River Gage #12413500 located at Cataldo, ID (Lehmann 2006). Data consisted of river measurements from 1987 to 2005 taken at noon and midnight daily. Error bars indicated standard deviation of river height monthly average. 24
- Figure 5.** Water table depths at sampling point well A, B, C, and D along the sampling transect at Black Rock Slough. 25
- Figure 6.** (Left) Soil profile at hand dug pit in Black Rock Slough near point B showing the historic seasonally high water table depth. Scale is in decimeters. The region in which charcoal was found is clearly evident at approximately 3.5 dm. (Right) Close-up of historic seasonally high water table depth. 29
- Figure 7.** Soil profile near point C along the Black Rock Slough sampling transect. Mottling exists from the soil surface to approximately 10 cm. Note the lack of distinct boundary between the red and gray soils. 30
- Figure 8.** Average elemental concentrations for red and gray colored soils taken from Black Rock Slough sampling transect. R – refers to red colored soil, G – refers to gray-colored soil, A – refers to the 0 – 10 cm sampling depth, and B – refers to the 10 – 20 cm sampling depth. Error bars represent the standard deviation of the sample average from 4 independent samples. Raw data are in Appendix A, Table A-5. 33
- Figure 9.** Average elemental concentrations for red and gray colored soils taken from mottled regions on Black Rock Slough sampling transect. R – refers to red colored soil, G – refers to gray colored soil, A – refers to the 0 – 10 cm sampling depth, and B – refers to the 10 – 20 cm sampling depth. Error bars represent the standard deviation of the average from 4 independent samples. Raw data are in Appendix A, Table A-5. 34
- Figure 10.** Two examples of Fe and Mn-rich cemented aggregates (F/M). Grid size is 1.6 mm. 36
- Figure 11.** Examples of Fe and Mn-rich cemented aggregates in which the surface color is mixed. The grid size is 1.6 mm. 37
- Figure 12.** Two examples of Fe enriched cemented redoximorphic features (F). Grid size is 1.6 mm. 38
- Figure 13.** Examples of fine sand aggregates (S). Grid size is 1.6 mm. 38
- Figure 14.** Examples of coarse-sand aggregates (A). Grid size is 1.6 mm. 39

Figure 15. Examples of root channel linings or pipestems (RC). Grid size is 1.6 mm.	40
Figure 16. Examples of biological (left) and non-weathered mineral (right) particles found after wet-sieving (O). Grid size is 1.6 mm.	40
Figure 17. Distribution of aggregated redoximorphic features from points A, B, and D within Black Rock Slough sampling transect. Percentages are relative to the total number of particles counted. Raw data is in Appendix A-6 through A-16.	42
Figure 18. Distribution of Fe/Mn-cemented aggregated feature categories collected from points A, B, and D within the Black Rock Slough sampling transect. Distribution is arranged by sampling point and sampling depth. Raw data are in Appendix A-6 through A-16.	43
Figure 19. Arsenic, Mn, and Fe concentrations in 1 – 2 mm sized aggregated redoximorphic features. S is fine sand aggregates, A is coarse sand aggregates, F/M is Fe/Mn-cemented aggregates, O are biological particles or primary minerals, F is Fe-cemented aggregates, and RC is cemented root channel linings. Error bars represent standard deviation of element averages. Error bars may be obscured by markers.	59
Figure 20. Manganese, Pb, and Fe concentrations in 1 – 2 mm sized aggregated redoximorphic features. S is fine sand aggregates, A is coarse sand aggregates, F/M is Fe/Mn-cemented aggregates, O are biological particles or primary minerals, F is Fe-cemented aggregates, and RC is cemented root channel linings. Error bars represent standard deviation of element averages. Error bars may be obscured by markers.	60
Figure 21. Manganese, Fe, and Pb enrichment in aggregated redoximorphic categories. Aggregated redoximorphic features are listed by category where O is biological or primary mineral particles, RC is cemented root-channel linings, S is fine sand aggregates, Ag is coarse sand aggregates, F/M are Fe/Mn aggregates, and F are Fe aggregates.	62
Figure 22. Manganese, P, and Cd concentrations in aggregated redoximorphic features. Aggregated redoximorphic features are listed by category where O is biological or primary mineral particles, RC is cemented root-channel linings, S is fine sand aggregates, Ag is coarse sand aggregates, F/M are Fe/Mn aggregates, and F are Fe aggregates. Error bars represent standard deviation of element averages. Error bars may be obscured by markers.	63
Figure 23. Iron and manganese concentration ratios for six categories of Fe/Mn-cemented aggregates collected at points A, B, and D along the Black Rock Slough sampling transect.	64
Figure D- 1. Diffraction patterns from clay-sized soil particles taken at the 0-5 cm depth near sampling point B. Vermiculite, muscovite, kaolinite, lepidocrocite, and quartz are the predominate minerals identified.	107
Figure D-2. Diffraction patterns for Mg-glycol and K treated clay-sized soil particles taken at the 0-5 cm depth near sampling point B. Chlorite, muscovite, and kaolinite are the predominate minerals identified.	108
Figure D-3. X-ray diffraction patterns for very fine sand and silt powder mounts of soil sampled at the 0 – 5 cm depth.	109
Figure D-4. X-ray diffraction patterns for clay-sized soil particles indicating the presence of quartz, chlorite, kaolinite, and muscovite at the 5-28 cm depth.	110

Figure D-5. X-ray diffraction patterns for clay-sized soil particles indicating the presence of chlorite, kaolinite, and muscovite at the 5-28 cm depth.	111
Figure D-6. X-ray diffraction patterns for clay-sized soil particles indicating the presence of quartz, chlorite, kaolinite, and muscovite at the 28-33 cm depth.	112
Figure D-7. X-ray diffraction patterns for clay-sized soil particles indicating the presence of chlorite, kaolinite, and muscovite at 28-33 cm depth.	113
Figure D-8. X-ray diffraction patterns for silt and very-fine sand sized particles indicating the presence of quartz at 33-46 cm depth.	114
Figure D-9. X-ray diffraction patterns for clay-sized soil particles indicating the presence of chlorite, muscovite, and kaolinite 33-46 cm depth.	115
Figure E-1. Comparison of category averaged Fe and Zn concentrations from Fe/Mn-cemented aggregates collected at points A, B, and D within the Black Rock Slough sampling transect.	117
Figure E-2. Comparison of category averaged Fe and As concentrations from Fe/Mn-cemented aggregates collected at points A, B, and D within the Black Rock Slough sampling transect.	117
Figure E-3. Comparison of category averaged Fe and Pb concentrations from Fe/Mn-cemented aggregates collected at points A, B, and D within the Black Rock Slough sampling transect.	118
Figure E-4. Comparison of category averaged Fe and Mn concentrations from Fe/Mn-cemented aggregates collected at points A, B, and D within the Black Rock Slough sampling transect.	118
Figure E-5. Comparison of category averaged Fe and Cd concentrations from Fe/Mn-cemented aggregates collected at points A, B, and D within the Black Rock Slough sampling transect.	119
Figure E-6. Comparison of category averaged Fe and P concentrations from Fe/Mn-cemented aggregates collected at points A, B, and D within the Black Rock Slough sampling transect.	119
Figure E-7. Comparison of category averaged Mn and Pb concentrations from Fe/Mn-cemented aggregates collected at points A, B, and D within the Black Rock Slough sampling transect.	120
Figure E-8. Comparison of category averaged Mn and Zn concentrations from Fe/Mn-cemented aggregates collected at points A, B, and D within the Black Rock Slough sampling transect.	120
Figure E-9. Comparison of category averaged Mn and P concentrations from Fe/Mn-cemented aggregates collected at points A, B, and D within the Black Rock Slough sampling transect.	121
Figure 10. Comparison of category averaged Mn and As concentrations from Fe/Mn-cemented aggregates collected at points A, B, and D within the Black Rock Slough sampling transect.	121

Figure E-11. Comparison of category averaged Mn and Cd concentrations from Fe/Mn-cemented aggregates collected at points A, B, and D within the Black Rock Slough sampling transect.....	122
Figure E-12. Comparison of category averaged S and P concentrations from Fe/Mn-cemented aggregates collected at points A, B, and D within the Black Rock Slough sampling transect.....	122
Figure E-13. Comparison of category averaged S and Mn concentrations from Fe/Mn-cemented aggregates collected at points A, B, and D within the Black Rock Slough sampling transect.....	123
Figure E-14. Comparison of category averaged S and Fe concentrations from Fe/Mn-cemented aggregates collected at points A, B, and D within the Black Rock Slough sampling transect.....	123
Figure E-15. Comparison of category averaged S and As concentrations from Fe/Mn-cemented aggregates collected at points A, B, and D within the Black Rock Slough sampling transect.....	124
Figure E-16. Comparison of category averaged S and Cd concentrations from Fe/Mn-cemented aggregates collected at points A, B, and D within the Black Rock Slough sampling transect.....	124
Figure E-17. Comparison of category averaged S and Pb concentrations from Fe/Mn-cemented aggregates collected at points A, B, and D within the Black Rock Slough sampling transect.....	125
Figure E-18. Comparison of category averaged S and Zn concentrations from Fe/Mn-cemented aggregates collected at points A, B, and D within the Black Rock Slough sampling transect.....	125
Figure E-19. Comparison of category averaged As and Cd concentrations from Fe/Mn-cemented aggregates collected at points A, B, and D within the Black Rock Slough sampling transect.....	126
Figure E-20. Comparison of category averaged As and P concentrations from Fe/Mn-cemented aggregates collected at points A, B, and D within the Black Rock Slough sampling transect.....	126
Figure E-21. Comparison of category averaged As and Pb concentrations from Fe/Mn-cemented aggregates collected at points A, B, and D within the Black Rock Slough sampling transect.....	127
Figure E-22. Comparison of category averaged As and Zn concentrations from Fe/Mn-cemented aggregates collected at points A, B, and D within the Black Rock Slough sampling transect.....	127
Figure E-23. Comparison of category averaged Cd and P concentrations from Fe/Mn-cemented aggregates collected at points A, B, and D within the Black Rock Slough sampling transect.....	128
Figure E-24. Comparison of category averaged Cd and Pb concentrations from Fe/Mn-cemented aggregates collected at points A, B, and D within the Black Rock Slough sampling transect.....	128

Figure E-25. Comparison of category averaged P and Pb concentrations from Fe/Mn-cemented aggregates collected at points A, B, and D within the Black Rock Slough sampling transect **129**

Figure E-26. Comparison of category averaged P and Zn concentrations from Fe/Mn-cemented aggregates collected at points A, B, and D within the Black Rock Slough sampling transect **129**

Figure E-27. Comparison of category averaged Zn and Pb concentrations from Fe/Mn-cemented aggregates collected at points A, B, and D within the Black Rock Slough sampling transect **130**

Figure E-28. Comparison of category averaged Cd and Zn concentrations from Fe/Mn-cemented aggregates collected at points A, B, and D within the Black Rock Slough sampling transect **130**

List of Tables

Table 1. Field measurement data for pH, Eh, temperature, and well depth taken from sampling point wells along the Black Rock Slough transect. Well depth is measured from the soil surface to the water surface. A well depth of zero indicates water at the soil surface. NT indicates that a measurement was not taken.	26
Table 2. Profile description for Black Rock Slough sampling transect point A.	27
Table 3. Profile description for Black Rock Slough sampling transect point B.	27
Table 4. Profile description for Black Rock Slough sampling transect point C.	27
Table 5. Texture analysis results of soils taken at ~ 30 m and ~ 15 m west of point B on the Black Rock Slough sampling transect. Raw data are in Tables A-4.	28
Table 6. Elemental concentrations from depth-composited (0 – 45 cm) matrix soil collected from the upper 7.5 cm of intact soil cores collected along four points (A, B, C, and D) along the sampling transect at Black Rock Slough. Standard DST6 and Sample Prep G-1 are ACME Laboratories in-house quality assurance samples.	30
Table 7. Common elemental ranges for soils and selected averages for soils (from Lindsay 1979).....	31
Table 8. Table modified from Hoffman (1995) , Bender (1991), and Rabbi (1994). Data presented here are representative of selected pre-mining metal background concentrations (mg/kg) taken from lake sediments located near the CDA River. Samples M-91-B and T-91-B were taken from Medicine Lake and Thompson Lake. Sample KB results are from Killarney Lake. Sample BR-91-B was taken from Bull Run Lake approximately 550 yards from the Black Rock Slough sampling transect. Mount Mazama and Mount St. Helens ash was identified by its chemical fingerprint and employed as a time reference point. Pre and post mining sediments were also determined by the distinct difference in metal concentration.	31
Table 9. Average elemental concentrations in the 6 categories of features in the 1 to 2 mm size fraction recovered from points A, B, and D on the Black Rock Slough sampling transect. Standard deviation of replicates is within parentheses. Averaged standard reference material (SRM) recovery percentages are shown with standard deviation in parentheses. Raw data are in Appendix A, Table A - 17	44
Table A-1. pH values of soils sampled from designated sampling points (A, B, C, and D) along the transect at Black Rock Slough. Sample identification is in the format X-Y-Z where X is the sample point, Y is the replicate number, and Z is the depth (a= 0-15 cm, b= 15-30 cm, c=30-45 cm). Not enough soil was present to accurately measure pH in sample a-2-a.	76
Table A-2. Matrix soil bulk density determined from 3 intact soil cores sampled in triplicate from 3 depths along the Black Rock Slough sampling transect. Sample designation is written in the format X-#-XX where X is the sample site, # is the replicate number, and XX is the (0 – 15 cm, 15 – 30 cm, and 30 – 45 cm).	77

Table A-3. Matrix soil bulk density determined from 3 intact soil cores sampled in triplicate from 3 depths along the Black Rock Slough sampling transect. Sample designation is written in the format X-#-XX where X is the sample site, # is the replicate number, and XX is the (0 – 15 cm, 15 – 30 cm, and 30 – 45 cm).	78
Table A-4. Particle size data from soil collected from a pit approximately 15 meters from Black Rock Slough sampling transect at point B. A sample was collected in layer of dark colored soil, burnt wood, and charcoal that was found in all pits at approximately 35 cm. Soil 8 was a composited sample collected from the top 20 cm of soil approximately 30 meters east of point B along the Black Rock Slough sampling transect.	79
Table A-5. Samples analyzed for selected elements based on visual soil coloration. Red colored soils indicate an environment that support the presence of Fe and/or Mn oxides, while grey soil color is indicative of reducing conditions that may deplete Fe and/or Mn from soil particle surfaces. The labeling, #-(R, G)-(A, B) represents the plot number sampled, enrichment (R) or depletion (G) of Fe and/or Mn, and 0-10 cm depth (A) or 10 – 20 cm depth (B). Standard reference material (SRM – 2711) results are referenced to samples analyzed by superscript lettering. SRM – 2711 elemental composition concentrations listed per NIST (2003)	80
Table A-6. Summary of redoximorphic feature by category gathered from sampling location A for three depths. Sample identification is in the format X-Y-Z where X is the sampling point, Y is the replicate number, and Z is the depth (a= 0-15 cm, b= 15-30 cm, c=30-45 cm).	83
Table A-7. Summary of redoximorphic feature by category gathered from sampling location A for three depths. Sample identification is in the format X-Y-Z where X is the sampling point, Y is the replicate number, and Z is the depth (a= 0-15 cm, b= 15-30 cm, c=30-45 cm).	84
Table A-8. Summary of redoximorphic feature by category gathered from sampling location A for three depths. Sample identification is in the format X-Y-Z where X is the sampling point, Y is the replicate number, and Z is the depth (a= 0-15 cm, b= 15-30 cm, c=30-45 cm).	85
Table A-9. Summary of redoximorphic feature by category gathered from sampling location B for three depths. Sample identification is in the format X-Y-Z where X is the sampling point, Y is the replicate number, and Z is the depth (a= 0-15 cm, b= 15-30 cm, c=30-45 cm).	86
Table A-10. Summary of redoximorphic feature by category gathered from sampling location B for three depths. Sample identification is in the format X-Y-Z where X is the sampling point, Y is the replicate number, and Z is the depth (a= 0-15 cm, b= 15-30 cm, c=30-45 cm).	87
Table A-11. Summary of redoximorphic feature by category gathered from sampling location B for three depths. Sample identification is in the format X-Y-Z where X is the sampling point, Y is the replicate number, and Z is the depth (a= 0-15 cm, b= 15-30 cm, c=30-45 cm).	88
Table A-12. Summary of redoximorphic feature by category gathered from sampling location D for three depths. Sample identification is in the format X-Y-Z where X is the sampling point, Y is the replicate number, and Z is the depth (a= 0-15 cm, b= 15-30 cm, c=30-45 cm).	89

Table A-13. Summary of redoximorphic feature by category gathered from sampling location D for three depths. Sample identification is in the format X-Y-Z where X is the sampling point, Y is the replicate number, and Z is the depth (a= 0-15 cm, b= 15-30 cm, c=30-45 cm).	90
Table A-14. Summary of redoximorphic feature by category gathered from sampling location D for three depths. Sample identification is in the format X-Y-Z where X is the sampling point, Y is the replicate number, and Z is the depth (a= 0-15 cm, b= 15-30 cm, c=30-45 cm).	91
Table A-15. Counts, averages, and standard deviations of Fe and Fe/Mn-cemented redoximorphic features collected from samples collected at three depths (0-15, 15-30, 30-45 cm) at points A, B, and D along the sampling transect in Black Rock Slough. The % column refers to the percentage of each category as compared to the sum of features counted.	92
Table A-16. Counts, averages, and standard deviations of Fe and Fe/Mn-cemented redoximorphic features collected from samples collected at three points (A, B, and D) at three depths (0-15, 15-30, 30-45 cm) along the sampling transect in Black Rock Slough. The % column refers to the percentage of each category as compared to the sum of features counted.	93
Table A-17. Fe and Fe/Mn-cemented redoximorphic feature and other collected particle selected elemental concentrations from ICP-AES analysis listed by category. Elements are presented in ppm (mg/kg).....	94
Table B-1. File names of aggregated redoximorphic feature photographs on attached CD – ROM.	97
Table C- 1. Averaged results from elemental analysis of digested redoximorphic features after being washed for 24 hours in a 5% Na-hexametaphosphate solution. Values are presented in ppm (mg/kg). Standard deviation of the sample averages are in parentheses.	103

Chapter 1: Research Setting and Problem: Mine Waste - Contaminated Soils in the Coeur d'Alene River Basin

1.1 Introduction

Mining activities during the last 100 years in the Silver Valley Mining District of Northern Idaho (Figure 1) have caused excessive As, Cd, Pb, and Zn enrichment of sediments in the floodplains of the Coeur d'Alene (CDA) River Basin in Idaho. The contaminated sediments are derived from erosion of contaminated riverbanks and river bottoms, as well as dumping of mine tailings directly in the river. Receptors on these mine-impacted soils include wildlife, farms, recreational areas, and rural residences. Heavy metal mobility throughout the CDA River Basin is considered to present significant long-term ecotoxicological risks to the local biosphere and nearby communities.

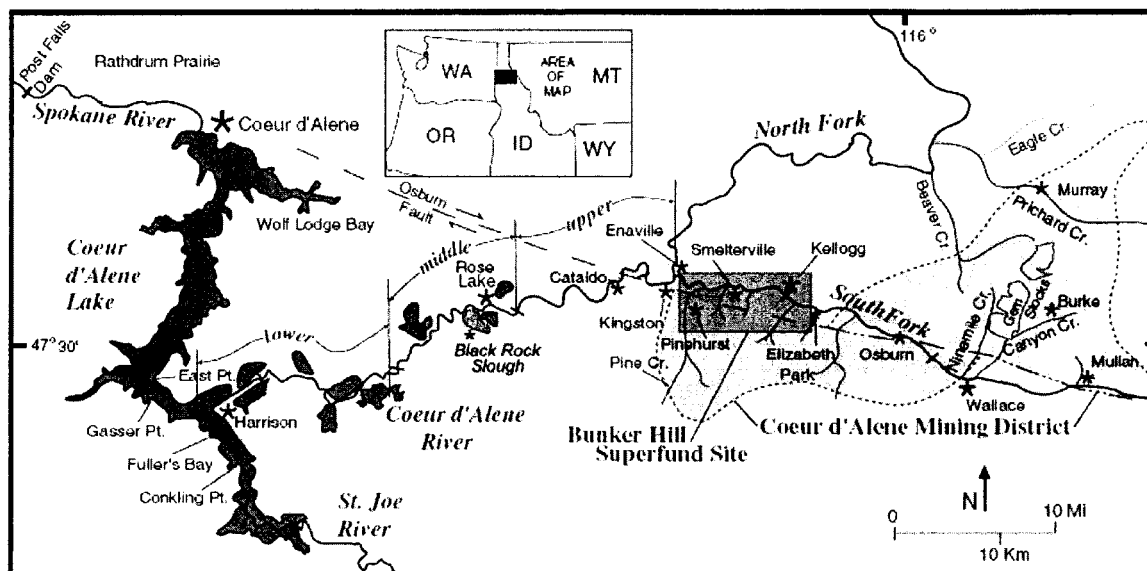


Figure 1. General Map of the Coeur d'Alene (CDA) mining district, CDA River, and Lake CDA. Also shown is the Bunker Hill Superfund site and lateral lakes associated with the CDA River. Map modified from Bookstrom (2001).

1.2 History of Mining in the Silver Valley

Mining began in the CDA –Silver Valley Region beginning in the 1880s. Silver and lead were the primary metals of interest. Subsequently, several of the richest silver and lead mines in the world were developed in the Silver Valley. Production of lead and silver required the acquisition of ore rock either through placer mining, hydraulic blasting to uncover minerals, or hard-rock mining, (Chapman 2000).

Initially ore was processed by crushing it and passing it through a vibrating jig table to separate economically viable ores. In the 1920s finely crushed ore was processed using flotation separation. Tailings, or mine wastes consisting of sand to clay-sized particles were disposed of in nearby tributaries of the Coeur d'Alene River because storage capabilities in the region were topographically limited (Long 1998). Ore processing technology advanced around the 1920s, increasing metal recovery efficiency from finely ground ore rock by using flotation separation. The waste from the flotation separator consisted of smaller size particles than prior ore-processing methods, resulting in increased river transport of particles.

Environmental damages from the Coeur d'Alene mining region became apparent as early as 1900 (Long 1998). Containments for waste tailings were built in the late 1920s and 1930s. Attempts to recover tailings deposited in the CDA River by the Mine Owners Association using dredges were made from the early 1930s to the late 1960s. In 1968 it became illegal for mine owners to dump

mill waste into rivers or tributaries, and impoundments were required for tailings (Long 1998).

Bookstrom et al. (2004) estimated that 190 kilotons per year of river-borne sediments were deposited on the CDA River Valley floodplains between 1980 and 1993. Of that amount, approximately 120 kilotons of silt and clay-sized particles were estimated to be deposited in floodplain marshes and lakes. Approximately 177 ± 35 kilotons of Pb has been deposited along the CDA floodplains from 1903 to 1993 (Bookstrom et al. 2004). It has been estimated that up to 700 million tons of contaminated sediment entered the basin since the mining activities began (Horowitz et al. 1995), contaminating ~95% of the entire floodplain habitat (EPA 2003).

1.3 Geological Composition of the Silver Valley

Silver, lead, and zinc are concentrated in the Belt Basin (Bookstrom et al. 1999). These Precambrian argillites, siltstones, and quartzites comprise the Silver Valley mining region (Gillerman 2001). Ores removed from these rocks contain galena [PbS], sphalerite [(Zn, Fe²⁺) S], and tetrahedrite [(Cu, Fe, Ag, Zn)₁₂Sb₄S₁₃] (Ross and Savage 1967). Other gangue minerals found in this region include quartz [SiO₂], siderite [FeCO₃], pyrrhotite [FeS], chalcocite [Cu₂S], and pyrite [FeS₂] (Bennett et al. 1989). The tailings that were directly dumped into CDA River tributaries or escaped from breached impoundments settled in the main stem of CDA River near Cataldo Idaho where a decreased gradient occurs. Sediments enriched in Pb, Zn, Cd, Fe, and Mn were transported

from the CDA River bed and riverbanks to Coeur d'Alene Lake, or were deposited on nearby floodplains during frequent flooding events. The metal-rich sediments are estimated to exceed 100 million tons, covering thousands of acres, and have impacted areas as far west as the Spokane River flood channel (EPA 2003).

1.4 Superfund (CERCLA) Site Designation

In 1983, the Bunker Hill Mining and Metallurgical Complex was designated as a superfund site under the Comprehensive Environmental Response, Compensation, and Liability Act (CERCLA) and placed on the national priority list (NPL). The 54.4 – square kilometer Bunker Hill Superfund site was extended in 2002 to include CDA River Valley Basin (Operable Unit 3) (EPA 2003). Proposed remedies to Operable Unit 3 include excavation and disposal of contaminated soils and river bank sediments, surface water treatments, riverbank stabilization, and soil treatments to reduce metal bioavailability.

1.5 Coeur d'Alene River Basin

The CDA River Basin contains 11 lateral lakes with thousands of acres of associated wetlands (U.S. Fish and Wildlife Service 2005a). Wetlands provide a host of functions, including flood protection, sediment control, erosion control, and fish and wildlife habitat (Tiner 1999). Many of the lateral lakes along the CdA River and their associated wetlands are feeding, resting, and nesting areas for birds migrating along the Pacific Flyway. (U.S. Fish and Wildlife Service 2005).

There are 226 different mammal, bird, reptile, and fish species believed to be native to the Coeur d'Alene sub-basin, including 3 endangered or threatened species (Coeur d'Alene Tribe 2001). Land uses in the CDA River Basin also include recreation and agriculture (U.S. Fish and Wildlife Service 2005).

The site being studied is located approximately 27 kilometers southeast of Coeur d'Alene, Idaho on the northern shore of Bull Run Lake next to the Black Rock Slough wetland area. The study area receives approximately 127 cm of precipitation a year (USGS 2005). However substantial wetting of the soils occurs through the influx of groundwater, which is directly influenced by Coeur d'Alene Lake and CDA River water levels. The lake and river levels vary with the water level maintenance at the Post Falls Dam resulting from power management (Coeur d'Alene Tribe 2005).

Deposition of metal-enriched sediments from CDA River floodwaters has occurred at sites along the CDA River floodplains, including Bull Run Lake and Black Rock Slough with common frequency. Bull Run Lake is the first lateral lake along the south side of the CDA River, and the area receives significant flood sediments (Rabbi 1994). The fluvial material settles out in this region due to rapidly decreasing water velocity and vegetation growth, which results in floodwater energy loss and subsequent sediment deposition.

Sediments in excess of 1,000 mg/kg Pb line the CDA River bed to an average thickness of 2.6 m (Bookstrom et al. 1999). Historically, the CDA River has risen to moderate and major flood stages at least ten times (NOAA 2006) since measurements began by the USGS in April 1911 (U.S. Geological Survey

2005). Bookstrom et al. (2004) estimated a depositional rate for palustrine lateral marshes at 4.0 cm/decade. This rate is based on sediment deposition from 1903 to 1980. Since 1980 flood events have continued to deposit metal-enriched sediments, e.g., in 2002 a flood deposited 1 cm of metal – enriched sediment on a farm field downriver of Black Rock Slough (Gerulf and Strawn 2005).

Regulators and site managers generally categorize soil contamination status based on total metal concentration (mg/kg soil). Extensive reports have been prepared on metal contamination distribution within the CDA River Basin (Bookstrom et al. 2001; Box et al. 2001; Bookstrom et al. 2004). From this information decisions regarding risks and remediation are made. However, risk assessment based on total metal concentration is costly, inaccurate and ineffective. Remediation efforts at the Bunker Hill Operable Unit 1 and 2 Superfund site have resulted in the removal of over 300,000 truckloads of soil and an estimated expenditure of \$150 million (EPA 2006). In fact, recent efforts by EPA are proposing to change current risk assessments to take into account speciation of soil contaminants, in addition to total concentration (Hogue 2004). In light of this, the goal of the research presented in this thesis is to provide information on sequestered contaminants in the soils in the lower CDA River Basin.

1.6 Pedologic Features in Chemically Reactive Wetland Environments

Wetland or hydric soils are biologically and chemically dynamic due to changing water table heights. It is well known that metals adsorb or interact with

various soil components, thereby changing their speciation, bioavailability and toxicity, and fate and transport. For example, Fe and Mn oxides demonstrate a strong affinity for lead and other trace metals (Dong et al. 2001; Green et al. 2003; O'Reilly and Hochella 2003; Neaman et al. 2004). Iron and Mn oxides have point of zero charge (PZC) that range from 2 – 5 (Mn oxides) and 6.8 – 8 (Fe oxides) (Cornu et al. 2005). The wide range of PZC values of the two oxides allows for greater adsorptive capacity over a wide pH range. In hydric soils, redox potential and pH influence the solubility and mobility of iron and manganese oxides (Vepraskas and Faulkner 2001). The mobility of iron and manganese oxides is indicated by enrichment and depletion within wetland soils. Microbial respiration in seasonally flooded soils often results in Fe(III) and Mn(III, IV) becoming reduced, which promotes mineral dissolution. Metals associated with these species through adsorption or coprecipitation may be released as a result of dissolution. Conversely, during oxic soil conditions, reduced Fe and Mn oxidize and precipitate out of solution as (hydr)oxide minerals. Metal contaminants can coprecipitate with the oxides or sorb on the surfaces. Cyclical oxidizing and reducing soil conditions result from fluctuating water tables and promote the formation of three types of redoximorphic features: redox concentrations, redox depletions, and reduced matrix (Vepraskas 2001). Examples of these features include concretions, nodules, and zones of Fe/Mn enrichment and depletion known as mottling. Mottled color patterns occur within the upper capillary fringe of the water table, or in horizons that were historically impacted by the water

table as a result of reducing and oxidizing conditions that facilitated the translocation of Fe and Mn (Tiner 1999).

Mottles are a color pattern resulting from Fe and Mn (hydr) oxide concentration or depletion (Vepraskas 2001). Iron and Mn enrichment can be found lining pore spaces and root channels as soft material that cannot be easily removed without breaking apart (Vepraskas 1992). Root channels that have hardened to the point where physical extraction of intact aggregates from the soil is possible are also described as pipestems (Bidwell et al. 1968). Nodules and concretions are examples of cemented aggregations of soil particles that can be removed from the surrounding matrix. As opposed to nodules, concretions have visible concentric rings around a point or plane, and thus the terms are not interchangeable (Schoeneberger et al. 2002). Redoximorphic features are generally referred to as concentrations and/or depletions. In this chapter the term Fe/Mn-cemented aggregate will be used to refer to redoximorphic features that resist fracturing during sieving, and appear to be comprised of particles held together with Fe and Mn oxides.

The translocation of reduced elements such as Fe(II) and Mn(II) under saturated soil conditions to oxidizing, aerated regions produces zones of Fe and Mn enrichment (Vepraskas 2001). Trace metal affinity of Fe and Mn has long been recognized (McKenzie 1977; Schwertmann and Taylor 1977). The presence of redox concentrations may lead to enrichment of trace metals relative to the soil matrix. Investigating the speciation of the minerals and distribution patterns of redoximorphic concentrations in mine tailing-impacted CDA River

floodplain soils will enhance the ability to manage the site so that potential toxicity to humans and animals will be reduced.

1.7 Research Hypotheses

I hypothesize that contaminants (As, Cd, Pb, and Zn) in the soils in the CDA River Basin are not homogeneously distributed. Specifically, processes leading to Fe/Mn-cemented aggregate formation promote contaminant enrichment relative to the bulk matrix soil. Studies have reported similar enrichments in nodules and concretions in marine and terrestrial environments (Palumbo et al. 2001; Hlawatsch et al. 2002; Manceau et al. 2003; Marcus et al. 2004).

Because Fe and Mn oxides are subject to reductive dissolution, the speciation of the associated contaminants is dynamic. Many elements associated with the oxides (e.g., Pb and Zn) will be released when the solids are reductively dissolved. As a result, redox cycling causes even non-redox sensitive elements to change their speciation, influencing their availability for transport, bio-uptake, and remediation.

The second hypothesis being tested is that the type of Fe/Mn-cemented aggregate varies with respect to topography and water table depth. Several studies of the interior architecture of Fe/Mn nodules and concretions are available (Harriss and Troup 1969; Palumbo et al. 2001; Manceau et al. 2003). However studies examining the characteristics of nodules and concretions formed *in situ* are limited. Analyses by Lindbo et al. (2000) and D'Amore et al.

(2004) are examples of such studies. Lindbo et al. (2000) investigated nodule formations in a severely eroded loess soil with a developed fragipan. The authors hypothesized that nodule formation begins with soil peds becoming fully coated with Fe and Mn during periods of oxidative concentration. During periods of reductive depletion the exterior of the soil ped is consumed, with Fe and Mn migrating and concentrating in the center of the nodule. Lindbo et al. (2000) suggested that nodules were fragments of the weathering fragipan. The Lindbo et al. (2000) study found that nodules were common in the eluvial horizon which is supported by similar findings by Rhoton et al. (1993). Rhoton et al. (1993) found the maximum concentration of nodules corresponded to the surface of the seasonally perched water table. D'Amore et al. (2004) investigated nodule and concretion formation in a wetland environment and provided theories of their genesis. D'Amore et al. (2004) found Fe/Mn aggregates in varying degrees of development at three study sites, each comprised of a different-aged soil. The concreted feature development progress was based on Fe and Mn concentrations in the matrix soil. The authors suggested that nodule formation is favored over concretion formation in a silt-loam soil texture. They also found greater concretion mass in the region above the water table that experiences cyclical wetting and drying. Lindbo et al. (2000) and D'Amore et al. (2004) cited several studies and theses in which Fe/Mn nodules and concretions were investigated (Somera 1967; Phillippe et al. 1971; Schwertmann and Fanning 1976; Rhoton et al. 1993). Review of these papers revealed few studies that

focused on the development and variety of Fe/Mn-rich cemented redoximorphic features.

1.8 Research Objectives

The objectives of the study are to classify and characterize the redoximorphic features in CDA River floodplain soils by determining (1) physical characteristics, (2) elemental composition, and (3) spatial distribution of Fe/Mn-cemented aggregates.

The visual identification and classification of redoximorphic features along with an accurate measurement of trace metal concentrations based on depth will provide an estimation of Fe/Mn -cemented aggregate distribution and heterogeneity of metal(loid) concentrations. This knowledge will provide insight into how pedological processes impact contaminant speciation, which will aid in risk assessment, management, and remediation.

Chapter 2: Pedogenic Cycling of Contaminants in a Mine Waste-impacted Wetland

2.1 Introduction

The CDA River Basin encompasses thousands of hectares of seasonally flooded wetlands, marshes, and riparian regions. The Black Rock Slough area lies within the CDA River Basin west of Cataldo, ID and adjacent to both the CDA River and Bull Run Lake in Kootenai County, Idaho (Figure 2). It is an area that metal(loid) enriched sediment has been deposited from CDA River flooding events, and experiences fluctuating water table heights throughout the year.

Black Rock Slough is an area that offers recreation opportunities, such as biking along the converted Union Pacific railroad, camping, and sport fishing. Black Rock Slough is inhabited by several species of raptors and waterfowl (Coeur d'Alene Tribe 2001), and is a migratory bird stopover. Because of these human and wildlife uses, risks of exposure to the contaminants in the soils exist at the site.

The focus of this study was to categorize the redoximorphic features found within a typical CDA River Basin wetland, determine the elemental composition of the features, and to estimate the enrichment density of trace metals within redoximorphic features as compared to the bulk matrix soil.

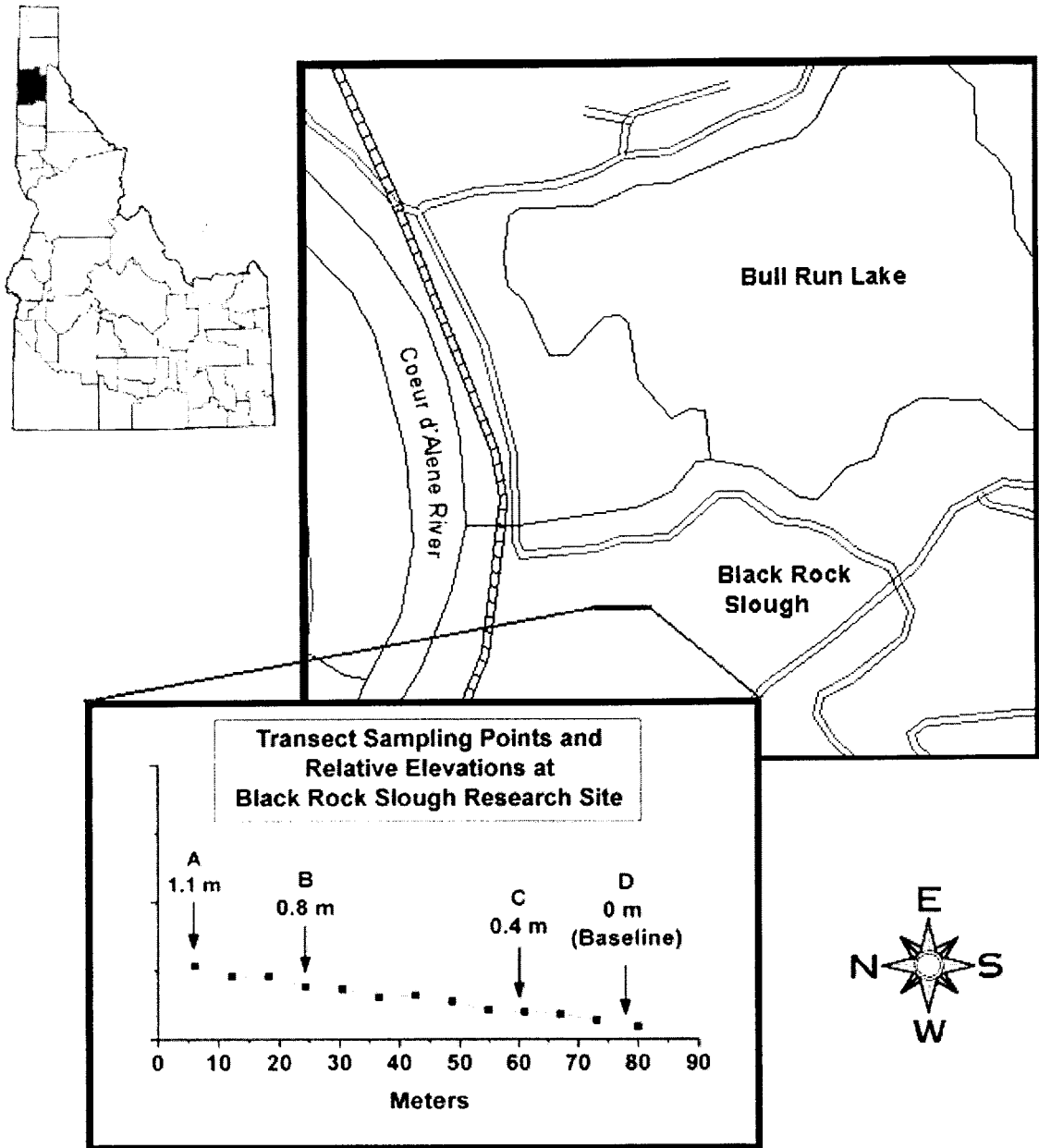


Figure 2. Map of the Black Rock Slough sampling site, location of sampling points, and illustration of the topographical slope change.

2.2 Materials and Methods

2.2.1 Site Description

The soils in the lower CDA Basin are mapped as either Slickens or Pywell Muck soil units (Weisel 1981). Pywell Muck is a deep and poorly-drained soil formed in medium to strongly acidic organic materials, has little to no slope, and occurs within floodplain areas. Runoff is slow with erosion hazards considered slight (Weisel 1981). Pywell Muck can be converted to farm or grazing land with proper drainage (Weisel 1981). The Slickens unit is a stratified soil that is composed of chemically-treated milled rock from the CDA mining district, alluvium from yearly riverbank overflow, and organic material (Weisel 1981). The research site has substantial vegetation coverage. Plant species include *Spirea douglasii* Hook. (Rose Spirea), *Phalaris arundinacea* L. (Reed Canarygrass), *Carex vesicaria* L. (Blister Sedge), and *Agrostis scabra* Willd. (Rough Bentgrass), which are listed in the 1988 *National List of Plant Species That Occur in Wetlands* (USFWS 1988).

A transect approximately 78 meters in length was established at Black Rock Slough. Four sampling points, designated A, B, C, and D, were selected along the transect (Figure 2). This transect was selected along a zone of undisturbed soil that had a decreasing slope from the northern sample point (A) to the southern sample point (D). A 2.4-meter well was installed using 5-centimeter diameter standard slotted-well sleeve at each sampling site for the purpose of measuring soil water pH, redox potential, temperature, and water

table depth. The transect was chosen to compare differences in redoximorphic features observed in a drier, high elevation site, to a wetter, low elevation site.

2.2.2 Soil Collection

Intact soil cores were retrieved in September 2004 from the Black Rock Slough sampling transect points A, B, C, and D (Figure 2) at 0-15, 15-30, and 30-45 cm depths. Three replicates from each sampling depth were collected. An impact soil-corer with 15-cm long, 5-cm-diameter plastic sleeve inserts was used to collect the samples. The replicate sampling was done within a meter radius of each sampling point. Each sampled core was capped, labeled, stored on ice, and transferred to a freezer for storage.

2.2.3 Soil pH Measurement

Prior to analysis, the frozen soil cores were allowed to thaw at room temperature. The top 2.5 cm of soil was extruded from the plastic sleeve, sliced with a stainless steel knife, and allowed to air dry. The remaining soil was later sieved to collect redoximorphic features. Approximately 10 grams of the air-dried soil and 10 mL triple distilled water (TDW) were placed in a 50 mL beaker for a 1:1 pH measurement. Samples that contained less than 10 grams of soil were measured using the same ratio but a smaller mass and volume of TDW. The results of the pH measurement are listed in Table A-1.

2.2.4 Soil Profile Determination

After collecting the soil cores, a pit was excavated in undisturbed soil near sampling points A, B, and C to approximately 90 cm to facilitate soil profile description. Each description contains data defining soil texture, color, horizonation, redoximorphic features, and unique characteristics as outlined in Soil Survey Methods Manual (Soil Survey Division Staff 1993).

2.2.5 Particle-Size Analysis

Soil was collected from two locations within Black Rock Slough for the purpose of soil particle-size determination. The first sample point was approximately 30 m east of point B on the sampling transect. Soil at this point was taken at 0 – 15 cm and 15 – 30 cm from intact cores and composited. The second soil sampled was approximately 15 m east of point B on the sampling transect. The samples from this sampling point were taken from five depths (0 – 10, 10 – 30, 30 – 60, 60 – 80 cm, and at ~ 35 cm). The 35-cm depth was sampled because of the presence of a darker brown color and burnt wood fragments. The other depths corresponded to horizons with distinct color change. The two soil collections were size fractionated using methods outlined in McDaniel (2004a).

2.2.6 Collection and Analysis of Mottled Soil

Selection criteria of soils having Fe and Mn (hydr) oxide enrichment and depletion from the Black Rock Slough study site were based on mottled coloring.

Iron-enriched samples were defined as those that exhibited a reddish brown to red color on the soil particle faces and soils having an Fe-depletion were gray-colored. The Munsell hue designation for the red colored soils ranged from 2.5 YR to 7.5 YR. The soil classified as being Fe-depleted in oxides was generally gray, with chromas of 1 or 2. Samples were collected from four plots separated by ~ 4 meters between sampling transect points A and B (Figure 2) at two depths; 0-10 cm and 10-20 cm. Samples were hand separated by Fe concentration or depletion as judged by soil color. The separated soil samples were air-dried, lightly crushed, and passed through a 2-mm sieve (approximately 2 – 5% of the soil particles were greater than 2 mm and remained consolidated on plants roots). The air-dried samples were digested in an aqua regia and HF solution as outlined in EPA Method 3052 (EPA 1996). The digested soil solution was passed through a 0.22- μ m filter and diluted to 50 mL in triple distilled water. The samples were then analyzed for As, Cd, Fe, Mn, P, Pb, S, and Zn using a Thermo Electron ICP-AES (IRIS Model) in the University of Idaho Soil Chemistry laboratory.

2.2.7 Visual Examination of Na-hexametaphosphate Collected Particles

An experiment was designed to test the effectiveness of separating the cemented aggregates from the matrix soil to ensure accurate visual characterization of the features. The goal of this experiment was to observe if there would be a noticeable removal of matrix soil from the aggregated particles

using Na-hexametaphosphate (Na-HMP) compared to features washed with TDW.

Soil was collected from an area approximately 28 m east of sampling point B along the Black Rock Slough sampling transect and was wet-sieved using 1 and 2 mm standard soil sieves. The particles in the 1 – 2 mm size fraction were collected, allowed to air-dry, and were mixed thoroughly. The samples were then split into triplicate subsamples and 5 photographs were taken of each subsample using a Nikon CoolPix 4300 digital camera mounted on a Nikon SMZ-10 Stereomicroscope. The samples were placed in 125 mL Erlenmeyer flasks and 100 mL of 5% Na-hexametaphosphate was added. The flasks were placed on a shaker table and rotated at 175 rpm for 24 hours. The Na-HMP-washed samples were transferred to a 425 μm sieve and rinsed thoroughly with TDW. After air-drying, the Na-HMP washed aggregates were digitally photographed. The photographs were visually compared with the photographs of particles taken prior to Na-HMP washing. Signs of fracturing, distinct color changes or dissolution of the material were evaluated.

The pre- and post-wash particle comparison did not reveal any noticeable changes to the physical condition of the particles collected. There was no apparent reduction in the number of particles washed. Elemental analyses of pre- and post-wash samples are in Appendix C, Table C-1.

Digital photography and visual inspection revealed that the clarity of the aggregated redoximorphic features was not enhanced enough by the Na-

hexametaphosphate wash to make the procedure worthwhile. Examples of pre-wash and post-wash aggregated redoximorphic features are shown in Figure 3.

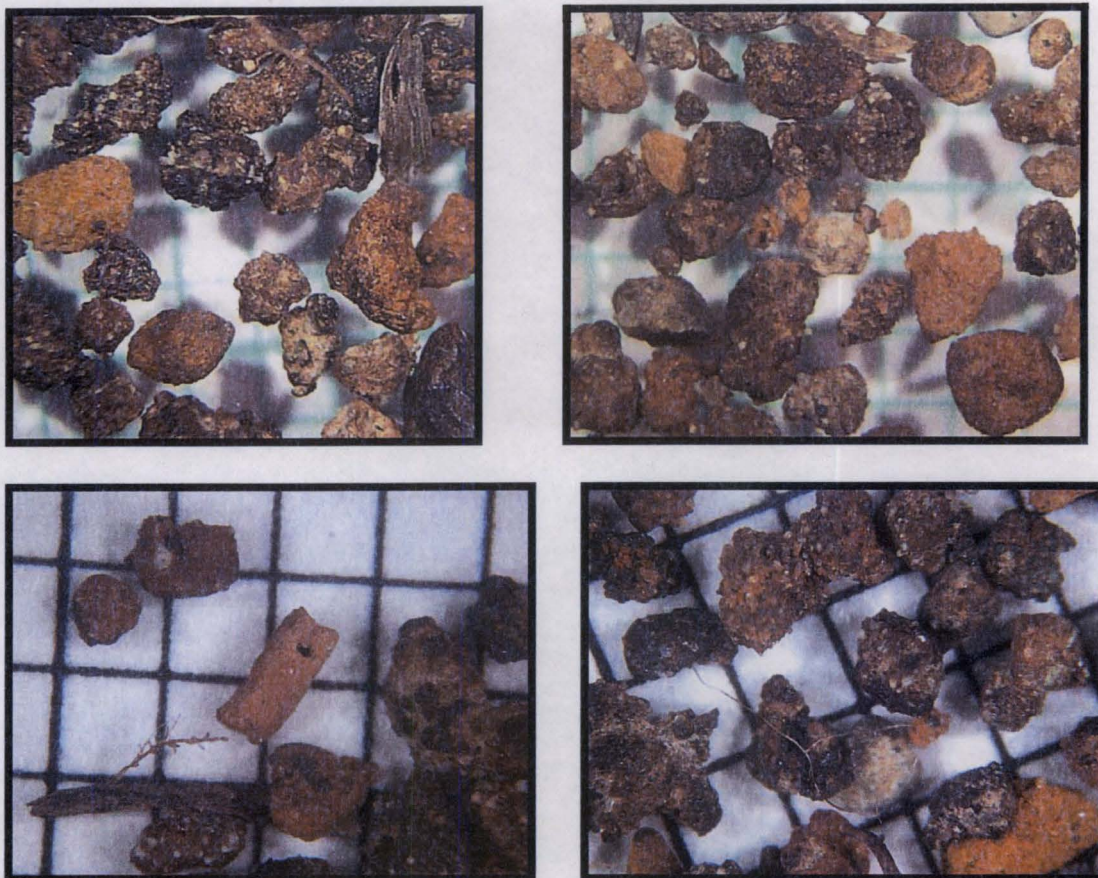


Figure 3. Aggregated redoximorphic features photographed before (top two photos) and after (bottom two photos) washing with 5% Na-hexametaphosphate solution.

2.2.8 Fe/Mn-Cemented Redoximorphic Feature Collection Sieving Method

The 12.5 cm of soil remaining from the intact cores used for pH measurements was extruded into a nest of standard 20-cm-diameter soil sieves. Soil remaining on the inside of the plastic liner was washed with TDW into the sieve nest. The nest of sieves consisted of 2mm, 1mm, 850 μ m, and 425 μ m mesh sizes. A Fritsch Analysette-3 Pro Microprocessor Sieve Shaker was used to agitate the sieves with a cycling amplitude modulation. The soil was rinsed with distilled water to promote dispersion and aggregate separation. The sieve

shaker was operated with an amplitude setting of 1.5 mm for a period of 20 minutes per sample wash. Additional washes were conducted when root mass hindered the release of soil. The resulting size-separated particles were collected in polypropylene beakers by washing the sieve mesh with TDW. The loss of particles during transfer was estimated through visual observation to be less than 1%. The washed particles were air dried and stored in glass vials. The collected particles were not washed with a Na-hexametaphosphate solution because the previous experiment revealed no change in the observed physical properties of the particles.

2.2.8.1 Separation and Selection Method

Visual inspection of the 1 – 2 mm soil particles showed five distinct categories of redoximorphic particles that had distinct color and morphology. The particles were categorized into 6 classes: Fe and Mn-rich aggregates (F/M), Fe aggregates (Fe), fine sand aggregates (S), coarse sand aggregates (A), Fe-cemented root channel linings (RC), and particles that consisted of either unweathered mineral fragments or biological material (O). Due to time constraints this study focused only on the categorization of the 1 to 2 mm size particles.

Particle selection and counting were conducted manually using fine-tipped stainless steel tweezers and a Nikon SMZ-10 Stereomicroscope (10x eyepiece, 0.66 – 4 (6:1) zoom, and 0.53 main lens). Particles were selected from all 36

samples taken along the Black Rock Slough transect in the 1 – 2 mm sized - fraction.

To count the cemented redoximorphic features the samples were evenly spread onto a 1/16" (~1.6 mm) grid, identified, and total numbers of each category within the microscope's viewable area (approximately 9 grid squares) were tabulated. Five field of view areas were counted. Each area viewed was digitally photographed. Digital photographs are presented in Appendix B.

Cemented redoximorphic aggregates from sampling points A, B, and D within the 1 – 2 mm size were categorized and counted to determine particle distribution and characteristics. Aggregates collected from sampling point C were not analyzed due to time considerations and similarity between water table levels at points C and D. Particle in the 1 – 2 mm size class represent a common size fraction noted in literary sources. The remaining particle size classes were stored for future analysis.

2.2.8.2 Digestion and Analysis Method

The 6 categories of aggregated redoximorphic features were finely ground in an agate mortar and pestle in preparation for acid digestion. The samples were digested using an aqua regia/HF digestion process outlined by EPA Method 3052 (EPA 1996). The digestion procedure employed 9 mL, 3 mL, and 2 mL of HNO₃, HF, and HCl, acids respectively. A CEM Mars – 5 Closed Vessel Microwave Digestion System was used to dissolve the samples. Sample vessel

pressure and temperature were controlled such that neither parameter exceeded 190 psi nor 190 C° for the 30 minute digestion time.

Digestions were done in duplicate or triplicate. Sample masses ranged between 0.0805 grams for the fine sand aggregates to 0.2056 grams for the Fe/Mn aggregates. Two samples of NIST SRM – 2711 and one composite acid blank were digested in each run. The digested samples were passed through a 0.22 µm filter into a 50 mL plastic volumetric flask and brought to level using TDW.

Concentrations of As, Cd, Fe, Mn, P, Pb, and Zn in the digest were measured on a Thermo Electron ICP-AES (IRIS Model) using Thermo Electron TEVA™ Version 1.5.0 analytical software.

2.2.9 Matrix Soil Elemental Analyses

Soil cores collected at 0 -15 cm, 15 - 30 cm, and 30 - 45 cm near sampling points A, B, C, and D were weighed, oven dried at 105 °C for 24 hours, and weighed again to collect data necessary to determine bulk density (Appendix A, Tables A-2, A-3). The oven-dried cores were split lengthwise to facilitate sampling of matrix soil. Soil was sampled from the upper 7.5 cm of each of the cores. The soil was gently crushed and composited by mortar and pestle. The resulting mixture represents a composite of soil from the surface to the 45 cm depth. The composited samples were sent to ACME Analytical Laboratories Ltd., Vancouver, British Columbia for acid digestion and analysis. ACME Laboratory quality assurance and control practices employ two blank reagent samples, one

standard sample with known elemental concentrations (STD DST6) to monitor digestion accuracy, and one granite sample (G-1) to evaluate mechanical process contamination.

2.3. Results

The Black Rock Slough study site is a wetland environment that is subjected to seasonal water table fluctuations resulting from Coeur d'Alene Lake water management. Generally the CDA River rises to its highest average height around April (Figure 4) and decreases to its lowest average height in September. The water table fluctuations (Figure 5) at sampling points A-D (Figure 2) are correlated to CDA River fluctuations.

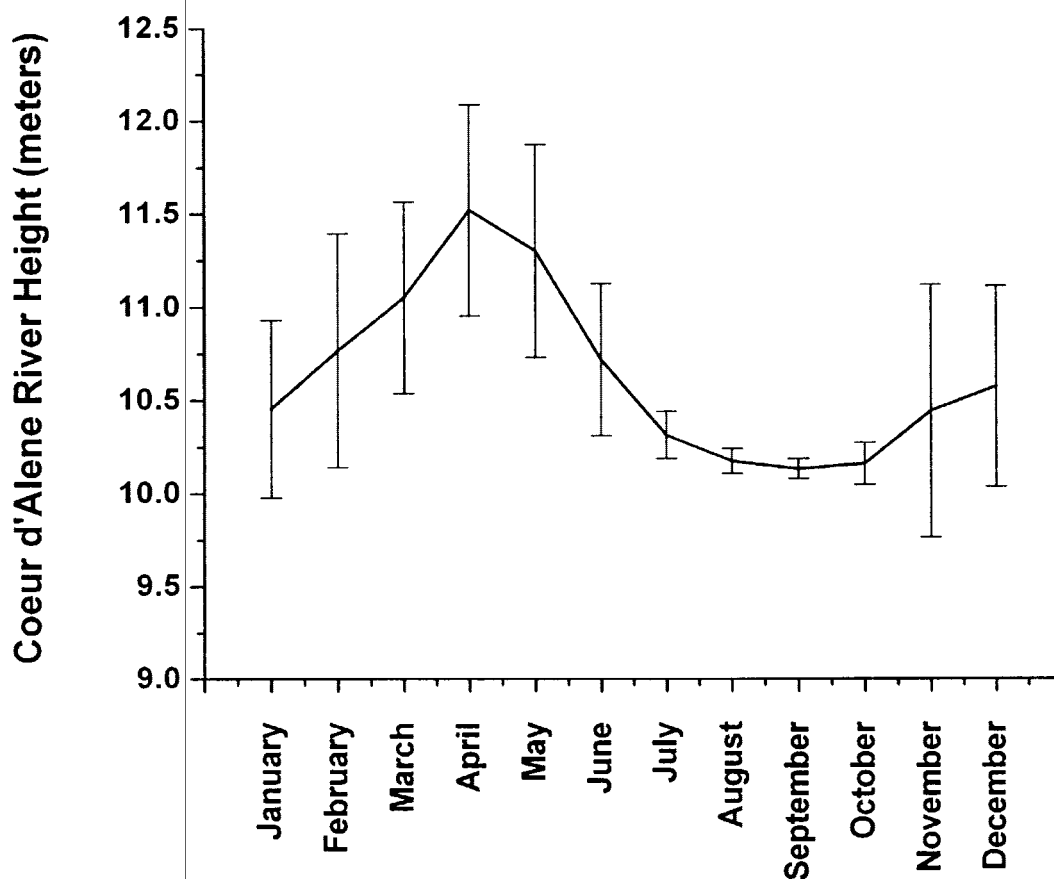


Figure 4. Coeur d'Alene River averaged monthly heights as recorded by USGS River Gage #12413500 located at Cataldo, ID (Lehmann 2006). Data consisted of river measurements from 1987 to 2005 taken at noon and midnight daily. Error bars indicated standard deviation of river height monthly average.

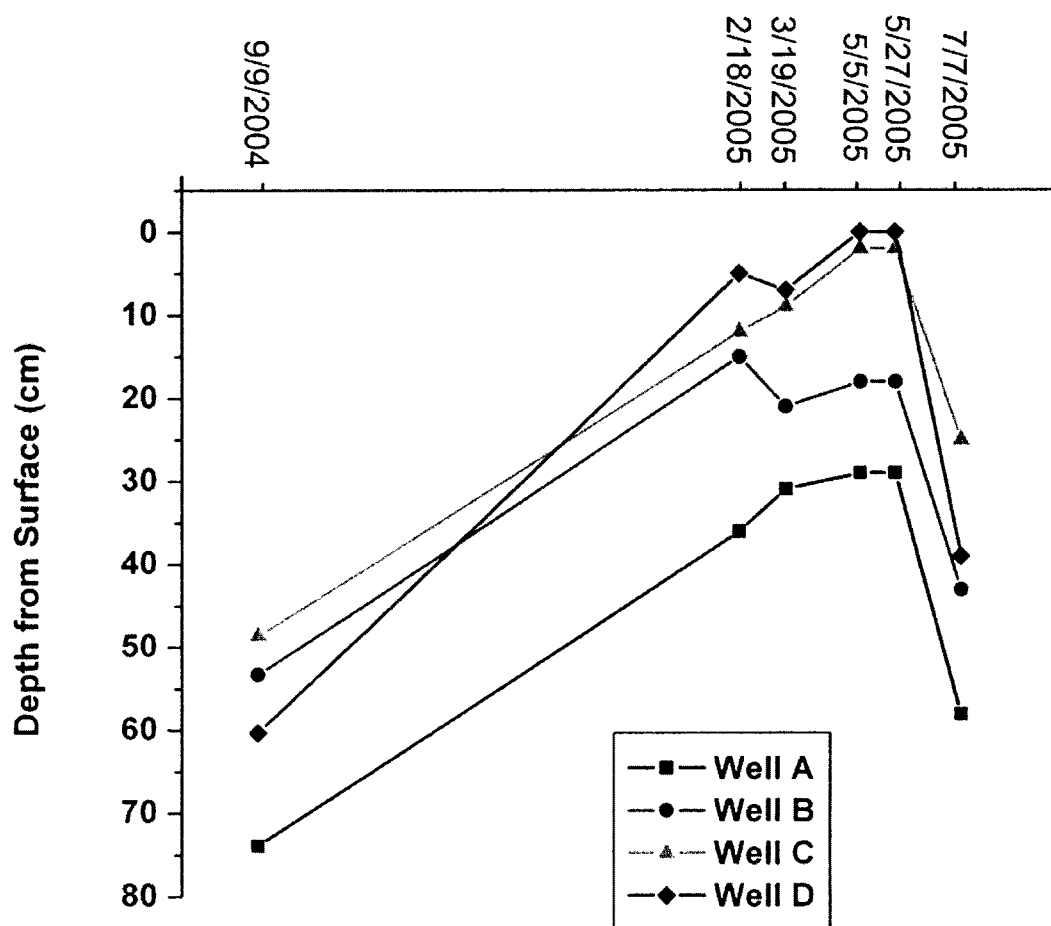


Figure 5. Water table depths at sampling point well A, B, C, and D along the sampling transect at Black Rock Slough.

The rising water levels and seasonal change in temperature within Black Rock Slough soils resulted in anaerobic activity as evidenced by the decreasing Eh values (Table 1). Well water pH values varied slightly (Table 1). Well temperatures corresponded to the seasonal warming (Table 1).

The soil at the Black Rock Slough site best fit the description of a Slickens series. Soil profiles at sampling points A, B, and C are described in Tables 2 - 4.

Table 1. Field measurement data for pH, Eh, temperature, and well depth taken from sampling point wells along the Black Rock Slough transect. Well depth is measured from the soil surface to the water surface. A well depth of zero indicates water at the soil surface. NT indicates that a measurement was not taken.

Measurement	Date	Sampling Point Well			
		A	B	C	D
pH					
	2/18/05	NT	NT	NT	NT
	3/19/05	5.66	5.70	5.37	6.29
	5/5/05	NT	NT	NT	NT
	5/27/05	5.54	5.3	5.3	5.43
	7/7/05	4.74	5.74	5.79	5.79
Eh (mV)					
	2/18/05	250 (464)*	250 (464)	246 (466)	233 (447)
	3/19/05	295 (505)	282 (496)	289 (503)	270 (484)
	5/5/05	233 (443)	195 (402)	210 (417)	205 (412)
	5/27/05	241 (448)	125 (332)	163 (370)	165 (372)
	7/7/05	195 (402)	15 (222)	75 (282)	101 (308)
Temp (°C)					
	2/18/05	4	3	2	2
	3/19/05	5	4	4	4
	5/5/05	9.4	11.1	10	11.1
	5/27/05	10.6	11.1	11.1	13.3
	7/7/05	13.3	13.3	13.3	15
Depth (cm)					
	9/9/04	73	53	48	60
	2/18/05	36	15	12	5
	3/19/05	31	21	9	7
	5/5/05	29	18	2	0
	5/27/05	29	18	2	0
	7/7/05	58	43	25	39

* Eh numbers in parentheses are redox potential corrections for an Ag/AgCl electrode to a hydrogen electrode per Vepraskas (2001).

Table 2. Profile description for Black Rock Slough sampling transect point A.

Horizon A: 0-9 cm. Red (2.5 YR 4/8) moist silt loam; very fine granular structure; very friable, slightly sticky and non plastic; no clay films; many very fine, fine, and medium roots. A platy accumulation of Fe is present at the horizon boundary.

Horizon C1: 9-28 cm. Dark Gray (5 YR 4/1) moist silt loam, single grain, very friable, non-sticky and non-plastic; no clay films; moderately few very fine and fine roots; common, medium, prominent, red (2.5 YR 4/8) moist concentrations.

Horizon C2: 28-33 cm. Light brownish gray (10 YR 6/2) moist silt loam, single grain, very friable, non-sticky and non-plastic; no clay films; few very fine roots; few, fine, prominent, strong brown (7.5 YR 5/6) moist concentrations.

Horizon C3: 33-74 cm. Pale brown (10 YR 6/2) moist silt loam, single grain, very friable, non-sticky and non-plastic; no clay films; few very fine roots, charcoal fragments approximately between 5 mm to 1 cm in length found in a 5 cm band at the 35 cm depth.

Table 3. Profile description for Black Rock Slough sampling transect point B.

Horizon A: 0-5 cm. Red (2.5 YR 4/8) moist silt loam, very fine granular structure; very friable, slightly sticky and non plastic; no clay films; many very fine, fine, and medium roots.

Horizon C1: 5-28 cm. Reddish gray (2.5 YR 5/1) moist silt loam, single grain, very friable, non-sticky and non-plastic; no clay films; moderately few very fine and fine roots; common, medium, prominent, red (2.5 YR 4/8) moist concentrations.

Horizon C2: 28-33 cm. Pinkish gray (5 YR 6/2) moist silt loam, single grain, very friable, non-sticky and non-plastic; no clay films; moderately few very fine and fine roots; few, medium, prominent, red (2.5 YR 4/8) moist concentrations.

Horizon C3: 33-46 cm. Light brownish gray (10 YR 6/2) moist silt loam, single grain structure, very friable, non-sticky and non-plastic; no clay films; few very fine roots; few, medium, prominent, red (2.5 YR 4/8) moist concentrations. Charcoal fragments approximately between 1 mm to 3 mm in length found in a 5-cm band at the 33-cm depth.

Table 4. Profile description for Black Rock Slough sampling transect point C.

Horizon A: 0-8 cm. Dark red (2.5 YR 3/6) moist silt loam, very fine granular structure; very friable, slightly sticky and non plastic; no clay films; many very fine, fine, and medium roots.

Horizon C1: 8-20 cm. Gray (5 YR 6/1) silt loam moist, single grain, very friable, non-sticky and non-plastic; no clay films; moderately few very fine and fine roots; few, medium, prominent, dark red (2.5 YR 3/6) moist concentrations.

Horizon C2: 20-56 cm. Gray (10 YR 6/1) silt loam moist, single grain, very friable, non-sticky and non-plastic; no clay films; moderately few very fine and fine roots; few, medium, prominent, dark red (2.5 YR 3/6) moist mottles. Charcoal fragments approximately between 1mm to 3 mm in length found in a 2 cm band at the 35 cm depth.

The floodplain topography within the Black Rock Slough study site transect had less than a 2% slope, with an overall elevation change of approximately 1.1 meters across 79.2 meters (Figure 2). The geographical positioning near the CDA River, vegetation growth, and slope of the Black Rock Slough provided conditions that were favorable to flood sediment-load deposition and retention. Well water depths measured indicated that the water table is closer to the surface as the transect progresses south (Table 1).

The soils collected from locations ~30 and ~15 meters from the sampling transect were a silt loam and loam texture (Table 5). The soil sampled at ~30 meters east of the transect consists of approximately 27 – 36% sand, 55 – 63% silt, and approximately 9% clay. Soils sampled from ~15 meters from the transect consisted of 10 – 45 % sand, 47 – 78 % silt, and 8 – 18 % clay-sized particles.

Table 5. Texture analysis results of soils taken at ~ 30 m and ~ 15 m west of point B on the Black Rock Slough sampling transect. Raw data are in Tables A-4.

Samples	Sand	Silt	Clay	USDA Texture Class
Composite Sample 1 ^a	36%	55%	9%	Silt Loam
Composite Sample 2 ^a	27%	63%	10%	Silt Loam
Pit Sample 1 ^b	10%	78%	12%	Silt Loam
Pit Sample 2 ^c	37%	55%	8%	Silt Loam
Pit Sample 3 ^d	45%	47%	8%	Loam
Pit Sample 4 ^e	27%	60%	13%	Silt Loam
Pit Sample 5 ^f	28%	54%	18%	Silt Loam

Notes a: Soil collected approximately 30 m east of Sample Point B and composited. Soil taken approximately 15 m east of Sample Point B at 5 distinct depths: **b:** 0 – 10 cm, **c:** 10 – 30 cm, **d:** 30 – 60 cm, **e:** 60 – 80 cm, and **f:** taken from a region of darker soil with charcoal fragments at ~ 35 cm.

At sampling point A, the high water table historically lies at approximately 10 cm from the soil surface as indicated by an abrupt boundary between the

upper Fe enriched (red) soil and the lower soil consisting of Fe concentrations and depletions (red and gray intermixed) soil (Figure 6). Concentrations were present between 5 cm and 56 cm. At sampling point C, an abrupt boundary between the soil surface and Fe concentrated and depleted soil did not exist, however Fe concentrations and depletions occurred in top 10 cm of the soil (Figure 7). A layer consisting of darkened soil and charcoal approximately 3-to-5 cm thick was found in the three pits excavated for profile descriptions at approximately 35 cm in depth. Presence of charcoal at a consistent 35-cm depth at all sites indicates uniform sediment deposition along the transect. Charcoal may have resulted from the burning of vegetation on site or deposition by flood waters, which followed forest fires that burned approximately 1.2 million hectares in northern Idaho and western Montana in 1910 (Wilma 2003). Soil pH was acidic and ranged between 3.9 and 5.1 (Table A-1).



Figure 6. (Left) Soil profile at hand dug pit in Black Rock Slough near point B showing the historic seasonally high water table depth. Scale is in decimeters. The region in which charcoal was found is clearly evident at approximately 3.5 dm. (Right) Close-up of historic seasonally high water table depth.



Figure 7. Soil profile near point C along the Black Rock Slough sampling transect. Mottling exists from the soil surface to approximately 10 cm. Note the lack of distinct boundary between the red and gray soils.

Successive flooding events have contaminated the Black Rock Slough site with metal(loids) carried by CDA River sediments. Elevated levels of As, Cd, Pb, S, and Zn are present in the soil, as well as increased concentrations of Fe and Mn (Table 6). Elements are enriched compared to average soil elemental concentrations (Lindsay (1979)) (Table 7) and pre-mining era sediment element concentrations (Table 8).

Table 6. Elemental concentrations from depth-composited (0 – 45 cm) matrix soil collected from the upper 7.5 cm of intact soil cores collected along four points (A, B, C, and D) along the sampling transect at Black Rock Slough. Standard DST6 and Sample Prep G-1 are ACME Laboratories in-house quality assurance samples.

Matrix	As	Cd	Fe	Mn	P	Pb	Zn
Soil	(mg/kg)						
Point A	156	15.7	92,900	3,500	720	4,840	2,350
Point B	140	8.00	93,500	1,180	860	7,230	2,350
Point C	169	9.10	77,900	1,200	930	4,980	1,820
Point D	103	5.50	55,900	1,040	1,040	4,250	1,190
Standard DST6	25	5.6	40,400	972	1,000	35.4	173
G-1	4	0.1	25,900	782	890	21.1	55

Table 7. Common elemental ranges for soils and selected averages for soils (from Lindsay 1979)

Element	Common Range for Soils (mg/kg)	Selected Average for Soils (mg/kg)
As	1 – 50	5
Cd	0.01 – 0.70	0.06
Fe	7,000 – 550,000	38,000
Mn	20 – 3,000	600
P	200 – 5,000	600
Pb	2 – 200	10
S	30 – 10,000	700
Zn	10 – 300	300

Table 8. Table modified from Hoffman (1995), Bender (1991), and Rabbi (1994). Data presented here are representative of selected pre-mining metal background concentrations (mg/kg) taken from lake sediments located near the CDA River. Samples M-91-B and T-91-B were taken from Medicine Lake and Thompson Lake. Sample KB results are from Killarney Lake. Sample BR-91-B was taken from Bull Run Lake approximately 550 yards from the Black Rock Slough sampling transect. Mount Mazama and Mount St. Helens ash was identified by its chemical fingerprint and employed as a time reference point. Pre and post mining sediments were also determined by the distinct difference in metal concentration.

Element	M-91-B (mg/kg)	T-91-B (mg/kg)	KB (mg/kg)	BR-91-B (mg/kg)
As	16-30	15-25	31-42	5 - 12
Cd	2-4	1-3	Below Detection Limit	5 - 31
Fe	17,900-22,000	11,600-13,500	14,100 – 30,000	25,600 - 34,500
Mn	249-518	56-181	320 – 800	510 -1,114
Pb	122-518	56-181	Below Detection Limit - 90	15 - 327
Zn	140-496	77-207	170 - 510	60 - 1,453

2.3.1 Results of Fe Concentrated and Fe Depleted Soil Elemental Analysis

The *in situ* effects of oxidizing and reducing conditions on elemental distribution are shown in Figures 8 and 9. Elemental concentrations of Fe - enriched (reddish-colored soil) or depleted (gray-colored soil) regions within the soil are listed in Table A-5.

Arsenic concentrations in the mottled soil features ranged between 27.2 mg/kg and 167 mg/kg and were different between the Fe enriched and the Fe depleted soils. The Fe-enriched soil had nearly twice the As concentration as the Fe-depleted soil.

The concentration of Cd varied from 1.18 mg/kg to 16.0 mg/kg in the Fe concentrated and depleted soil samples. The concentrations of Cd, however, did not show a large difference between the red and gray-colored soil samples. Cadmium was noticeably different between the 0 – 10 cm and 10 – 20 cm Fe enriched soil samples.

Iron concentration differences between the soil concentrations and depletions were large, from 26,600 mg/kg to 112,000 mg/kg. The red soil fraction contained an average of 67,800 mg/kg more Fe than the gray soils. The difference between the two depths of the gray soils was also noticeable; however, the concentrations of Fe in the two depths of the red soils did not differ greatly.

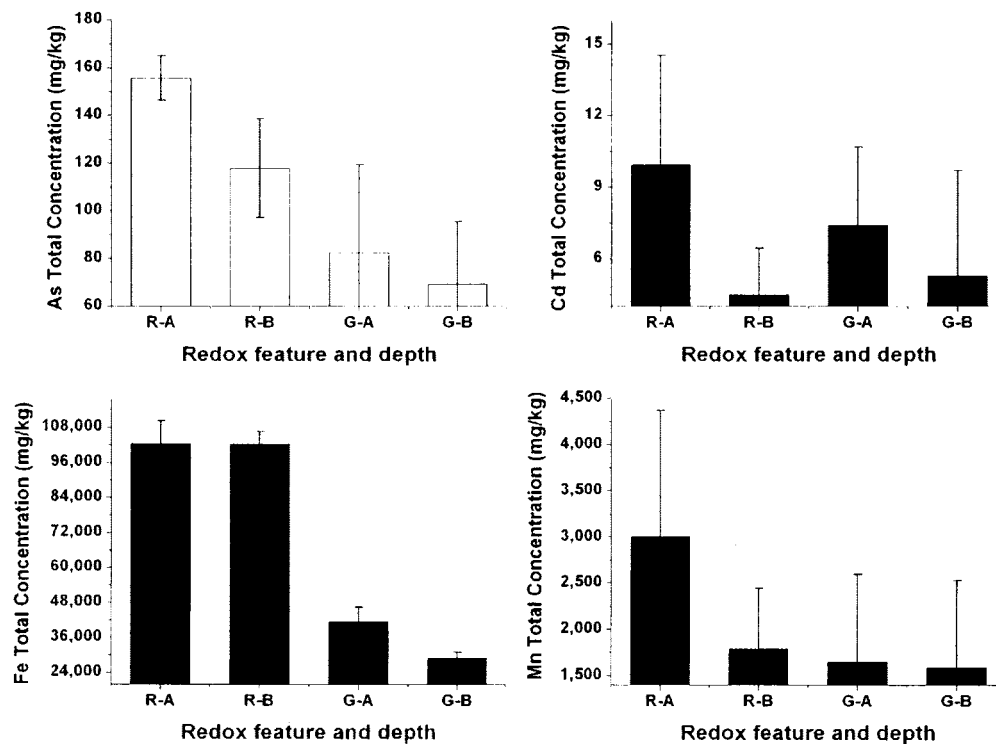


Figure 8. Average elemental concentrations for red and gray colored soils taken from Black Rock Slough sampling transect. R – refers to red colored soil, G – refers to gray-colored soil, A – refers to the 0 – 10 cm sampling depth, and B – refers to the 10 – 20 cm sampling depth. Error bars represent the standard deviation of the sample average from 4 independent samples. Raw data are in Appendix A, Table A-5

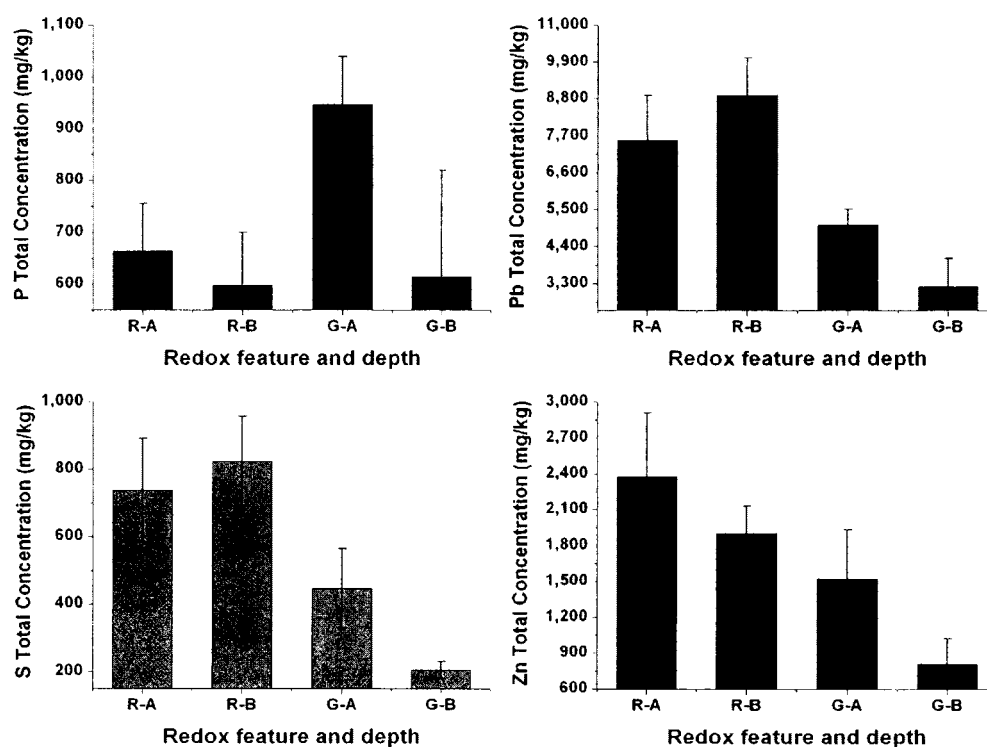


Figure 9. Average elemental concentrations for red and gray colored soils taken from mottled regions on Black Rock Slough sampling transect. R – refers to red colored soil, G – refers to gray colored soil, A – refers to the 0 – 10 cm sampling depth, and B – refers to the 10 – 20 cm sampling depth. Error bars represent the standard deviation of the average from 4 independent samples. Raw data are in Appendix A, Table A-5.

The concentration of Mn ranged from 480 mg/kg to 4,870 mg/kg. There were no clear trends in Mn concentrations between Fe enriched and Fe depleted soils.

Concentrations of P ranged from 252 mg/kg to 1,040 mg/kg. In the 0 – 10 cm soil samples the concentration of P between the Fe-enriched and depleted soil was noticeably different. Phosphorus concentration in the upper and lower depths of the Fe-enriched soils was not markedly different. The difference between concentrations of the upper and lower depths of the Fe-depleted soil was noticeably different.

There were distinct differences in Pb concentrations between Fe-enriched and depleted samples. The difference between the upper and lower depths of the Fe-enriched soil had less obvious differences; however the Fe-depleted fractions in the two depths were distinctly different. The samples have a Pb concentration range of 686 mg/kg to 10,300 mg/kg.

Differences in sulfur concentrations were noticeable between the Fe-enriched and depleted samples and the 0 -10 cm and 10 - 20 cm gray soils. Sulfur showed large differences in the 0 – 10 cm and 10 – 20 cm gray soils. Sulfur varied between 159 mg/kg and 979 mg/kg.

The range of concentrations for Zn was 562 mg/kg to 3,020 mg/kg. Zinc concentration had appreciable differences in the Fe-enriched and depleted soil samples, 0 – 10 cm and 10 – 20 cm red soil samples, and the 0 – 10 cm and 10 – 20 cm depths of the gray soils.

Precision of the ICP-AES analysis conducted on Fe concentrated and depleted soil samples were measured using NIST SRM-2711 (Montana Soil:

Moderately elevated trace element concentrations). The recovery percentage of the reference soil ranged from 79% to 160% (Table A-5). The 160% recovery was only for one set of data for As concentrations. This value likely resulted from incorrect calibration of the As line since recovery percent for other elements were within 10% of expected values for those samples. The majority of the element recovery values for the standards were within 10% of the expected values.

2.3.2 Results of Aggregated Redoximorphic Feature Characterization

2.3.2.1 Fe and Mn-Rich Cemented Aggregates (F/M) (Figure 10):

The Fe/Mn-cemented aggregates are very dark and brown to black, indicating the presence of Mn oxides (Rhoton et al. 1993). Particles in this category were strongly cemented as determined by attempting to crush with the fingers (Schoeneberger et al. 2002). These particles also resisted fracturing from pressure by tweezers. The typical Fe/Mn aggregate was generally blocky oblate or blocky equant in shape, subangular in sphericity, and had a rough surface (Stoops 2003). The surfaces of these particles had intermixed reddish-brown and black coloring (Figure 11).

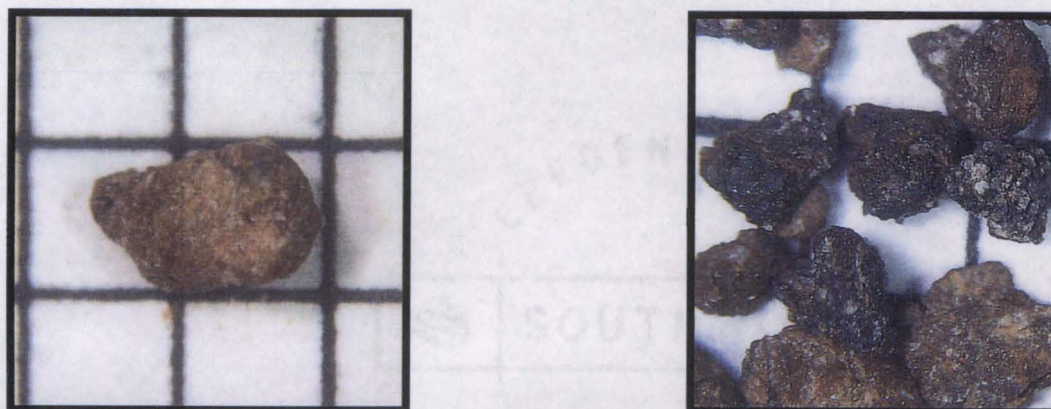


Figure 10. Two examples of Fe and Mn-rich cemented aggregates (F/M). Grid size is 1.6 mm

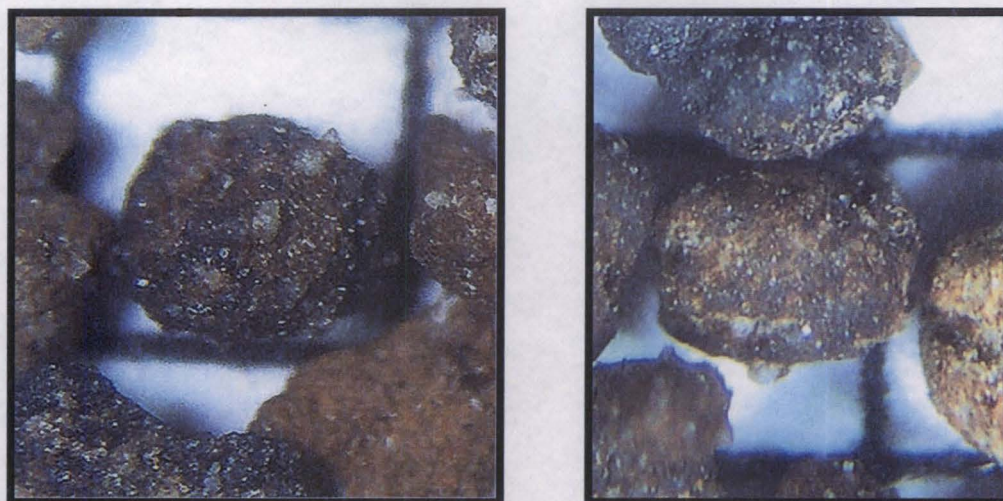


Figure 11. Examples of Fe and Mn-rich cemented aggregates in which the surface color is mixed. The grid size is 1.6 mm.

2.3.2.2 Fe-cemented Aggregates (Fe) (Figure 12):

Iron-cemented aggregates are orange-red in color resulting from the presence of Fe-oxide coatings. These particles have a noticeable lack of black color, suggesting the lack of oxidized Mn. Particles in this category are more weakly cemented than the Fe/Mn-cemented aggregates. The Fe aggregates tended to be globular oblate in shape, rounded sphericity, and had an undulating surface roughness (Stoops 2003). The Fe-cemented aggregates were nearly always rounded or oval in shape. Iron nodules that were encountered with angles were devoid of sharp edges.

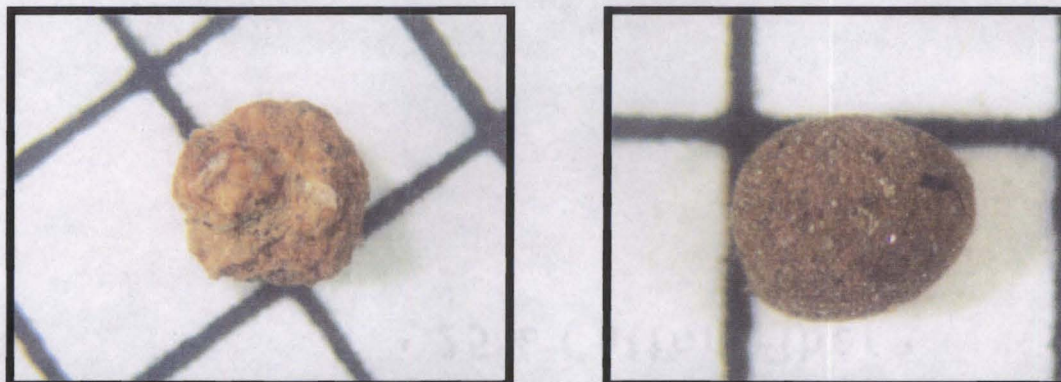


Figure 12. Two examples of Fe enriched cemented redoximorphic features (F). Grid size is 1.6 mm.

2.3.2.3 Fine Sand Aggregates (S) (Figure 13):

Soil particles grains are weakly cemented and are gray due to increased depletion of Fe and Mn-oxides. The particles have a cementing agent present that allowed particles to remain whole after mechanical sieving; however, the cementing agent appears to be minimal such that coloration is undetectable. Fine sand aggregates were found to be a globular shape and most often equant in sphericity. The particles were well rounded with a smooth surface (Stoops 2003). The term “fine sand” was used as a distinguishing term during initial aggregated redoximorphic feature observations and does not indicate actual particle size. The aggregate’s particle-size was not determined.

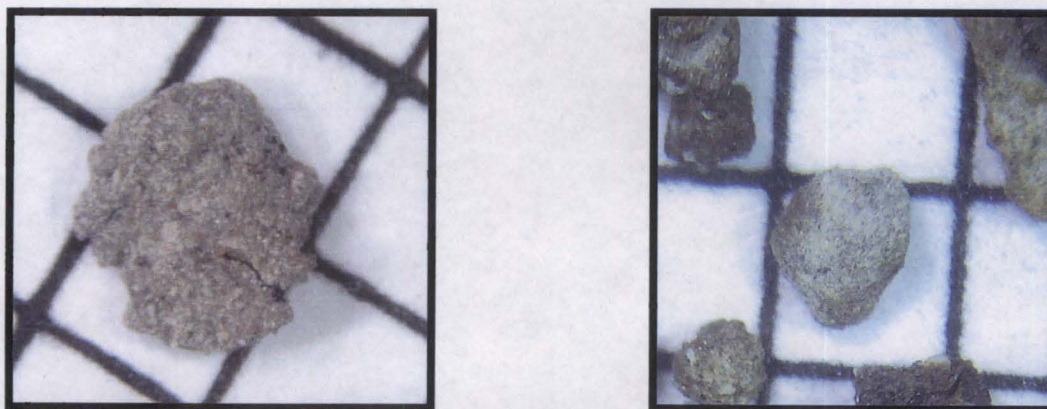


Figure 13. Examples of fine sand aggregates (S). Grid size is 1.6 mm.

2.3.2.4 Coarse Sand Aggregates (A) (Figure 14):

Particles forming this category have a dark-brown to black core and are impregnated with grains that are larger than what constitutes the particle-size makeup of the core. The term "coarse sand" was used as a distinguishing term during initial aggregated redoximorphic feature observations and does not indicate actual particle size. The aggregate's particle-size was not determined. In most cases, the center nodule resembled an oval Fe/Mn aggregate. The sand appeared colorless, indicating a possible lack of oxide coatings. These particles were moderately to strongly cemented. Coarse sand aggregates were always globular in shape and equant, rounded, and had a rough surface.

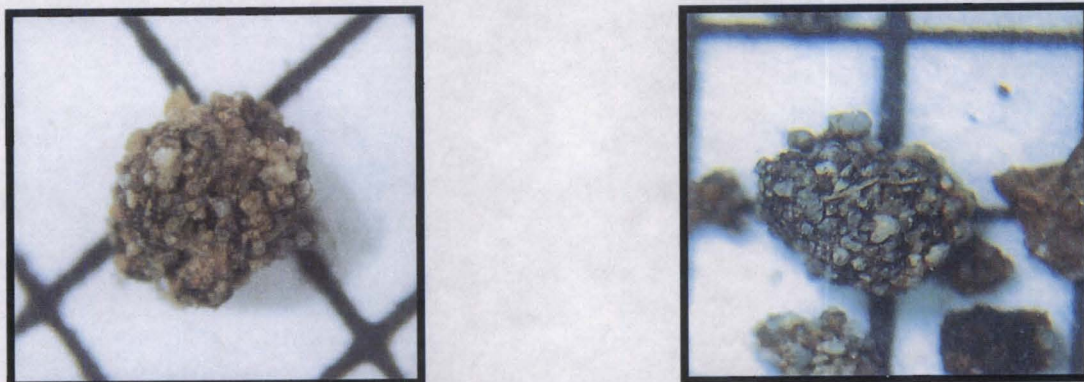


Figure 14. Examples of coarse-sand aggregates (A). Grid size is 1.6 mm.

2.3.2.5 Fe Root Channel Linings (RC) (Figure 15):

These particles varied in length from approximately 1.0 mm to 3.5 mm and often resembled fractured segments of larger root channels. These particles were uniquely defined by a distinct central channel that a plant root occupied. The particle colors ranged from slightly reddish to dark brown. The cemented root channel linings were often cylindrical and prolate. The root channels were most often rounded and had smooth surfaces (Stoops 2003). These particles

were weakly to strongly cemented, but were fragile due to their cylindrical shape with often hollow centers and occasionally fractured when moved with tweezers. Many root channels were globular in shape and equant due to fracturing during the sieving process or during movement while in storage.

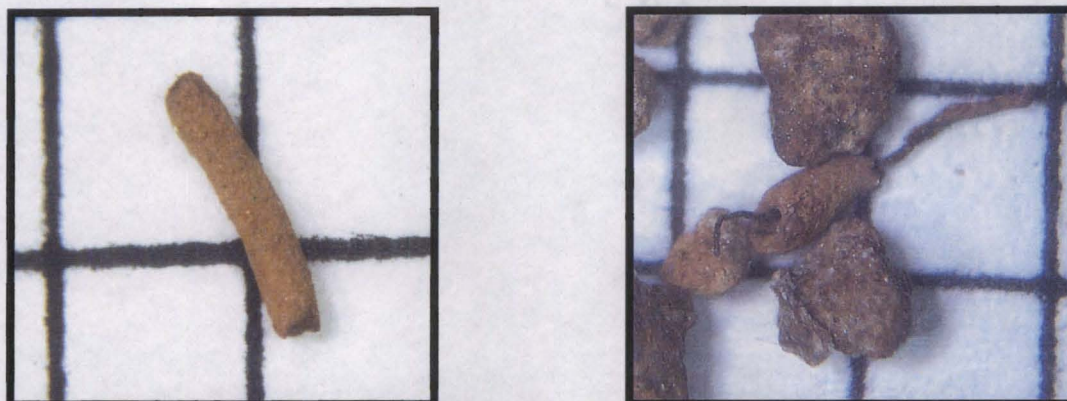


Figure 15. Examples of root channel linings or pipestems (RC). Grid size is 1.6 mm.

2.3.2.6 Other Particulates (O) (Figure 16):

These particles are comprised of either organic (e.g. roots, seeds, insect exoskeleton fragments, charcoal) or primary mineral components (e.g. mica sheets, quartz fragments). As a result of the variety of particles associated with this category, the shape, equidimensionality, degree of roundness, and surface roughness were not consistent.

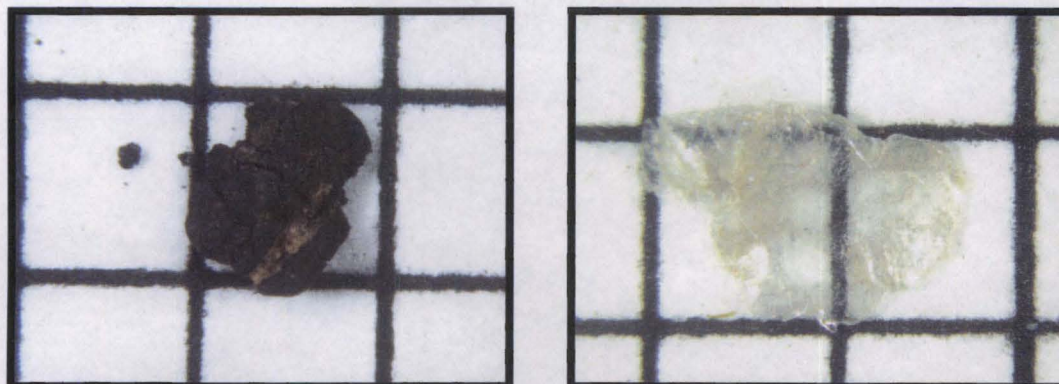


Figure 16. Examples of biological (left) and non-weathered mineral (right) particles found after wet-sieving (O). Grid size is 1.6 mm.

2.3.3 Distribution and Concentration of Cemented Redoximorphic Aggregates

Digital images taken during categorization procedure are listed in Appendix B. Cemented redoximorphic aggregate distribution (Figures 17 and 18 Appendix A, Tables A-6 – A-16) and element composition (Table 9) within the Black Rock Slough soil varied depending on the depth and landscape position. Overall distribution of aggregated redoximorphic particles decreased with depth; however, coarse sand aggregates (A) increased with depth at point A and root channel linings (RC) increased with depth at point D. Particle distribution within the sampling points was dominated by the Fe/Mn-cemented aggregates with the greatest observed percentage of Fe/Mn-cemented aggregates (63%) at point B. By depth, Fe/Mn-cemented aggregates were common at both the 0 – 15 cm and 15 – 30 cm depths. Fe-cemented aggregates were common at the lower and wetter point D. Fe-cemented aggregates were less common at the wetter point B when compared to point A which has a higher landscape profile. Fine sand aggregates (S) were less common at point B. Organic material and non-weathered mineral counts increased with depth and were common in the 30 - 45 cm depth of all sampling points. Point B had the highest percentage of the organic material and non-weathered minerals.

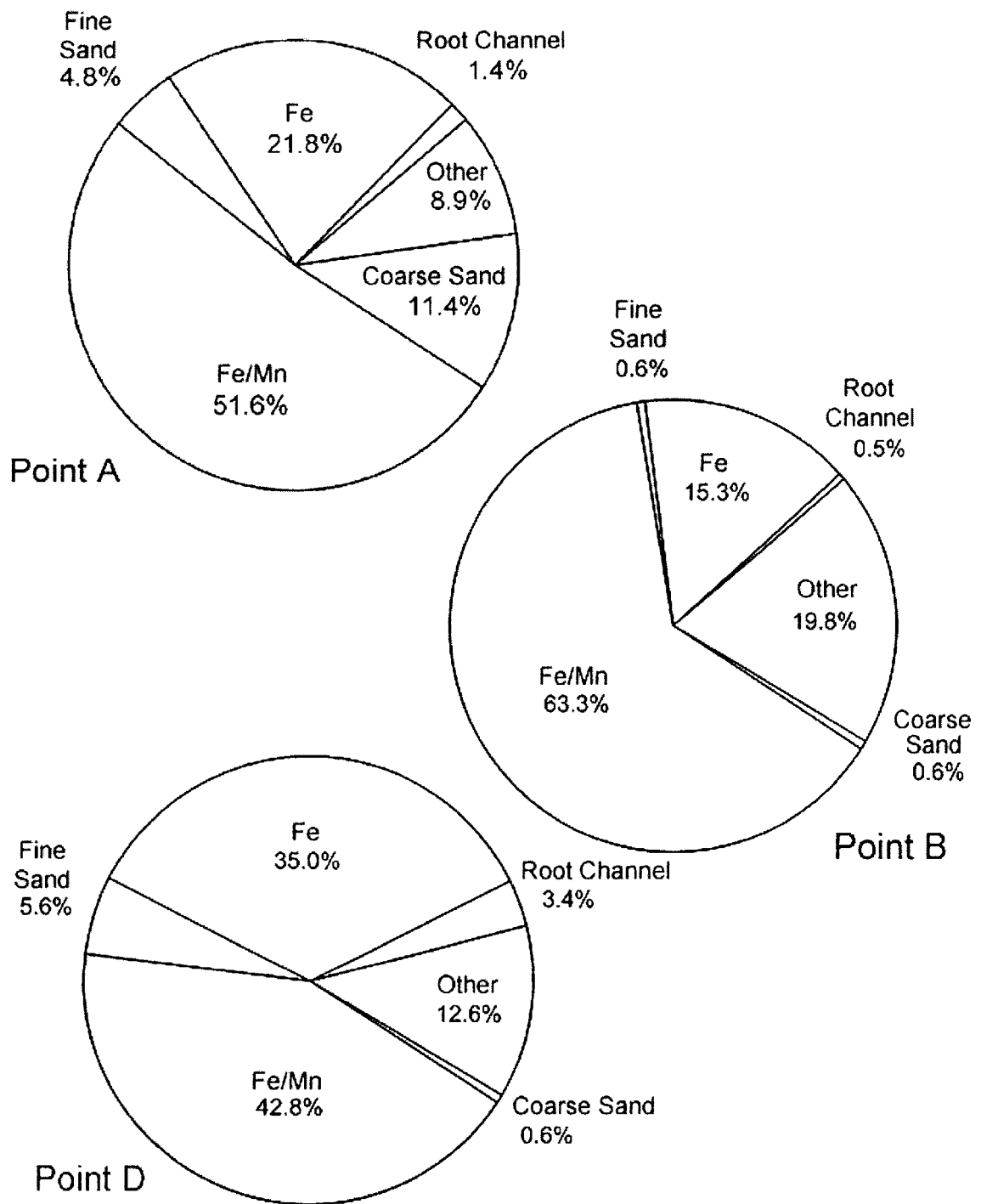


Figure 17. Distribution of aggregated redoximorphic features from points A, B, and D within Black Rock Slough sampling transect. Percentages are relative to the total number of particles counted. Raw data is in Appendix A-6 through A-16.

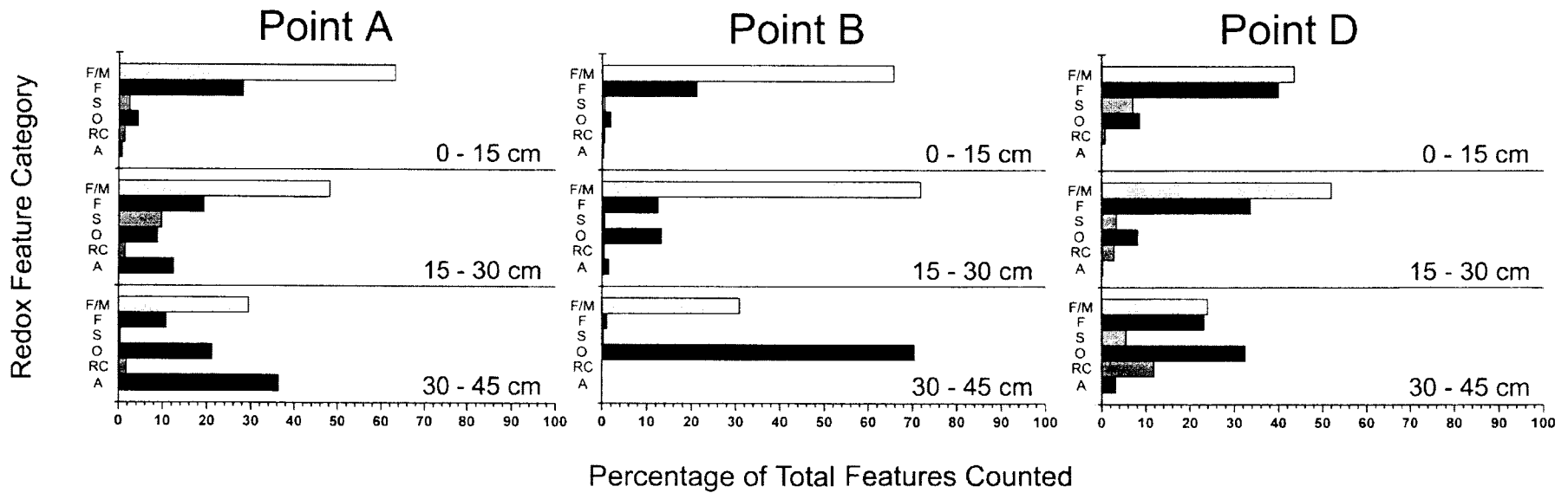


Figure 18. Distribution of Fe/Mn-cemented aggregated feature categories collected from points A, B, and D within the Black Rock Slough sampling transect. Distribution is arranged by sampling point and sampling depth. Raw data are in Appendix A-6 through A-16.

Table 9. Average elemental concentrations in the 6 categories of features in the 1 to 2 mm size fraction recovered from points A, B, and D on the Black Rock Slough sampling transect. Standard deviation of replicates is within parentheses. Averaged standard reference material (SRM) recovery percentages are shown with standard deviation in parentheses. Raw data are in Appendix A, Table A - 17

Sample Name	As (mg/kg)	Cd (mg/kg)	Fe (mg/kg)	Mn (mg/kg)	P (mg/kg)	Pb (mg/kg)	S (mg/kg)	Zn (mg/kg)
Other (O) ^a	102 (9.1)	50.8 (0.8)	97,300 (357.8)	9,760 (33.9)	3,780 (229)	13,720 (8.0)	1,150 (52.7)	1,840 (78.2)
Root Channel (RC) ^a	182 (4.8)	26.1 (0.6)	138,000 (2,020)	3,230 (49.4)	2,130 (26.6)	9,240 (147)	1,120 (35.8)	1,060 (18.3)
Fine Sand Aggregate (S) ^a	64.0 (2.0)	16.2 (0.1)	43,200 (304)	3,880 (149)	1,250 (32.8)	6,830 (226)	1,010 (22.1)	1,350 (10.9)
Coarse Sand Aggregates (A) ^b	37.6 (8.1)	43.9 (0.7)	39,400 (902)	29,500 (675)	1,250 (42.2)	16,800 (982)	603 (24.0)	1,130 (24.9)
Fe/Mn-cemented Aggregates (F/M) ^b	59.2 (6.8)	38.2 (0.5)	70,600 (4,020)	34,600 (6,980)	1,370 (25.0)	26,800 (4,370)	1,230 (20.8)	1,430 (9.2)
Fe-cemented Aggregates (F) ^b	148 (7.5)	23.8 (0.5)	114,000 (4,330)	5,280 (231)	780 (42.6)	9,710 (485)	1,280 (43.6)	1,950 (65.7)
SRM - 2711 Recovery Percentage ^a	108% (0.7%)	92% (1%)	92% (1%)	94% (2%)	95% (1%)	99% (1%)	132% (1%)	99% (2%)
SRM - 2711 Recovery Percentage ^b	91% (8%)	89% (6%)	93% (2%)	104% (2%)	132% (51%)	97% (2%)	109% (1%)	99% (1%)

2.4 Cemented Redoximorphic Aggregate Distribution and Elemental Concentration Results

Iron manganese-rich cemented aggregates (F/M) were the most abundant in all three sample sites (Tables A-6 – A-16), comprising 43% to 61% of the total particles counted. These particles were strongly cemented and resisted fracturing. The average Fe content of the Fe/Mn-rich cemented aggregates was 70,600 mg/kg. The average Mn content was 34,600 mg/kg. The Fe:Mn ratio in the Fe/Mn rich cemented aggregates is approximately 2:1. The Fe/Mn-rich cemented aggregates were enriched in Cd, P, Pb, and S (Table A – 17) when compared to bulk soils average concentrations (Tables 6 and 9).

Iron-cemented aggregates (F) were the next most abundant category found in the 1-to-2-mm size range comprising approximately 18% to 35% of total particles (Tables A-6 – A-16). These cemented aggregates had the second highest average Fe content of approximately 114,000 mg/kg. The Mn content was 5,280 mg/kg. The Fe:Mn ratio is 21:1. The oxidized Fe concentrations were enriched in Cd, Pb, and S compared to bulk soils (Tables 6 and 9).

Root-channel linings (RC) were among the lowest percentage of 1 – 2 mm particles (0.7% to 3.4%) (Tables A-6 – A-16). The average Fe content for the root channel linings was the highest of all 1 – 2 mm particle classes at 138,000 mg/kg. The average Mn content of the root channel particles was 3,230 mg/kg. The Fe:Mn ratio for root channel linings is 43:1. The Fe root channel linings were enriched in As, Cd, P, Pb, and S (Table 9) compared to the bulk soils (Table 6).

The highest As and lowest Zn concentration in the 1 – 2 mm particles was sequestered in cemented root channel linings (Table 9).

The aggregated coarse sand aggregates (A) comprised 11.4% of the 1 to 2 mm particles found in the drier, northern sampling site A (Tables A-6 – A-16), but were uncommon (0.6%) in the wetter southern sampling areas of Site B and D. The average Fe content for the aggregated coarse sand particles was 39,400 mg/kg and the average Mn content was 29,500 mg/kg. The Fe:Mn ratio is 1.3. The coarse sand aggregates were enriched in Cd, P, and Pb (Table 9) compared to the bulk soil (Table 6). The highest Cd concentrations, except for biological material, were found in the coarse sand aggregates. The lowest As and S concentrations were found in the coarse sand aggregates.

Fine sand aggregates (S) comprised 0.7% to 5.6% of the 1 – 2 mm particles (Tables A-6 – A-16). Observations of these particles were uncommon (~0.7%) at site B compared to site A and D. The average Fe content for the sand aggregates was 43,200 mg/kg and the Mn content was 3,880 mg/kg. The Fe:Mn ratio is 11:1. The fine sand aggregates were not markedly enriched in P compared to the bulk soils enriched in As, Cd, P, Pb, S, and Zn (Tables 6 and 9). The sand aggregates had the lowest Cd concentration.

The category defined as other (O), consisting of organic (e.g. exoskeletal remains, charcoal, roots) and primary mineral particles (e.g. mica), comprised approximately 9% to 20% (Tables A-6 – A-16) of the particles counted. The mineral and biological particles had an average Fe content of 97,300 mg/kg and the average Mn content was 9,760 mg/kg. The Fe:Mn ratio was 10:1. Compared

to the bulk soil, the mineral and biological particles were enriched in Cd, P, Pb, and S (Tables 6 and 9). This category often had metal concentrations greater than the remaining categories, which can be attributed to the presence of a variety of functional groups associated with organic materials.

Within the six particle categories, Zn concentration was the least variable (Table 9). Zinc concentrations were the greatest in the mineral and biological particles (O) and the Fe-cemented aggregates (Fe). Sulfur was also consistent in concentration, except for the low concentration in the coarse sand aggregates (A), which had only ~ 50% as much S as the other particle classes. Arsenic, Cd, and Pb contents were highly variable among the six particle categories.

2.5 Discussion

2.5.1 Black Rock Slough Study Site

The Black Rock Slough study site is a wetland environment that is subjected to seasonal water table fluctuations. Figure 4 illustrates the CDA River rise to its highest average height around April and decreases to its lowest average height between August and October. Similarly, the water table height measured at the sampling point wells follows the change in river height. This evidence supports the controlling nature of the CDA River in regards to the groundwater table heights in the Black Rock Slough study area. It is during the early year when water rises to inundate the soil pores near the surface, reducing the amount of atmospheric oxygen present, and promoting reducing conditions. At the end of summer or beginning of the fall, as the water table height decreases, redox potential remains high. Acquiring additional measurements may indicate that redox potential decreases further with time before increasing. The lowering redox potential occurring with water table decrease may be attributed to saturation of soil pores in the vadose zone and the inability of atmospheric oxygen to penetrate to that soil depth.

The deposition of oxidized Fe and Mn on soil particles, primarily in the form of poorly – crystallized oxides occurs. X-ray diffraction analysis of soils showed that the only crystalline Fe oxide mineral present was lepidocrocite. Lepidocrocite forms as a result of slow oxidation of Fe^{2+} and often in mildly acidic (pH 4 – 5) environments. The presence of other crystalline Fe or Mn oxides was not detected. Results of the X-ray diffraction analysis are in Appendix D.

2.5.2 Soils Containing Fe and Mn Concentrations and Depletions

Redoximorphic processes in the wetland soils results in transport and precipitation/dissolution processes that create mottled soil colors and heterogeneous distribution of trace metals in the weathered mine-waste impacted soils. Metal concentrations varied between the Fe and Mn-enriched or depleted regions. Arsenic, Pb and Zn concentrations between the Fe and Mn-enriched and depleted areas were different.

Iron and manganese oxides have preferential adsorption sites for many metals. This is evidenced by the difference in Pb concentrations between the Fe-enriched and depleted soil samples. Lead is found to be approximately twice the concentration in the Fe-enriched soil as the Fe-depleted soil. In redox concentrations Fe is approximately 102,000 mg/kg, and 35,000 mg/kg in the depleted zones.

The presence of Fe and Mn concentrations and depletions indicate the translocation and consolidation of Fe and Mn from an initially homogeneous environment. The concentration of Fe and Mn within the soil of the Black Rock Slough sampling transect suggests a possible development route for Fe and Fe/Mn-rich aggregated redoximorphic features. Lindbo et al. (2000) investigated nodule formation in a loess soil containing a fragipan. They suggested that Fe and Mn migrate towards the center of the particle during redox conditions resulting in higher Fe and Mn concentrations at the center of the particle. D'Amore et al. (2004) hypothesized that development of nodules occurs as a result of Fe and Mn precipitation in small pores associated with fine soil particle size. The continued growth of these nodules results in the incorporation of matrix

soil grains as Fe and Mn further precipitate. In both the Lindbo et al. (2000) and D'Amore et al. (2004) studies, translocation of Fe and Mn from the bulk soil occurred, as indicated by the presence of depletions having low soil chroma values.

Movement of Fe as Fe^{2+} occurs either through diffusion or as the result of moving water (Vepraskas and Guertal 1992). As Fe is reduced from Fe^{3+} to Fe^{2+} , water movement resulting from transpiration of the plants draws the soluble Fe towards the soil surface. Atmospheric oxygen present in the Black Rock Slough soil oxidizes and promotes precipitation of Fe forming an abrupt region of Fe accumulation at a depth of 9 cm at site A (Table 2). Conversely, soil water at the water table surface and below is most likely devoid of enough oxygen to allow for any visually noticeable oxidation and precipitation of the Fe^{2+} .

2.5.3 Fe and Fe/Mn-Cemented Redoximorphic Features

2.5.3.1 Feature Development

Aggregated Fe and Fe/Mn-rich redoximorphic features can include both nodules and concretions; however the two features are not the same.

Schoeneberger et al. (2002) describes concretions as features with a visible presence of concentric layers around a point or plane, while nodules are cemented bodies that can be removed from the soil by hand. Both types of cemented aggregates have been observed in the Black Rock Slough soils.

Lindbo et al. (2000) collected nodules and intact soil samples from an eroded loess soil and proposed a formation process for the nodules. They

suggested that soil particles become coated with precipitated Fe and Mn during changing redox conditions and form roughly-angled nodules. After a period of time under reducing conditions the exterior of the nodule is dissolved and the Fe and Mn migrate towards the center of the particle forming a particle highly concentrated in Fe and Mn. Manceau et al. (2003) investigated nodules collected from an area near the Lindbo et al. (2000) site. The nodules were analyzed using synchrotron-based X-ray fluorescence, and Manceau et al. (2003) described a variable correlation between Fe and Mn in several nodules. In two nodules examined the exterior was enriched in Fe and depleted in Mn. In a third nodule the Fe-Mn correlation was 0.69 with distinct regions of non-overlapping Fe and Mn.

Aggregated redoximorphic particles collected in this study were composed of both nodules and concretions, and nodules appeared to comprise the majority of particles. However, some Fe/Mn-cemented aggregates collected in this study had visual evidence of varied Fe and Mn precipitation with distinct color variations, while other particles, e.g. Fe aggregates, were for the most part monochromatic red or gray.

D'Amore et al. (2004) found that nodule development in an Oregon wetland occurred in a silty textured soil. The particle sizes of soil found near the Black Rock Slough transect tended to be dominated by fine sands and silts (silt loam textures). The small pore sizes may provide a uniform initial point of accumulation. Once accumulation of Fe and Mn occurs, the smaller pores are connected through successive Fe and Mn accumulations to form a more-uniform cemented feature. However, the soil pore sizes may not provide the uniformity

and connectivity that promote the development of concretions. D'Amore et al. (2004) described finding concretion development from a silty clay soil in the same area. Soils at the Black Rock Slough study site contain a range of clay, from 8 to 18%. The presence of a smaller percentage of clay may explain the infrequent occurrence of concretions.

During the period of lowest redox potential measured the water table is at its lowest measured point. Dissolved Fe and Mn would be drawn towards the soil surface as a effect of the continued evapotranspiration until oxidative conditions resulted in re-precipitation of the two metals. Data suggest this depth is within 0 - 15 cm of the soil surface. In the region of decreased redox potential Fe and Mn would coprecipitate on existing nodules, concretions, or in soil pores.

The coarse-sand aggregates and Fe/Mn-cemented aggregates appear to have parallel development paths as the interiors of both have similar coloration and metal concentrations (Fe/Mn ratio of 1.3). Visually, the two categories differ only by the presence of sand grains present in the surface of the coarse-sand aggregates. The main body of both features is dark brown to black. The two features have similar average concentrations of P (1,250 mg/kg and 1,370 mg/kg) and Cd (43.9 mg/kg and 38.2 mg/kg). Average Mn concentrations in both categories are an order of magnitude higher than the bulk soils, and other redoximorphic features. The coarse sand aggregates and Fe/Mn-cemented aggregates have the highest average Pb concentration (16,800 mg/kg and 26,800 mg/kg respectively).

The root-channel linings and Fe-cemented aggregates had similar Fe concentrations, 138,000 mg/kg and 114,000 mg/kg respectively, As

concentrations, 182 mg/kg and 148 mg/kg respectively, and Pb concentrations, 9,240 mg/kg and 9,710 mg/kg respectively. Visually, the root-channel linings and Fe-cemented aggregates had similar coloring and appeared to only differ in shape. These similarities suggest that the two categories undergo similar formation processes.

The reported sizes of nodules and concretions vary. Cornu et al. (2005) examined nodules 1 mm to 20 mm in size, White and Dixon (1996) selected nodules sized 0.60 mm to 4 mm to analyze, and Schwertmann and Dixon (1976) investigated nodules ranging from 0.2 mm to > 2mm. The size of nodules or concretions in a soil is likely dependant on the redox potential of the soil and time of development. White and Dixon (1996) hypothesized that time and varying reduction potentials would promote Fe and Mn precipitation on or dissolution from the nodule surface. Decrease of soil solution redox potential over a period of time would reduce the nodule size through dissolution of coprecipitated Fe and Mn. This hypothesis may explain the smaller aggregated redoximorphic particle sizes found at Black Rock Slough.

The size of the nodules may also be attributed to the relatively recent influx of mine tailings over the last century and change in the hydrological nature of the CDA River. Riverine mine waste deposition from the late 1800s to 1968 increased Fe and Mn in the soil and provided essential components for the development of nodules and concretions. The Post Falls Dam water management in the spring and summer months result in artificially higher Coeur d'Alene Lake levels, which cause an increase in CDA River levels. The CDA River level increases water table levels in Black Rock Slough as soils warm and

microbial activity intensifies resulting in reducing wetland conditions. The artificial level management may have altered the saturation times of the CDA River Valley floodplain soils during summer months. Both the construction of the Post Falls Dam and mining inputs are relatively recent events; however, the time required to develop cemented Fe and Mn concentrations varies to a large extent on the soil and environmental conditions it experiences. Iron and Mn concentrations and depletions in redox affected soils have been shown to develop quickly (Vepraskas 2001); however, studies examining the development time for cemented redoximorphic aggregates minimal. The small size of the nodules in the CDA Basin soils are likely the results of the recent deposition of Fe and Mn-rich sediments combined with the groundwater fluctuations, which are controlled seasonally and by CDA Lake management.

2.5.3.2 Feature Location

Iron and Fe/Mn-cemented redoximorphic features occur in the soil where water table fringe fluctuations occur. Rhoton et al. (1993) described the location for maximum nodule development to be at the approximate surface of a seasonally perched water table. Water table levels reached high levels at approximately 30 cm (Point A) to 0 cm (Point D), however the vadose fringe extends above measured well depths. Consequently, the majority of Fe/Mn-cemented aggregates counted were located in the 0 – 15 cm depth. Fe/Mn-cemented aggregates decreased in number with depth. Sample point B had the greatest percent of Fe and Fe/Mn-cemented aggregates, where the maximum recorded water table was approximately 20 cm from the soil surface. The fewer

cemented aggregates counted from sample point D suggest longer periods of time with reducing conditions. Sample point A had cemented aggregates counts between those of points B and C, which suggests cycling of reducing and oxidizing conditions resulting from the zone of saturation above the measured water table depth.

The Fe/Mn-cemented aggregates category was found most commonly in the upper 15 cm of the soil; the depth most dramatically influenced by seasonal wetting and drying. The high percentage of Fe/Mn-cemented aggregates found in the upper 15 cm likely develop as a result of increased microbial activity, presence of mobile species of metals, and cyclical saturation and drying. Soluble Fe and Mn present in the soil water may remain as reduced species as lower Eh values result from microbial populations vigorously responding to warmer soil temperatures, outpacing atmospheric oxygen replenishment (Lynn and Austin 1998). Rising soil temperatures also increase plant growth, which boost evapotranspiration rates, drawing soil water with soluble Fe and Mn towards the surface. Oxygen is more likely present in the upper portion of the soil and may result in the increased oxidation of Fe and Mn.

The Fe/Mn-cemented aggregates are less abundant with depth. This can be attributed to a reduced presence of atmospheric oxygen. These Fe/Mn redoximorphic features were the only category to have a noticeable difference by depth. There was not an appreciable difference in Fe/Mn aggregate particles percentage between the three sampling sites.

The number of root channel linings counted from sampling area A was evenly spread between the three sampling depths. The roots (Tables 2 – 4) at

sampling points A and B are more concentrated in the A and C1 horizons where Fe and Mn concentrations and depletions tend to be common. The prominent vegetation type around sampling points A and B is Rough Bentgrass (*Agrostis scabra* Wild). The plant is adapted to medium and fine textured soils, has a rooting depth minimum of approximately 30.5 cm, and is thought to endure a minimum pH of 6.0 (USDA 2006a). In the wetter sampling area D, a distinct increase in root channel linings population was evident. The prominent vegetation around sampling points C and D is a mix of Reed Canarygrass (*Phalaris arundinacea* L.), Blister Sedge (*Carex vesicaria* L.), and Rose Spirea (*Spiraea douglasii menziesii* (Hook.) Presl). These species have a deeper minimum rooting depth and can tolerate a minimum soil pH of 4.5 to 5.5 (USDA 2006b; USDA 2006c; USDA 2006d). Many wetland plants, including Reed Canarygrass and Blister Sedge, are known to translocate O₂ to the rhizosphere through aerenchyma, which would promote Fe and Mn oxidation.

The aggregated coarse sand particles were only prominent at the northern sample point A where the population counts increased with depth. This population distribution indicates that reoxidization of Fe and Mn is occurring as the two elements move down through the soil profile. Sampling area A is saturated for less time throughout the year than the other sampling locations. This drier condition allows for the deeper movement and reprecipitation of soluble Fe and Mn in the lower depths. The grains imbedded in the particle surface can be possibly attributed to a greater sand content in the soil resulting from flood water bed load deposition closer to the CDA River. Fewer aggregated coarse sand particles found in the wetter sampling locations B and D may

indicate greater soil silt content or a preference for Fe and Mn to form Fe/Mn aggregates given a potentially increased soluble Fe presence.

The aggregated fine sand particles followed the trend of decreasing population as the sample depth increased, with sampling location D having the greatest concentration of aggregated fine sand particles. Given that sampling location D is the furthest sampling point from the CDA River, sediment deposition would consist of silt or clay-sized particles. The Fe concentration of a fine sand particle was similar to that of the aggregated coarse sand particles; however the Mn concentration is lower by nearly one order of magnitude, resulting in a lack of darker coloration. Seasonal fluctuations in water table depth allow oxidizing conditions that produce an accumulation of Fe oxides that cement finer sand particles to the point that particle fracture from mechanical separation is minimal.

The organic and primary mineral features found during microscope counts were distributed throughout all sampling locations and depths, with the lowest sampling depths having the most abundant particles. The particles are found predominantly in the historically high water table region, and biological activity is probably reduced, allowing decreased organic decomposition and weathering.

The data produced from this study suggest that soil water table height plays an important role in the formation of aggregated redoximorphic features. The change in categorical quantities of aggregated redoximorphic features was noticeable. Future studies conducted in a wetland soil experiencing more variance in water table heights, such that the upper portion of the soil is drier during much of the year, may provide more definitive data as to the effect of water table proximity to aggregated redoximorphic feature development.

2.5.3.3 Aggregated Redoximorphic Features < 1mm

While the 1 – 2 mm sized aggregated redoximorphic features were the only particle size examined due to time and monetary constraints, a sizeable volume of 850 μm – 1 mm and 425 μm - 850 μm sized particles were collected. The smaller sized particles appear to consist of nodules and concretions, similar to the 1 – 2 mm size fractions. Given the silty texture of soil at the Black Rock Slough site, smaller particles may be the majority of aggregated redoximorphic features present (Particle size data in Appendix A, Table A-4).

2.5.3.4 Feature Elemental Composition

Correlation analysis of elements in the redoximorphic features reveals several trends. Figures showing the element concentration comparisons are in Appendix E. Iron is positively correlated to both Zn and As (Figures E-1 and E-2), however is poorly correlated with P, Pb, Mn, and Cd concentrations (Figures E-3, E-4, E-5, and E-6). Root channel linings were outliers in the Fe-Zn correlation. The positive correlation between As and Fe has been documented in soils and sediments, and is due to the preferential adsorption of As to Fe oxides (Adriano 2001; Kabata-Pendias and Pendias 2001; Papassiopi et al. 2003). Hansel et al. (2002) described the dominant control of Fe on As in Fe(III) plaques on wetland plants. This finding is supported by the highest concentrations of As in cemented root channel linings (Figure 19). Decreased zinc in the Fe-cemented root channel aggregates is likely caused by plant rhizosphere processes, in which the plant absorb the Zn creating a local depletion, or releases exudates that mobilize the

Zn out of the rhizosphere.

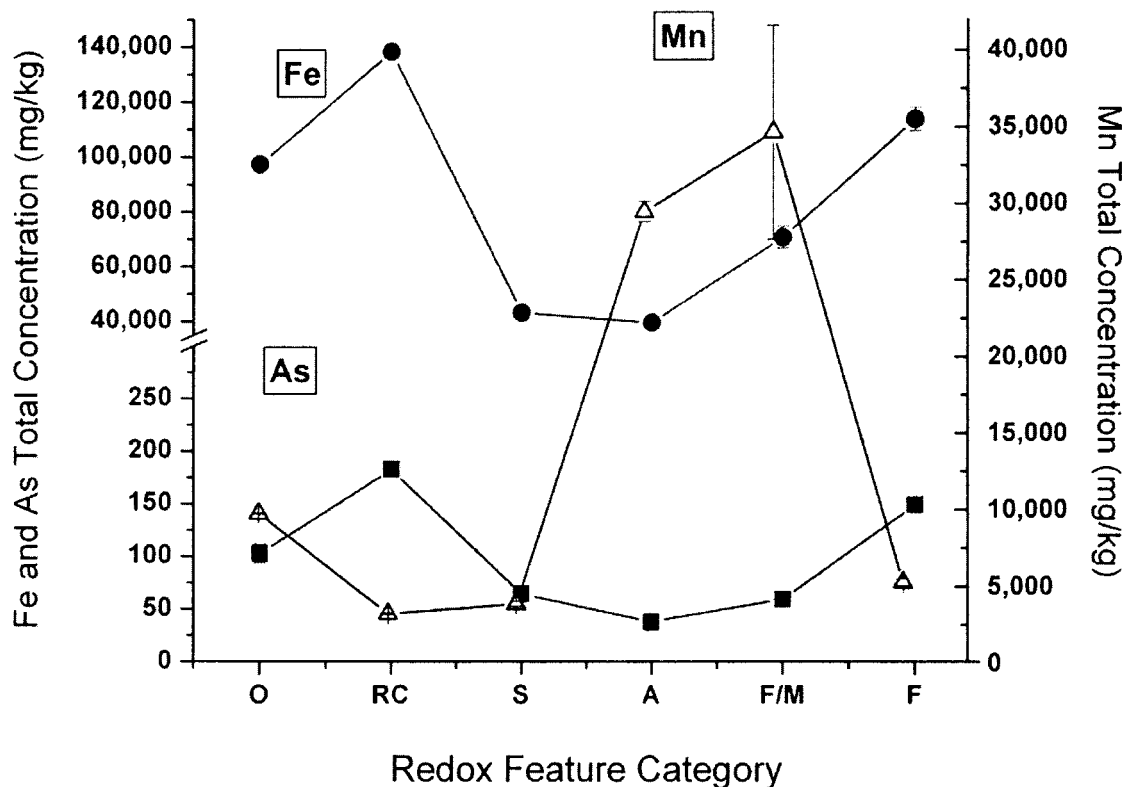


Figure 19. Arsenic, Mn, and Fe concentrations in 1 – 2 mm sized aggregated redoximorphic features. S is fine sand aggregates, A is coarse sand aggregates, F/M is Fe/Mn-cemented aggregates, O are biological particles or primary minerals, F is Fe-cemented aggregates, and RC is cemented root channel linings. Error bars represent standard deviation of element averages. Error bars may be obscured by markers.

Manganese concentrations were positively correlated with Pb

concentrations in the redoximorphic particles (Figures 20 and E-7). The Fe/Mn-cemented aggregates and coarse sand aggregates had the highest average concentration of Pb and Mn.. Manganese concentration was not correlated to Cd, Zn, P, and As (Figures E-8, E-9, E-10). Manganese and Cd are only poorly correlated; however, the biological and non-weathered mineral category (O) is clearly an outlier (Figure E-11).

Sulfur concentrations in the particles were not correlated to P, Mn, Fe, As, Cd, and Pb (Figures E-12, E-13, E-14, E-15, E-16, and E-17). Sulfur concentrations were positively correlated to Zn (Figure E-18). Sulfur concentrations varied between 604 mg/kg and 1,280 mg/kg, the coarse sand aggregate category, was the lowest S concentration particle category.

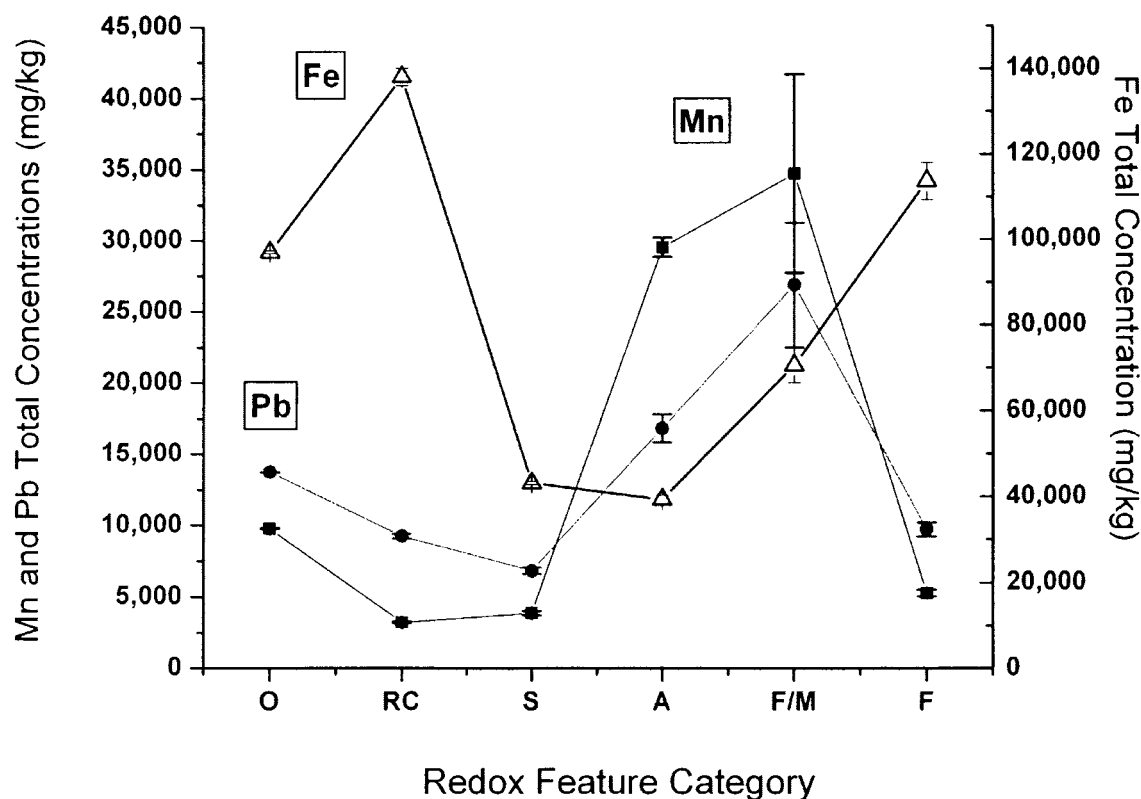


Figure 20. Manganese, Pb, and Fe concentrations in 1 – 2 mm sized aggregated redoximorphic features. S is fine sand aggregates, A is coarse sand aggregates, F/M is Fe/Mn-cemented aggregates, O are biological particles or primary minerals, F is Fe-cemented aggregates, and RC is cemented root channel linings. Error bars represent standard deviation of element averages. Error bars may be obscured by markers.

2.5.3.5 Iron and Manganese Enrichment

Redoximorphic features appear to be created by the precipitation of Fe and Mn on particle surfaces and within soil pores. Redox conditions within the soil control the precipitation and dissolution of Fe and Mn so a ratio of Fe to Mn may suggest similar development paths amongst Fe/Mn-cemented aggregates. Coarse sand aggregates (A) and Fe/Mn-cemented aggregates (F/M) have similar physical features and element concentrations. The noticeable physical differences are the coarse sand aggregate's sand grains imbedded in the surface of a dark brown to dark black mass and its frequent spherical shape. Both types of particles have high average Pb concentrations an order of magnitude higher than the other categories (Figure 21). Manganese concentrations were approximately 6 times higher than other categories. Both the coarse sand aggregates and the Fe/Mn-cemented aggregates have similar Cd concentrations (Figure 22). The Fe-Mn ratios for these particles are 1.3 (A) and 2.0 (F/M) (Figure 23).

Fe-cemented aggregates (F) and cemented root channel linings (RC) also appear similar both physically and chemically. The features often were the same color and had a smooth to undulating surface roughness. Both root channel linings and Fe-cemented aggregates had Fe concentrations nearly twice the concentration of the Fe/Mn-cemented aggregates. These features had As concentrations twice that of the other categories and had similar Cd and Pb concentrations. The Fe-Mn ratios for these two categories are 21.5 (F) and 42.8 (RC) (Figure 23).

Given the physical and chemical concentration similarities of the two groups of Fe/Mn-cemented aggregates including Fe-Mn ratios, it appears that these categories may have undergone similar developmental conditions.

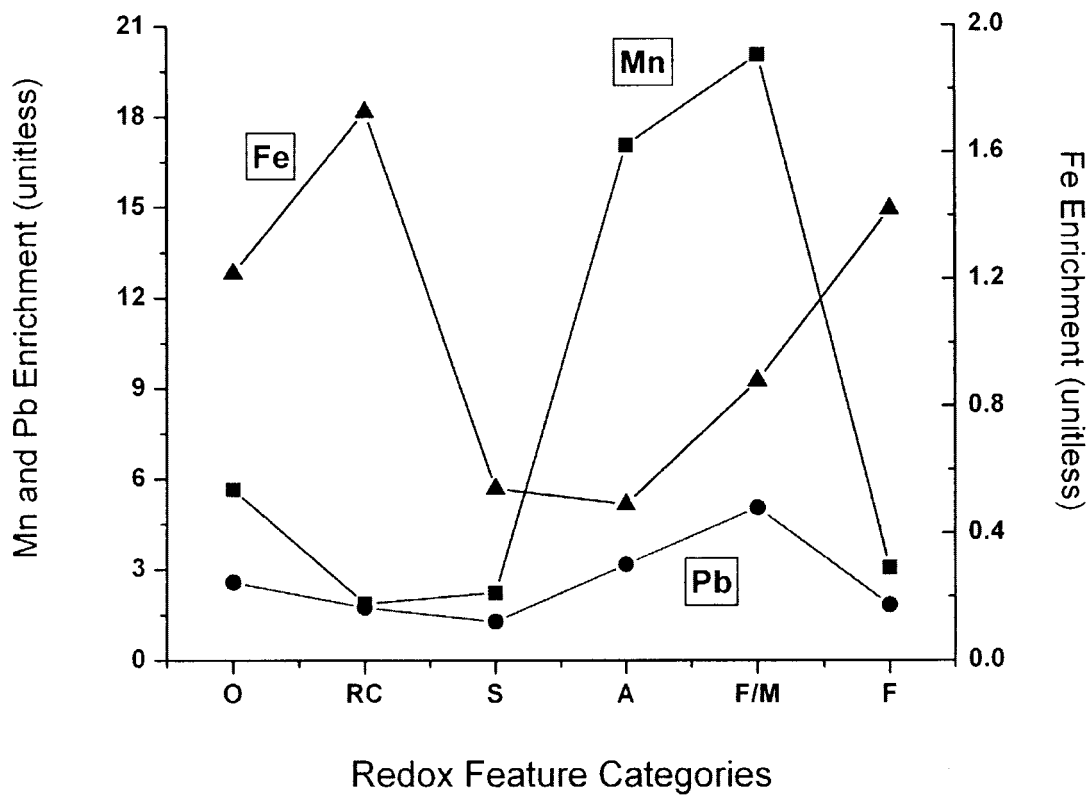


Figure 21. Manganese, Fe, and Pb enrichment in aggregated redoximorphic categories. Aggregated redoximorphic features are listed by category where O is biological or primary mineral particles, RC is cemented root-channel linings, S is fine sand aggregates, Ag is coarse sand aggregates, F/M are Fe/Mn aggregates, and F are Fe aggregates.

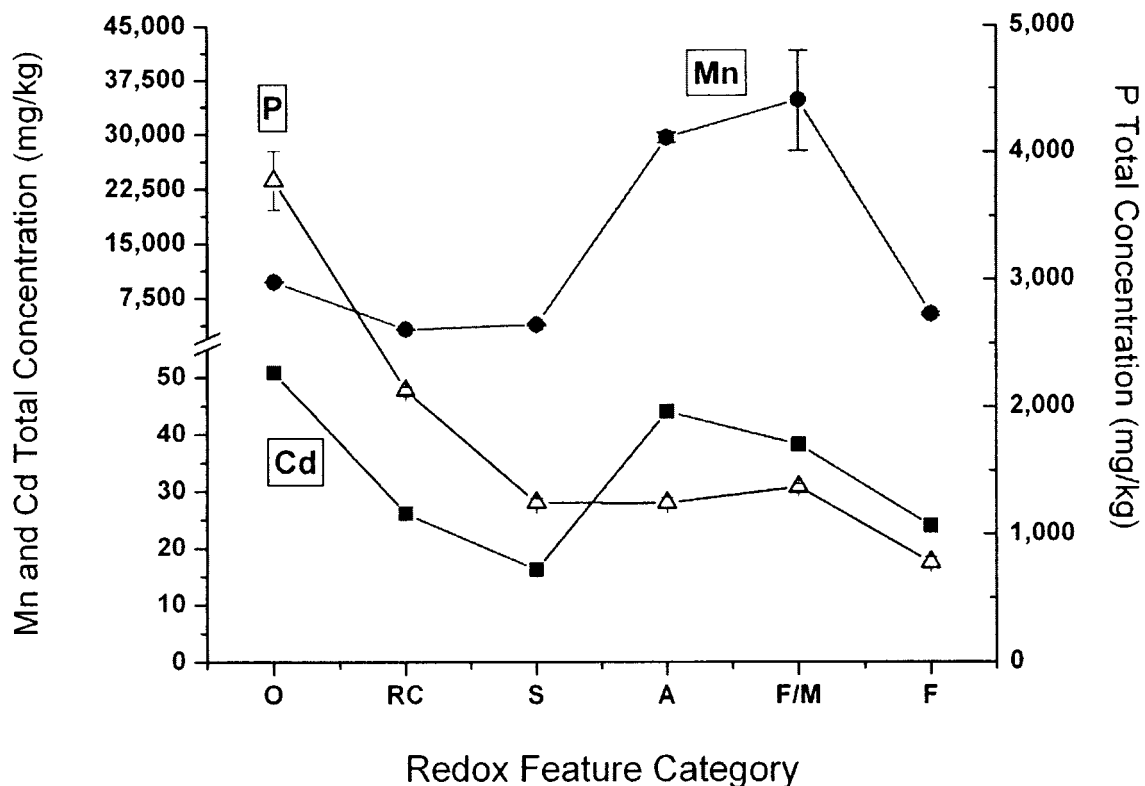


Figure 22. Manganese, P, and Cd concentrations in aggregated redoximorphic features. Aggregated redoximorphic features are listed by category where O is biological or primary mineral particles, RC is cemented root-channel linings, S is fine sand aggregates, Ag is coarse sand aggregates, F/M are Fe/Mn aggregates, and F are Fe aggregates. Error bars represent standard deviation of element averages. Error bars may be obscured by markers

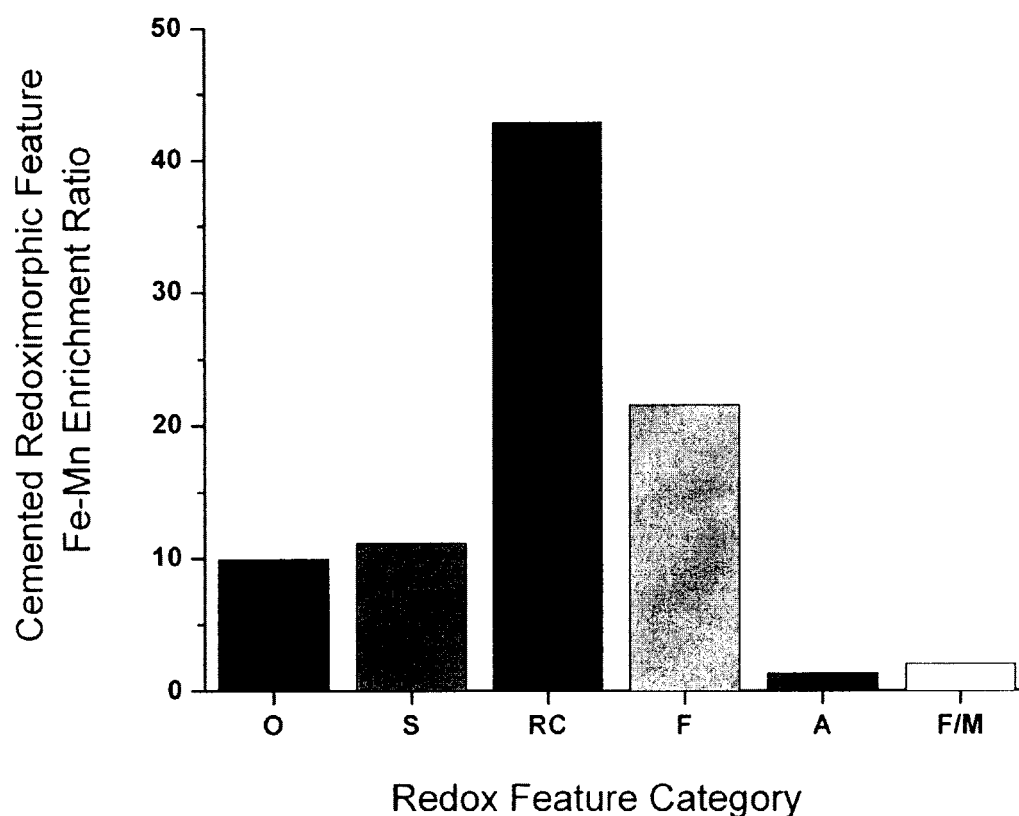


Figure 23. Iron and manganese concentration ratios for six categories of Fe/Mn-cemented aggregates collected at points A, B, and D along the Black Rock Slough sampling transect.

2.6 Conclusions

There exists within the mine-waste contaminated soils of Black Rock Slough several chemically and physically distinct redoximorphic features. Concentrations of trace metals increase as the scale of the feature is reduced.

Lead is enriched in Fe-enriched soil, while Fe-depleted soil has lower Pb concentrations than that of average bulk soil. Aggregated redoximorphic features had increased concentrations of trace metals when compared to Fe and Mn concentrations and bulk soil. Data suggest that Fe-enriched concentrations may provide the initial point of development for aggregated redoximorphic features.

Iron/Mn-rich cemented aggregates, Fe-cemented aggregates, and aggregated fine-sand particles populations decreased with depth. Cemented root channel linings increased with depth and were more prominent at sites with water table levels closer to the soil surface.

Aggregated redoximorphic feature sizes were predominantly less than 2 mm. However, a substantial amount of sub-millimeter redoximorphic features were collected. The reduction potential experienced in the Black Rock Slough study site may limit precipitation of Fe or Mn oxides onto the feature surface and restrict the overall size of the feature.

Chapter 3: Summary

Biogeochemical reactions in the wetland soils in the Coeur d'Alene River Basin create redoximorphic features such as iron oxide enriched and depleted regions that have centimeter-scale variability, and Fe and Mn oxide cemented aggregates that are sand size and smaller particles. Within the resulting distinct mineralogical features, the concentration of potentially-toxic elements is variable, with concentration differences between the contaminant enriched and depleted features of nearly an order of magnitude. The research presented in this thesis describes the physical characteristics, element concentration, and distribution of the redoximorphic features within the mine-waste contaminated wetland at Black Rock Slough. While the information in this thesis provides important characterization of the wetland and contaminant features, to better understand the mechanisms responsible for their formation and contaminant sequestration more research on the mineralogy and molecular speciation of the contaminants is needed.

Continuous monitoring of redox cycling within the Black Rock Slough through in-place redox potential monitoring systems would allow for more complete information from which to assess how redox potential impacts feature development. Within approximately 80 meters of the Black Rock Slough sampling transect there is a change in cemented aggregated redoximorphic feature population. Redox potential within the areas of feature development could be continuously monitored now that the population densities are known.

Visual inspection, description, and categorization of the cemented aggregated redoximorphic features provided data related to redox potential changes and metal movement within the soil. Acquiring thin sections of the soil at distinct points during the redox potential change would provide samples that can be analyzed using electron microprobe and x-ray diffraction techniques to identify metal speciation and mineral development

Knowledge of metal distribution in mine-waste impacted soils would benefit from measurement of cemented redoximorphic aggregate masses. This would allow for a more accurate illustration of metal distribution within a soil.

Iron and Mn-rich cemented aggregates (F/M) and Fe-rich cemented aggregates (F) comprise the majority of categories found, while coarse sand aggregates (A) and cemented root channel linings (RC) are less common. Expanding redoximorphic feature collection to other regions of the Black Rock Slough and other wetlands that have been affected by mine-waste contamination may provide a more comprehensive picture of the redoximorphic feature categories described here.

The use of wetland areas bordering the CDA River by waterfowl and human beings emphasizes the need to understand the bioavailability of metals within the soil. The redoximorphic features have provided evidence of sequestration of potentially toxic metals released from weathered mine-wastes. However, the ability to retain these metals under varying wetland soil conditions is poorly understood. Conducting experiments that mimic the conditions occurring within a wetland soil using cemented redoximorphic features would clarify how the dynamic biogeochemical changes occurring within the wetland will

impact contaminant solubility, and therefore bioavailability and potential for transport. Furthering the pedological knowledge of redoximorphic feature development in wetland soils will allow for remediation efforts to be more focused and fiscally efficient. The understanding of adsorptive capacities of the different redoximorphic feature categories provides a basis for understanding contaminant speciation and cycling in wetland environments that is necessary to properly manage the contaminated sites.

References

- Adriano, D. C. (2001). Trace elements in the terrestrial environment. New York, Springer-Verlag.
- Bender, S. F. (1991). Investigation of the chemical composition and distribution of mining wastes in Killarney Lake, Coeur d'Alene Area, Northern Idaho. Department of Geology. Moscow, University of Idaho: 1-98.
- Bennett, E. H., P. L. Siems, et al. (1989). The Geology and History of the Coeur d'Alene Mining District, Idaho. Guidebook to the Geology of Northern and Western Idaho and Surrounding Area. V. E. Chamberlain, Breckenridge, R. M., Bonnicksen, B. Moscow, ID, Idaho Geological Survey. **28**: 137-156.
- Bidwell, O., D. Gier, et al. (1968). "Ferromagnesian pedotubules on roots of *Bromus inermis* and *Adropogon gerardii*." Intern. Congress Soil Science Trans. **IV**: 683-692.
- Bookstrom, A., S. Box, et al. (2001). Lead-Rich Sediments, Coeur d'Alene River Valley, Idaho: Area, Volume, Tonnage, and Lead Content, U.S. Geological Survey: 1-79.
- Bookstrom, A., S. Box, et al. (2004). Baseline and historic depositional rates and lead concentrations, floodplain sediments, Lower Coeur d'Alene River, Idaho. Spokane, USGS: 1-118.
- Bookstrom, A., S. Box, et al. (1999). Digital map of surficial geology, wetlands, and deepwater habitats, Coeur d'Alene River Valley, Idaho. Spokane, United States Geological Survey: 1-121.
- Box, S., A. Bookstrom, et al. (2001). Geochemical analyses of soils and sediments, Coeur d'Alene drainage basin, Idaho: Sampling, analytical methods, and results, US Geological Survey: 1-206.
- Cescas, M., E. Tyner, et al. (1970). "Ferromanganiferous Soil Concretions: A scanning electron microscope study of their micropore structures." Soil Science Society of America Proceedings **34**: 641-644.
- Chapman, R. (2000). History of Idaho's Silver Valley: 1878-2000. Kellogg, ID, Chapman Publishing.
- Coeur d'Alene Tribe. (2005, 10/16/2005). "Lake Management Challenges." Retrieved 10/16/2005, 2005, from <http://www.cdatribe-nsn.gov/depts/lake/challenges.asp#03> Dam.
- Coeur d'Alene Tribe (2001). Coeur d'Alene Subbasin Summary (including Coeur d'Alene Lake and all tributaries), Northwest Power Planning Council: 1-104.

- Cornu, S., V. Deschatrettes, et al. (2005). "Trace element accumulation in Mn-Fe-oxide nodules of a planosolic horizon." Geoderma **125**(1-2): 11-24.
- D'Amore, D., S. Stewart, et al. (2004). "Saturation, Reduction, and the Formation of Iron-Manganese Concretions in the Jackson-Frazier Wetland, Oregon." Soil Science Society of America Journal **68**: 1012-1022.
- Dong, D., Y. Li, et al. (2001). "Investigation of Fe, Mn oxides and organic material in surface coatings and Pb, Cd adsorption to surface coatings developed in different natural waters." Microchemical Journal **70**: 25-33.
- EPA (1996). Method 3052 - Microwave Assisted Acid Digestion of Siliceous and Organically Based Matrices.
- EPA. (2003). "Region 10 Superfund: Bunker Hill / Coeur d'Alene Basin - Record of Decision (ROD)." Retrieved 3/21/2004, 2004, from [http://yosemite.epa.gov/R10/CLEANUP.NSF/basin/Record+of+Decision+\(ROD\)](http://yosemite.epa.gov/R10/CLEANUP.NSF/basin/Record+of+Decision+(ROD)).
- EPA. (2006, 4/1/2006). "Bunker Hill Operable Units 1 and 2, SuperFund, US EPA." Retrieved 5/4/2006, 2006, from http://www.epa.gov/superfund/accomp/success/bunker_ou12.htm.
- Gasparatos, D., D. Tarenidis, et al. (2005). "Microscopic structure of soil Fe-Mn nodules: environmental implication." Environmental Chemistry Letters **2**: 175-178.
- Gerulf, M. and D. G. Strawn (2005). Effects of Weathering on Recent Flood Deposits on the South Fork of the Coeur d'Alene River. Environmental Science Program. Moscow, University of Idaho: 1-45.
- Gillerman, V. (2001). Idaho Mining and Geology. Moscow, Idaho Geological Survey: 1 pg.
- Green, C., D. Heil, et al. (2003). "Heavy Metals in the Environment: Solubilization of Manganese and Trace Metals in Soils Affected by Acid Mine Runoff." Journal of Environmental Quality **32**: 1323-1334.
- Hansel, C., S. La Force, et al. (2002). "Spatial and Temporal Association of As and Fe Species on Aquatic Plants Roots." Environmental Science and Technology **36**(9): 1988-94.
- Harriss, R. and A. Troup (1969). "Freshwater ferromanganese concretions: Chemistry and internal structure." Science **166**(3905): 604-606.
- Hickey, M. and J. Kittrick (1984). "Chemical Partitioning of Cadmium, Copper, Nickel and Zinc in Soils and Sediments Containing High Levels of Heavy Metals." Journal of Environmental Quality **13**(3): 372-76.

- Hlawatsch, S., Garbe-Schonberg C., et al. (2002). "Trace metal fluxes to ferromanganese nodules from the western Baltic Sea as a record for long-term environmental changes." Chemical Geology **182**(2-4): 697-709.
- Hoffman, M. (1995). Characterization of heavy metal contamination in two lateral lakes of the lower Coeur d'Alene River Valley, Northern Idaho. Geology. Moscow, University of Idaho: 1-76.
- Hogue, C. (2004). "Metallic Refinement." Chemical and Engineering News **82**: 23-24.
- Horowitz, A., K. Elrick, et al. (1995). "A summary of the effects of mining and related activities on the sediment-trace element geochemistry of Lake Coeur d'Alene, Idaho, USA." Journal of Geochemical Exploration **52**: 135-144.
- Jackson, M. L. (1956). Soil Chemical Analysis - Advanced Course. Madison, University of Wisconsin.
- Kabata-Pendias, A. and H. Pendias (2001). Trace elements in soils and plants. Boca Raton, Fla., CRC Press.
- Lehmann, K. (2006). Email concerning data readings from USGS River Gauge #12413500 near Cataldo, ID. P. Hickey. Moscow.
- Lindbo, D., F. Rhoton, et al. (2000). "Fragipan degradation and nodule formation in glossic fragiudalfs of the Lower Mississippi River Valley." Soil Science Society of America Journal **64**(5): 1713-1722.
- Lindsay, W. (1979). Chemical Equilibria in Soils. New York, John Wiley and Sons.
- Long, K. R. (1998). Production and Disposal of Mill Tailings in the Coeur d'Alene Mining Region, Shoshone County, Idaho; Preliminary Estimates. Tucson, U.S. Geological Survey: 1-14.
- Lynn, W. and W. Austin (1998). "Oxymorphic Manganese (Iron) segregations in a wet soil catena in the Willamette Valley, Oregon." Soil Science Society of America Special Publication **54**: 209-226.
- Manceau, A., N. Tamura, et al. (2003). "Molecular-scale speciation of Zn and Ni in soil ferromanganese nodules from loess soils of the Mississippi Basin." Environmental Science and Technology **37**(1): 75-80.
- Marcus, M., A. Manceau, et al. (2004). "Mn, Fe, Zn and As speciation in a fast-growing ferromanganese marine nodule." Geochimica et Cosmochimica Acta **68**(14): 3125-3136.

- McDaniel, P. A. (2004a, 7/1/2005). "Sample Preparation " Retrieved 1/22/2004, 2004.
- McDaniel, P. A., Falen, A. (2004 a). "Soil sample preparation." Retrieved 2/16/2004, 2004, from <http://soils.ag.uidaho.edu/pedology/Analyses/Psdprep.pdf>.
- McKenzie, R. (1977). Manganese Oxides and Hydroxides. Minerals in Soil Environments. J. B. Dixon, Weed, S.B. Madison, Soil Science Society of America: 181-193.
- Neaman, A., F. Mouele, et al. (2004). "Improved methods for selective dissolution of Mn oxides: applications for studying trace element associations." Applied Geochemistry **19**: 973-79.
- NIST. (2003). "Certificate of Analysis: Standard Reference Material 2711." Retrieved 9/23, 2003, from https://srmors.nist.gov/certificates/view_cert2gif.cfm?certificate=2711.
- NOAA. (2006, 1/12/2006). "Advanced Hydrological Prediction Service: Coeur d'Alene at Cataldo." Retrieved 1/13/2006, 2006, from <http://ahps2.wrh.noaa.gov/ahps2/hydrograph.php?wfo=otx&gage=ctli1&view=1,1,1,1,1,1>.
- O'Reilly, S. and M. Hochella (2003). "Lead sorption efficiencies of natural and synthetic Mn and Fe-oxides." Geochimica et Cosmochimica Acta **67**(23): 4471-87.
- Palumbo, B., A. Bellanca, et al. (2001). "Trace metal partitioning in Fe-Mn nodules from Sicilian soils, Italy." Chemical Geology **173**(4): 257-269.
- Papassiopi, N., K. Vaxevanidou, et al. (2003). "Investigating the use of iron reducing bacteria for the removal of arsenic from contaminated soils." Water, Air, and Soil Pollution: Focus **3**(3): 81-90.
- Phillippe, W., R. Blevins, et al. (1971). "Distribution of concretions from selected soils of the inner bluegrass region of Kentucky " Soil Science Society of America Proceedings **36**: 171-173.
- Plouffe, A., G. Hall, et al. (2001). "Leaching of loosely bound elements during wet grain size separation with sodium hexametaphosphate: implications for selective extraction analysis." Geochemistry: Exploration, Environment, Analysis **1**(2): 157-162.
- Rabbi, F. (1994). Trace element geochemistry of bottom sediments and waters from the lateral lakes of Coeur d'Alene River, Kootenai County, North Idaho. Geology. Moscow, University of Idaho: 1-256.

- Rhoton, F., J. Bigham, et al. (1993). "Properties of iron-manganese nodules from a sequence of eroded fragipan soils." Soil Science Society of America Journal **57**: 1386-1392.
- Ross, S. and C. Savage (1967). Idaho Earth Science: Geology, Fossils, Climate, Water, and Soils. Moscow, Idaho Bureau of Mines and Geology.
- Schoeneberger, P., D. Wysocki, et al. (2002). Field Book for Describing and Sampling Soils, Version 2.0. Lincoln, Agriculture Dept., Natural Resources Conservation Service, National Soil Survey Center.
- Schwertmann, U. and D. Fanning (1976). "Iron-manganese concretions in hydrosequences of soils in Loess in Bavaria." Soil Science Society of America Journal **40**: 731-738.
- Schwertmann, U. and R. Taylor (1977). Iron Oxides. Minerals in Soil Environments. J. B. Dixon, Weed, S.B. Madison, Soil Science Society of America: 145-180.
- Soil Survey Division Staff (1993). Soil Survey Manual. Washington, U.S. Government Printing Office.
- Somera, R. (1967). Iron and Manganese distribution and seasonal oxidation changes in soils of the Willamette drainage sequence. Department of Soils. Corvallis, Oregon State University. **Master of Science**: 1-78.
- Stoops, G. (2003). Guidelines for analysis and description of soil and regolith thin sections. Madison, Soil Science Society of America, Inc.
- Thoral, S., J. Rose, et al. (2005). "XAS study of iron and arsenic speciation during Fe(II) oxidation in the presence of As(III)." Environmental Science and Technology **39**(24): 9478-9485.
- Tiner, R. (1999). Wetland Indicators: A guide to wetland identification, delineation, classification, and mapping. Boca Raton, Lewis Publishers.
- U.S. Fish and Wildlife Service. (2005). "Chapter 1: Introduction." Retrieved 10/21/2005, 2005.
- U.S. Fish and Wildlife Service. (2005). "Chapter 6: Wildlife Resources." Retrieved 10/16/2005, 2005, from http://www.fws.gov/pacific/ecoservices/envicon/nrda/pdf/h-Chapter_6_Wildlife_Resources.pdf.
- U.S. Fish and Wildlife Service. (2005a). "Chapter 9: Riparian Resources." Retrieved 10/22/2005, 2005, from http://www.fws.gov/pacific/ecoservices/envicon/nrda/pdf/k-Chapter_9_Riparian_Resources.pdf.

- U.S. Geological Survey. (2005). "Station 12413500 Coeur d'Alene River NR Cataldo, Idaho " Retrieved 10/15/2005, 2005, from <http://pubs.usgs.gov/wri/wri934076/stations/12413500.html>; http://waterdata.usgs.gov/id/nwis/uv/?site_no=12413500.
- USDA. (2006a). "Conservation Plant Characteristics for: *Agrostis scabra* Willd. (rough bentgrass) AGSC5." Retrieved 1/12/2006, 2006, from http://plants.nrcs.usda.gov/cgi_bin/plant_attribute.cgi?symbol=AGSC5.
- USDA. (2006b). "Conservation Plant Characteristics for: *Phalaris arundinacea* L. (reed canarygrass) PHAR3 Auburn." Retrieved 1/12/2006, 2006, from http://plants.nrcs.usda.gov/cgi_bin/topics.cgi?earl=plant_attribute.cgi&symbol=PHAR3.
- USDA. (2006c). "Conservation Plant Characteristics for: *Carex vesicaria* L. (blister sedge) CAVE6." Retrieved 1/12/2006, 2006, from http://plants.nrcs.usda.gov/cgi_bin/topics.cgi?earl=plant_attribute.cgi&symbol=CAVE6.
- USDA. (2006d). "Conservation Plant Characteristics for: *Spiraea douglasii* Hook. (rose spirea) SPDO Bashaw." Retrieved 1/13/2006, 2006, from http://plants.nrcs.usda.gov/cgi_bin/topics.cgi?earl=plant_attribute.cgi&symbol=SPDO.
- USFWS. (1988). "1988 National List of Plant Species that Occur in Wetlands." Retrieved 1/20/2006, 2006, from <http://www.fws.gov/nwi/bha/list88.html>.
- USGS. (2005). "Station 12413500 Coeur d'Alene River NR Cataldo, Idaho " Retrieved 10/15/2005, 2005, from <http://pubs.usgs.gov/wri/wri934076/stations/12413500.html>; http://waterdata.usgs.gov/id/nwis/uv/?site_no=12413500.
- Vepraskas, M. J. (1992). Redoximorphic features for identifying aquic conditions. Raleigh, North Carolina Agricultural Research Service: 1-33.
- Vepraskas, M. J. (2001). Morphological Features of Seasonally Reduced Soils. Wetland Soils: Genesis, Hydrology, Landscapes, and Classification. S. P. Faulkner, Vepraskas, M. J., Boca Raton, Lewis Publishing: 163-182.
- Vepraskas, M. J. and S. Faulkner (2001). Redox Chemistry of Hydric Soils. Wetland Soils: Genesis, Hydrology, Landscapes, and Classification. J. L. Richardson, Vepraskas, M. J. Boca Raton, Lewis Publishers: 85-106.
- Vepraskas, M. J. and W. Guertal (1992). Morphological indicators of soil wetness. Eighth International Soil Correlation Meeting, Lincoln, NE, U.S.D.A., Soil Cons. Serv., Nat. Soil Surv. Center.

- Weisel, C. (1981). Soil Survey of Kootenai County Area, Idaho. Washington, D.C., U.S. Government Printing Office.
- White, G. and J. Dixon (1996). "Iron and manganese distribution in nodules from a young Texas Vertisol." Soil Science Society of America Journal **60**: 1254-1262.
- Wilma, D. (2003). "Forest fires in Idaho and Montana burn three million acres of timber and kill 85 people on August 20 and 21, 1910." Retrieved 3/27, 2006, from http://www.historylink.org/essays/output.cfm?file_id=5488.

Appendix A: Cemented Redoximorphic Feature Data Tables

Table A-1. pH values of soils sampled from designated sampling points (A, B, C, and D) along the transect at Black Rock Slough. Sample identification is in the format X-Y-Z where X is the sample point, Y is the replicate number, and Z is the depth (a= 0-15 cm, b= 15-30 cm, c=30-45 cm). Not enough soil was present to accurately measure pH in sample a-2-a.

Sample Name	pH	Sample Name	pH
a-1-a	4.96	c-1-a	4.95
a-1-b	4.60	c-1-b	4.83
a-1-c	4.55	c-1-c	4.40
a-2-a	***	c-2-a	4.75
a-2-b	4.78	c-2-b	4.71
a-2-c	4.40	c-2-c	4.79
a-3-a	4.47	c-3-a	4.55
a-3-b	4.57	c-3-b	4.67
a-3-c	3.93	c-3-c	4.81
b-1-a	5.10	d-1-a	4.71
b-1-b	5.14	d-1-b	4.72
b-1-c	5.02	d-1-c	4.62
b-2-a	4.97	d-2-a	4.11
b-2-b	4.85	d-2-b	4.94
b-2-c	4.82	d-2-c	4.72
b-3-a	4.84	d-3-a	4.87
b-3-b	4.66	d-3-b	4.72
b-3-c	4.41	d-3-c	4.96

Table A-2. Matrix soil bulk density determined from 3 intact soil cores sampled in triplicate from 3 depths along the Black Rock Slough sampling transect. Sample designation is written in the format X-#-XX where X is the sample site, # is the replicate number, and XX is the (0 – 15 cm, 15 – 30 cm, and 30 – 45 cm).

Sample	Sample Mass Wet (g)	Sample Mass Dry (g)	Water Mass (Difference) (g)	Pan Tare (g)	Tube Tare (g)	Total Mass (g)	Tube Diameter (cm)	Core Length (cm)	Volume of Core (cm ³)	Bulk Density (g/cm ³)
a-1-a	590	409	181	120	48.5	361	4.80	15.3	277	1.30
a-1-b	646	477	170	124	48.5	428	4.80	15.3	277	1.50
a-1-c	630	450	180	123	48.5	402	4.80	15.3	277	1.50
a-2-a	493	366	128	120	0.00	366	4.80	13.0	235	1.60
a-2-b	620	458	163	123	48.5	409	4.80	15.3	277	1.50
a-2-c	606	427	179	100	48.5	379	4.80	15.3	277	1.40
a-3-a	553	385	168	109	48.0	337	4.80	15.3	277	1.20
a-3-b	532	418	114	122	0.00	418	4.80	14.0	253	1.60
a-3-c	500	401	99.5	120	0.00	401	4.80	13.0	235	1.70
Average	574	421	153	118	32.3	388.7	4.80	14.6	265	1.50
StDev	57.0	35.8	31.2	8.1	24.2	30.0	0.00	1.00	18.5	0.20
b-1-a	491	371	120	115	0.00	371	4.80	13.0	235	1.60
b-1-b	469	345	124	96.5	0.00	345	4.80	13.0	235	1.50
b-1-c	541	410	131	127	0.00	410	4.80	15.3	277	1.50
b-2-a	487	363	124	120	0.00	363	4.80	15.3	277	1.30
b-2-b	434	338	95.5	109	0.00	338	4.80	15.3	277	1.20
b-2-c	465	359	106	122	0.00	359	4.80	15.3	277	1.30
b-3-a	588	388	200	121	48.5	339	4.80	15.3	277	1.20
b-3-b	497	392	106	114	0.00	392	4.80	13.0	235	1.70
b-3-c	504	388	116	116	0.00	388	4.80	13.0	235	1.60
Average	497	373	126	115	5.40	367	4.80	14.3	258	1.40
StDev	45.0	23.6	30.4	8.80	16.2	25.3	0.00	1.20	21.9	0.20

Table A-3. Matrix soil bulk density determined from 3 intact soil cores sampled in triplicate from 3 depths along the Black Rock Slough sampling transect. Sample designation is written in the format X-#-XX where X is the sample site, # is the replicate number, and XX is the (0 – 15 cm, 15 – 30 cm, and 30 – 45 cm).

Sample	Sample Mass Wet (g)	Sample Mass Dry (g)	Water Mass (Difference) (g)	Pan Tare (g)	Tube Tare (g)	Total Mass (g)	Tube Diameter (cm)	Core Length (cm)	Volume of Core (cm ³)	Bulk Density (g/cm ³)
c-1-a	564	362.5	201.0	122.0	48.5	314.0	4.8	15.3	276.9	1.1
c-1-b	626	451.0	175.0	110.0	48.5	402.5	4.8	15.3	276.9	1.5
c-1-c	629	445.0	184.0	121.5	48.5	396.5	4.8	15.3	276.9	1.4
c-2-a	398	282.0	115.5	110.0	0.0	282.0	4.8	12.0	217.1	1.3
c-2-b	536	351.5	184.0	120.0	48.5	303.0	4.8	15.3	276.9	1.1
c-2-c	491	385.5	105.5	114.0	0.0	385.5	4.8	12.0	217.1	1.8
c-3-a	492	348.5	143.0	124.5	0.0	348.5	4.8	14.0	253.3	1.4
c-3-b	509	390.0	119.0	100.5	0.0	390.0	4.8	14.0	253.3	1.5
c-3-c	576	435.0	140.5	127.5	0.0	435.0	4.8	15.3	276.9	1.6
Average	535	383.4	151.9	116.7	21.6	361.9	4.8	14.3	258.4	1.4
StDev	73.3	54.8	35.0	8.7	25.6	52.3	0.0	1.4	25.4	0.2
d-1-a	487	345	142	121	0.00	345	4.80	14.0	253	1.40
d-1-b	581	445	134	124	0.00	445	4.80	15.3	277	1.60
d-1-c	559	425	134	120	0.00	425	4.80	15.3	277	1.50
d-2-a	525	368	157	111	0.00	368	4.80	15.3	277	1.30
d-2-b	534	413	122	103	0.00	413	4.80	14.0	253	1.60
d-2-c	457	358	98.5	123	0.00	358	4.80	11.0	199	1.80
d-3-a	525	373	153	122	0.00	373	4.80	15.0	271	1.40
d-3-b	533	410	124	120	0.00	410	4.80	14.0	253	1.60
d-3-c	533	396	137	121	0.00	396	4.80	14.0	253	1.60
Average	526	392	134	118	0.00	392	4.80	14.2	257	1.50
StDev	36.4	33.6	17.6	6.9	0.00	33.6	0.00	1.40	24.5	0.20

Table A-4. Particle size data from soil collected from a pit approximately 15 meters from Black Rock Slough sampling transect at point B. A sample was collected in layer of dark colored soil, burnt wood, and charcoal that was found in all pits at approximately 35 cm. Soil 8 was a composited sample collected from the top 20 cm of soil approximately 30 meters east of point B along the Black Rock Slough sampling transect.

Sample Depth	Very Coarse Sand	Coarse Sand	Medium Sand	Fine Sand	Very Fine Sand	Sand Total	Silt Total	Clay Total	Mass Recovery
0 - 10	0.0%	0.0%	0.0%	0.6%	9.0%	9.6%	78.7%	11.7%	-2.0%
10 - 30	0.1%	2.2%	0.2%	7.4%	26.9%	36.8%	54.8%	8.4%	0.6%
30 - 60	0.0%	0.0%	0.3%	17.6%	27.6%	45.5%	46.8%	7.7%	-1.6%
60 - 80	0.0%	0.1%	0.2%	0.6%	26.6%	27.4%	59.9%	12.7%	-25.8%
~ 35 cm	0.0%	0.0%	0.0%	3.8%	23.8%	27.7%	54.0%	18.3%	-26.1%
Soil 8	0.1%	0.0%	0.1%	6.8%	19.7%	26.6%	63.6%	9.8%	-0.8%

Note: Very coarse and coarse sand size fractions comprised a minor percentage of the soil despite the presence of 1 – 2 mm and 1 mm – 850 μ m sized particles. It is suspected that the use of a bleach solution to remove organic matter, heat, and use of mild sonic dispersion fragmented the cemented aggregated particles into smaller sand-sized particles.

Table A-5. Samples analyzed for selected elements based on visual soil coloration. Red colored soils indicate an environment that support the presence of Fe and/or Mn oxides, while grey soil color is indicative of reducing conditions that may deplete Fe and/or Mn from soil particle surfaces. The labeling, #-(R, G)-(A, B) represents the plot number sampled, enrichment (R) or depletion (G) of Fe and/or Mn, and 0-10 cm depth (A) or 10 – 20 cm depth (B). Standard reference material (SRM – 2711) results are referenced to samples analyzed by superscript lettering. SRM – 2711 elemental composition concentrations listed per NIST (2003)

Sample	As (mg/kg)	Cd (mg/kg)	Fe (mg/kg)	Mn (mg/kg)	P (mg/kg)	Pb (mg/kg)	S (mg/kg)	Zn (mg/kg)
1-R-A (1) ^c	154	9.47	111,000	3,410	730	9,190	979	2,700
1-R-A (2) ^c	145	8.24	108,000	2,240	711	8,470	897	2,540
1-R-A (3) ^c	133	10.1	109,000	1,900	730	8,070	896	2,560
2-R-A (1) ^a	146	4.03	102,000	1,400	678	8,600	746	2,120
2-R-A (2) ^a	149	4.13	100,000	1,370	700	8,930	749	2,130
2-R-A (3) ^a	159	4.47	102,000	1,640	684	8,950	754	2,150
3-R-A (1) ^a	160	14.7	107,000	4,490	537	6,560	736	3,020
3-R-A (2) ^a	165	16.0	106,000	4,870	524	6,800	725	2,960
4-R-A (1) ^a	162	10.6	88,200	3,010	686	686	535	1,720
4-R-A (2) ^a	167	11.0	95,800	3,730	749	749	564	1,850
1-R-B (1) ^d	119	6.30	99,000	1,690	663	9,500	832	2,130
1-R-B (2) ^d	101	6.72	102,000	1,500	686	9,690	886	2,220
1-R-B (3) ^d	95.1	6.82	99,400	1,640	654	9,400	844	2,170
2-R-B (1) ^a	119	1.18	108,000	1,190	558	9,900	827	1,690
2-R-B (2) ^a	124	2.05	112,000	1,300	557	10,300	901	1,910
2-R-B (3) ^a	108	2.50	105,000	1,340	579	9,920	824	1,710
3-R-B (1) ^a	103	3.98	98,700	2,630	472	8,500	934	1,960
3-R-B (2) ^a	102	5.12	103,000	2,870	465	8,760	972	2,050
4-R-B (1) ^b	149	4.67	99,600	1,510	673	7,410	645	1,660
4-R-B (2) ^b	146	5.21	99,200	1,510	706	7,500	628	1,690
1-G-A (1) ^b	120	10.2	49,100	1,170	907	5,760	573	2,060
1-G-A (2) ^b	120	10.3	48,300	807	932	5,590	573	2,050
2-G-A (1) ^a	48.7	2.91	39,400	954	1,020	5,180	437	1,360
2-G-A (2) ^a	44.5	2.74	37,600	727	1,040	5,090	438	1,360
3-G-A (1) ^d	67.4	9.92	37,500	1,840	844	4,470	411	1,670
3-G-A (2) ^d	47.8	9.08	39,700	2,250	834	5,000	668	1,580
3-G-A (3) ^d	49.7	8.67	37,100	1,540	795	4,290	372	1,520
4-G-A (1) ^b	105	7.69	39,500	3,160	1,010	4,990	301	1,090

Table A-5. Continued from previous page

Sample	As (mg/kg)	Cd (mg/kg)	Fe (mg/kg)	Mn (mg/kg)	P (mg/kg)	Pb (mg/kg)	S (mg/kg)	Zn (mg/kg)
4-G-A (2) ^p	112	7.13	42,400	2,620	1,000	4,620	285	1,080
1-G-B (1) ^p	93.0	13.2	27,000	3,180	492	2,430	168	1,120
1-G-B (2) ^p	79.3	11.5	27,100	2,960	486	2,140	178	1,060
1-G-B (3) ^p	82.4	10.7	26,600	2,830	512	2,370	159	1,050
2-G-B (1) ^p	70.2	2.19	29,500	484	737	3,420	208	774
2-G-B (2) ^p	96.5	1.86	30,900	1,940	799	4,840	217	829
3-G-B (1) ^p	79.7	3.69	30,800	1,110	252	3,880	206	822
3-G-B (2) ^p	77.5	3.16	31,400	842	522	3,490	230	801
4-G-B (1) ^a	27.2	4.48	27,900	1,600	803	2,960	240	562
4-G-B (2) ^a	33.0	3.27	28,000	732	811	2,550	210	575
SRM - 2711 ^a	110	33.9	27,000	648	866	1,170	387	363
SRM - 2711 ^a	114	33.7	27,500	617	861	1,172	825	381
SRM - 2711 ^a	106	33.3	26,000	633	847	1,170	467	374
SRM - 2711 ^a	111	33.1	26,600	633	868	1,170	411	360
SRM - 2711 ^b	167	34.1	26,500	625	788	1,180	326	381
SRM - 2711 ^b	183	34.0	26,900	612	764	1,120	329	378
SRM - 2711 ^b	169	34.3	26,600	633	778	1,150	376	373
SRM - 2711 ^b	156	32.6	24,800	586	718	1,080	368	344
SRM - 2711 ^c	105	34.0	28,200	640	811	1,130	380	375
SRM - 2711 ^c	98.8	32.1	27,900	632	790	1,120	390	384
SRM - 2711 ^d	119	41.6	27,200	685	917	1220	431	402
SRM - 2711 ^d	112	39.7	27,300	625	844	1170	510	371
SRM - 2711 ^d	126	42.4	27,000	680	916	1220	442	400

Table A-5. Continued from previous page

Sample	As (mg/kg)	Cd (mg/kg)	Fe (mg/kg)	Mn (mg/kg)	P (mg/kg)	Pb (mg/kg)	S (mg/kg)	Zn (mg/kg)
SRM – 2711 Elemental Composition Concentration	105 ± 8	41.70 ± 0.25	28,900 ± 600	638 ± 28	860 ± 70	1,162 ± 31	420 ± 10	350.4 ± 4.8
SRM – 2711 ^a Recovery %	105% (2.9%)	80.4% (0.8%)	92.6% (2.1%)	99.1% (2.0%)	100% (1.1%)	100% (0.3%)	124% (48.7%)	106% (2.8%)
SRM – 2711 ^b Recovery %	160% (13.0%)	80.5% (2.0%)	90.2% (4.0%)	95.2% (3.1%)	88.0% (4.1%)	97.1% (4.3%)	106% (2.7%)	105% (5.8%)
SRM – 2711 ^c Recovery %	97.0% (4.1%)	79.2% (3.2 %)	97.1% (0.5%)	99.7% (0.8%)	93.1% (1.7%)	97.1% (0.4%)	91.7% (1.7%)	108% (1.8%)
SRM – 2711 ^d Recovery %	113% (6.6%)	98.9% (3.3%)	94.1% (0.7%)	104% (5.2%)	104% (4.8%)	104% (2.3%)	110% (10.1%)	112% (5.0%)
SRM – 2711 ^d	119	41.6	27,200	685	917	1220	431	402
SRM – 2711 ^d	112	39.7	27,300	625	844	1170	510	371
SRM – 2711 ^d	126	42.4	27,000	680	916	1220	442	400
SRM – 2711 Elemental Composition Concentration	105 ± 8	41.70 ± 0.25	28,900 ± 600	638 ± 28	860 ± 70	1,162 ± 31	420 ± 10	350.4 ± 4.8
SRM – 2711 ^a Recovery %	105% (2.9%)	80.4% (0.8%)	92.6% (2.1%)	99.1% (2.0%)	100% (1.1%)	100% (0.3%)	124% (48.7%)	106% (2.8%)
SRM – 2711 ^b Recovery %	160% (13.0%)	80.5% (2.0%)	90.2% (4.0%)	95.2% (3.1%)	88.0% (4.1%)	97.1% (4.3%)	106% (2.7%)	105% (5.8%)
SRM – 2711 ^c Recovery %	97.0% (4.1%)	79.2% (3.2 %)	97.1% (0.5%)	99.7% (0.8%)	93.1% (1.7%)	97.1% (0.4%)	91.7% (1.7%)	108% (1.8%)
SRM – 2711 ^d Recovery %	113% (6.6%)	98.9% (3.3%)	94.1% (0.7%)	104% (5.2%)	104% (4.8%)	104% (2.3%)	110% (10.1%)	112% (5.0%)

Table A-6. Summary of redoximorphic feature by category gathered from sampling location A for three depths. Sample identification is in the format X-Y-Z where X is the sampling point, Y is the replicate number, and Z is the depth (a= 0-15 cm, b= 15-30 cm, c=30-45 cm).

Site, Repetition, Depth	Spot	Total Particles Counted	F/M	% of Total	F	% of Total	S	% of Total	O	% of Total	RC	% of Total	A	% of Total
a-1-a	1	34	21	61.8%	7	20.6%	2	5.9%	2	5.9%	1	2.9%	1	2.9%
a-1-a	2	33	22	66.7%	7	21.2%	1	3.0%	2	6.1%	1	3.0%	0	0.0%
a-1-a	3	38	25	65.8%	10	26.3%	0	0.0%	3	7.9%	0	0.0%	0	0.0%
a-1-a	4	42	22	52.4%	12	28.6%	3	7.1%	4	9.5%	0	0.0%	1	2.4%
a-1-a	5	30	17	56.7%	9	30.0%	3	10.0%	1	3.3%	0	0.0%	0	0.0%
	Sum	177	107	60.5%	45	25.4%	9	5.1%	12	6.8%	2	1.1%	20	1.1%
	Average	35.4	21.4	60.7%	9	25.3%	1.8	5.2%	2.4	6.5%	0.4	1.2%	0.4	1.1%
	StDev	4.7	2.9	6.1%	2.1	4.3%	1.3	3.8%	1.1	2.3%	0.5	1.6%	0.5	1.5%
a-1-b	1	40	15	37.5%	8	20.0%	12	30.0%	2	5.0%	1	2.5%	2	5.0%
a-1-b	2	48	26	54.2%	4	8.3%	10	20.8%	2	4.2%	1	2.1%	5	10.4%
a-1-b	3	43	17	39.5%	12	27.9%	8	18.6%	5	11.6%	0	0.0%	1	2.3%
a-1-b	4	31	13	41.9%	5	16.1%	10	32.3%	2	6.5%	0	0.0%	1	3.2%
a-1-b	5	52	21	40.4%	13	25.0%	13	25.0%	4	7.7%	0	0.0%	1	1.9%
	Sum	214	92	43.0%	42	19.6%	53	24.8%	15	7.0%	2	0.9%	10	4.7%
	Average	42.8	18.4	42.7%	8.4	19.5%	10.6	25.3%	3	7.0%	0.4	0.9%	2	4.6%
	StDev	8	5.2	6.6%	4	7.7%	1.9	5.8%	1.4	2.9%	0.5	1.3%	1.7	3.5%
a-1-c	1	39	10	25.6%	5	12.8%	0	0.0%	7	17.9%	2	5.1%	15	38.5%
a-1-c	2	32	7	21.9%	4	12.5%	0	0.0%	6	18.8%	0	0.0%	15	46.9%
a-1-c	3	40	17	42.5%	4	10.0%	1	2.5%	5	12.5%	1	2.5%	12	30.0%
a-1-c	4	25	9	36.0%	2	8.0%	0	0.0%	8	32.0%	1	4.0%	5	20.0%
	Sum	136	43	31.6%	15	11.0%	1	0.7%	26	19.1%	4	2.9%	47	34.6%
	Average	34	10.75	31.5%	3.75	10.8%	0.25	0.6%	6.5	20.3%	1	2.9%	11.75	33.8%
	StDev	7	4.3	9.5%	1.3	2.3%	0.5	1.3%	1.3	8.3%	0.8	2.2%	4.7	11.5%

Table A-7. Summary of redoximorphic feature by category gathered from sampling location A for three depths. Sample identification is in the format X-Y-Z where X is the sampling point, Y is the replicate number, and Z is the depth (a= 0-15 cm, b= 15-30 cm, c=30-45 cm).

Site, Repetition, Depth	Spot	Total Particles Counted	F/M	% of Total	F	% of Total	S	% of Total	O	% of Total	RC	% of Total	A	% of Total
a-2-a	1	49	26	53.1%	20	40.8%	0	0.0%	1	2.0%	2	4.1%	0	0.0%
a-2-a	2	53	35	66.0%	17	32.1%	0	0.0%	1	1.9%	0	0.0%	0	0.0%
a-2-a	3	47	29	61.7%	14	29.8%	2	4.3%	2	4.3%	0	0.0%	0	0.0%
a-2-a	4	57	32	56.1%	18	31.6%	2	3.5%	4	7.0%	1	1.8%	0	0.0%
a-2-a	5	56	38	67.9%	14	25.0%	1	1.8%	1	1.8%	1	1.8%	1	1.8%
	Sum	262	160	61.1%	83	31.7%	5	1.9%	9	3.4%	4	1.5%	1	0.4%
	Average	52.4	32	61.0%	16.6	31.9%	1	1.9%	1.8	3.4%	0.8	1.5%	0.2	0.4%
	StDev	4.3	4.7	6.3%	2.6	5.7%	1	2.0%	1.3	2.3%	0.8	1.7%	0.4	0.8%
a-2-b	1	39	24	61.5%	4	10.3%	0	0.0%	2	5.1%	0	0.0%	9	23.1%
a-2-b	2	45	23	51.1%	8	17.8%	0	0.0%	5	11.1%	2	4.4%	7	15.6%
a-2-b	3	34	18	52.9%	6	17.6%	0	0.0%	5	14.7%	2	5.9%	3	8.8%
a-2-b	4	58	25	43.1%	8	13.8%	1	1.7%	2	3.4%	0	0.0%	22	37.9%
a-2-b	5	49	21	42.9%	16	32.7%	0	0.0%	1	2.0%	0	0.0%	11	22.4%
	Sum	225	111	49.3%	42	18.7%	1	0.4%	15	6.7%	4	1.8%	52	23.1%
	Average	45	22.2	50.3%	8.4	18.4%	0.2	0.3%	3	7.3%	0.8	2.1%	10.4	21.6%
	StDev	9.2	2.8	7.8%	4.6	8.5%	0.4	0.8%	1.9	5.4%	1.1	2.9%	7.1	10.8%
a-2-c	1	29	5	17.2%	2	6.9%	0	0.0%	1	3.4%	0	0.0%	21	72.4%
a-2-c	2	26	3	11.5%	4	15.4%	0	0.0%	2	7.7%	0	0.0%	17	65.4%
a-2-c	3	15	2	13.3%	5	33.3%	0	0.0%	1	6.7%	0	0.0%	7	46.7%
	Sum	70	10	14.3%	11	15.7%	0	0.0%	4	5.7%	0	0.0%	45	64.3%
	Average	23.33	3.33	14.0%	3.67	18.5%	0	0.0%	1.33	5.9%	0	0.0%	15	61.5%
	StDev	7.4	1.5	2.9%	1.5	13.5%	0	0.0%	0.6	2.2%	0	0.0%	7.2	13.3%

Table A-8. Summary of redoximorphic feature by category gathered from sampling location A for three depths. Sample identification is in the format X-Y-Z where X is the sampling point, Y is the replicate number, and Z is the depth (a= 0-15 cm, b= 15-30 cm, c=30-45 cm).

Site, Repetition, Depth	Spot	Total Particles Counted	F/M	% of Total	F	% of Total	S	% of Total	O	% of Total	RC	% of Total	A	% of Total
a-3-a	1	29	19	65.5%	10	34.5%	0	0.0%	0	0.0%	0	0.0%	0	0.0%
a-3-a	2	67	47	70.1%	15	22.4%	0	0.0%	3	4.5%	1	1.5%	1	1.5%
a-3-a	3	64	41	64.1%	17	26.6%	1	1.6%	4	6.3%	1	1.6%	0	0.0%
a-3-a	4	67	41	61.2%	22	32.8%	0	0.0%	2	3.0%	1	1.5%	1	1.5%
a-3-a	5	51	38	74.5%	10	19.6%	2	3.9%	1	2.0%	0	0.0%	0	0.0%
	Sum	278	186	66.9%	74	26.6%	3	1.1%	10	3.6%	3	1.1%	2	0.7%
	Average	55.6	37.2	67.1%	14.8	27.2%	0.6	1.1%	2	3.1%	0.6	0.9%	0.5	0.6%
	StDev	16.3	10.7	5.3%	5.1	6.4%	0.9	1.7%	1.6	2.4%	0.5	0.8%	0.6	0.8%
a-3-b	1	55	24	43.6%	15	27.3%	1	1.8%	9	16.4%	1	1.8%	5	9.1%
a-3-b	2	58	33	56.9%	13	22.4%	0	0.0%	6	10.3%	0	0.0%	6	10.3%
a-3-b	3	43	24	55.8%	5	11.6%	3	7.0%	7	16.3%	0	0.0%	4	9.3%
a-3-b	4	21	13	61.9%	2	9.5%	2	9.5%	2	9.5%	2	9.5%	0	0.0%
	Sum	177	94	53.1%	35	19.8%	6	3.4%	24	13.6%	3	1.7%	15	8.5%
	Average	44.25	23.5	54.6%	8.75	17.7%	1.5	4.6%	6	13.1%	0.75	2.8%	5	7.2%
	StDev	16.8	8.2	7.8%	6.2	8.5%	1.3	4.4%	2.9	3.7%	1	4.5%	1	4.8%
a-3-c	1	32	15	46.9%	0	0.0%	0	0.0%	12	37.5%	1	3.1%	4	12.5%
a-3-c	2	40	14	35.0%	4	10.0%	0	0.0%	17	42.5%	0	0.0%	5	12.5%
	Sum	72	29	40.3%	4	5.6%	0	0.0%	29	40.3%	1	1.4%	9	12.5%
	Average	36	14.5	40.9%	2	5.0%	0	0.0%	14.5	40.0%	0.5	1.6%	4.5	12.5%
	StDev	5.7	0.7	8.4%	2.8	7.1%	0	0.0%	3.5	3.5%	0.7	2.2%	0.7	0.0%

Table A-9. Summary of redoximorphic feature by category gathered from sampling location B for three depths. Sample identification is in the format X-Y-Z where X is the sampling point, Y is the replicate number, and Z is the depth (a= 0-15 cm, b= 15-30 cm, c=30-45 cm).

Site, Repetition, Depth	Spot	Total Particles Counted	F/M	% of Total	F	% of Total	S	% of Total	O	% of Total	RC	% of Total	A	% of Total
b-1-a	1	46	23	50.0%	20	43.5%	2	4.3%	1	2.2%	0	0.0%	0	0.0%
b-1-a	2	58	26	44.8%	26	44.8%	0	0.0%	5	8.6%	1	1.7%	0	0.0%
b-1-a	3	58	31	53.4%	24	41.4%	2	3.4%	1	1.7%	0	0.0%	0	0.0%
b-1-a	4	50	30	60.0%	20	40.0%	0	0.0%	0	0.0%	0	0.0%	0	0.0%
b-1-a	5	40	21	52.5%	16	40.0%	2	5.0%	1	2.5%	0	0.0%	0	0.0%
	Sum	252	131	52.0%	106	42.1%	6	2.4%	8	3.2%	1	0.4%	0	0.0%
	Average	50.4	26.2	52.2%	21.2	41.9%	1.2	2.6%	1.6	3.0%	0.2	0.3%	0	0.0%
	StDev	7.8	4.3	5.5%	3.9	2.2%	1.1	2.4%	1.9	3.3%	0.4	0.8%	0	0.0%
b-1-b	1	53	32	60.4%	14	26.4%	1	1.9%	5	9.4%	0	0.0%	1	1.9%
b-1-b	2	52	37	71.2%	11	21.2%	0	0.0%	4	7.7%	0	0.0%	0	0.0%
b-1-b	3	44	30	68.2%	9	20.5%	0	0.0%	3	6.8%	0	0.0%	2	4.5%
b-1-b	4	52	38	73.1%	10	19.2%	0	0.0%	2	3.8%	0	0.0%	2	3.8%
b-1-b	5	49	40	81.6%	7	14.3%	0	0.0%	1	2.0%	1	2.0%	0	0.0%
	Sum	250	177	70.8%	51	20.4%	1	0.4%	15	6.0%	1	0.4%	5	2.0%
	Average	50	35.4	70.9%	10.2	20.3%	0.2	0.4%	3	6.0%	0.2	0.4%	1	2.1%
	StDev	3.7	4.2	7.7%	2.6	4.3%	0.4	0.8%	1.6	3.0%	0.4	0.9%	1	2.1%
b-1-c	1	24	10	41.7%	1	4.2%	1	4.2%	12	50.0%	0	0.0%	0	0.0%

Table A-10. Summary of redoximorphic feature by category gathered from sampling location B for three depths. Sample identification is in the format X-Y-Z where X is the sampling point, Y is the replicate number, and Z is the depth (a= 0-15 cm, b= 15-30 cm, c=30-45 cm).

Site, Repetition, Depth	Spot	Total Particles Counted	F/M	% of Total	F	% of Total	S	% of Total	O	% of Total	RC	% of Total	A	% of Total
b-2-a	1	46	23	50.0%	21	45.7%	0	0.0%	2	4.3%	0	0.0%	0	0.0%
b-2-a	2	71	58	81.7%	10	14.1%	0	0.0%	1	1.4%	1	1.4%	1	1.4%
b-2-a	3	82	70	85.4%	9	11.0%	0	0.0%	3	3.7%	0	0.0%	0	0.0%
b-2-a	4	104	74	71.2%	27	26.0%	0	0.0%	0	0.0%	2	1.9%	1	1.0%
b-2-a	5	75	58	77.3%	14	18.7%	0	0.0%	1	1.3%	1	1.3%	1	1.3%
	Sum	378	283	74.9%	81	21.4%	0	0.0%	7	1.9%	4	1.1%	3	0.8%
	Average	75.6	56.6	73.1%	16.2	23.1%	0	0.0%	1.4	2.1%	0.8	0.9%	0.6	0.7%
	StDev	20.9	20.1	14.0%	7.7	13.8%	0	0.0%	1.1	1.8%	0.8	0.9%	0.5	0.7%
b-2-b	1	33	15	45.5%	2	6.1%	0	0.0%	14	42.4%	0	0.0%	2	6.1%
b-2-b	2	36	13	36.1%	4	11.1%	1	2.8%	17	47.2%	0	0.0%	1	2.8%
b-2-b	3	8	1	12.5%	0	0.0%	0	0.0%	7	87.5%	0	0.0%	0	0.0%
	Sum	77	29	37.7%	6	7.8%	1	1.3%	38	49.4%	0	0.0%	3	3.9%
	Average	25.7	9.7	0.3	2.0	0.1	0.3	0.0	12.7	0.6	0.0	0.0	1.0	0.0
	StDev	15.4	7.6	17.0%	2	5.6%	0.6	1.6%	5.1	24.8%	0	0.0%	1	3.0%
b-2-c	1	41	23	56.1%	2	4.9%	0	0.0%	16	39.0%	0	0.0%	0	0.0%
b-2-c	2	44	15	34.1%	1	2.3%	0	0.0%	28	63.6%	0	0.0%	0	0.0%
b-2-c	3	40	15	37.5%	0	0.0%	0	0.0%	25	62.5%	0	0.0%	0	0.0%
b-2-c	4	34	8	23.5%	0	0.0%	0	0.0%	26	76.5%	0	0.0%	0	0.0%
	Sum	159	61	38.4%	3	1.9%	0	0.0%	95	59.7%	0	0.0%	0	0.0%
	Average	39.8	15.3	0.4	0.8	0.0	0.0	0.0	23.8	0.6	0.0	0.0	0.0	0.0
	StDev	4.2	6.1	13.6%	1	2.3%	0	0.0%	5.3	15.6%	0	0.0%	0	0.0%

Table A-11. Summary of redoximorphic feature by category gathered from sampling location B for three depths. Sample identification is in the format X-Y-Z where X is the sampling point, Y is the replicate number, and Z is the depth (a= 0-15 cm, b= 15-30 cm, c=30-45 cm).

Site, Repetition, Depth	Spot	Total Particles Counted	F/M	% of Total	F	% of Total	S	% of Total	O	% of Total	RC	% of Total	A	% of Total
b-3-a	1	50	23	46.0%	20	40.0%	1	2.0%	3	6.0%	2	4.0%	1	2.0%
b-3-a	2	71	49	69.0%	20	28.2%	0	0.0%	1	1.4%	1	1.4%	0	0.0%
b-3-a	3	72	50	69.4%	12	16.7%	1	1.4%	7	9.7%	2	2.8%	0	0.0%
b-3-a	4	62	45	72.6%	10	16.1%	1	1.6%	5	8.1%	1	1.6%	0	0.0%
b-3-a	5	52	36	69.2%	13	25.0%	0	0.0%	3	5.8%	0	0.0%	0	0.0%
	Sum	307	203	66.1%	75	126.0%	3	5.0%	19	31.0%	6	9.8%	1	2.0%
	Average	61.4	40.6	65.3%	15	25.2%	0.6	1.0%	3.8	6.2%	1.2	2.0%	0.2	0.4%
	StDev	10.3	11.3	10.9%	4.7	9.8%	0.5	0.9%	2.3	3.1%	0.8	1.5%	0.4	0.9%
b-3-b	1	43	39	90.7%	0	0.0%	0	0.0%	2	4.7%	2	4.7%	0	0.0%
b-3-b	2	38	37	97.4%	0	0.0%	0	0.0%	1	2.6%	0	0.0%	0	0.0%
b-3-b	3	51	41	80.4%	4	7.8%	1	2.0%	5	9.8%	0	0.0%	0	0.0%
b-3-b	4	50	39	78.0%	5	10.0%	0	0.0%	6	12.0%	0	0.0%	0	0.0%
b-3-b	5	38	31	81.6%	2	5.3%	0	0.0%	5	13.2%	0	0.0%	0	0.0%
	Sum	220	187	85.0%	11	23.1%	1	2.0%	19	42.2%	2	4.7%	0	0.0%
	Average	44	37.4	85.6%	2.2	4.6%	0.2	0.4%	3.8	8.4%	0.4	0.9%	0	0.0%
	StDev	6.3	3.8	8.1%	2.3	4.5%	0.4	0.9%	2.2	4.6%	0.9	2.1%	0	0.0%
b-3-c	1	40	8	20.0%	0	0.0%	0	0.0%	32	80.0%	0	0.0%	0	0.0%
b-3-c	2	45	10	22.2%	0	0.0%	0	0.0%	35	77.8%	0	0.0%	0	0.0%
b-3-c	3	34	11	32.4%	0	0.0%	0	0.0%	23	67.6%	0	0.0%	0	0.0%
b-3-c	4	39	10	25.6%	0	0.0%	0	0.0%	39	100.0%	0	0.0%	0	0.0%
b-3-c	5	31	5	16.1%	0	0.0%	0	0.0%	26	83.9%	0	0.0%	0	0.0%
	Sum	189	44	23.3%	0	0.0%	0	0.0%	155	409.3%	0	0.0%	0	0.0%
	Average	37.8	8.8	23.3%	0	0.0%	0	0.0%	31	81.9%	0	0.0%	0	0.0%
	StDev	5.4	2.4	6.1%	0	0.0%	0	0.0%	6.5	11.8%	0	0.0%	0	0.0%

Table A-12. Summary of redoximorphic feature by category gathered from sampling location D for three depths. Sample identification is in the format X-Y-Z where X is the sampling point, Y is the replicate number, and Z is the depth (a= 0-15 cm, b= 15-30 cm, c=30-45 cm).

Site, Repetition, Depth	Spot	Total Particles Counted	F/M	% of Total	F	% of Total	S	% of Total	O	% of Total	RC	% of Total	A	% of Total
d-1-a	1	47	9	19.1%	25	53.2%	3	6.4%	9	19.1%	1	2.1%	0	0.0%
d-1-a	2	47	11	23.4%	26	55.3%	3	6.4%	6	12.8%	1	2.1%	0	0.0%
d-1-a	3	47	15	31.9%	25	53.2%	3	6.4%	3	6.4%	1	2.1%	0	0.0%
d-1-a	4	54	12	22.2%	31	57.4%	7	13.0%	4	7.4%	0	0.0%	0	0.0%
d-1-a	5	49	12	24.5%	27	55.1%	5	10.2%	3	6.1%	2	4.1%	0	0.0%
	Sum	244	59	24.2%	134	54.9%	21	8.6%	25	10.2%	5	2.0%	0	0.0%
	Average	48.8	11.8	24.2%	26.8	54.8%	4.2	8.5%	5	10.4%	1	2.1%	0	0.0%
	StDev	3	2.2	4.7%	2.5	1.8%	1.8	3.0%	2.5	5.6%	0.7	1.4%	0	0.0%
d-1-b	1	27	10	37.0%	13	48.1%	3	11.1%	0	0.0%	1	3.7%	0	0.0%
d-1-b	2	54	17	31.5%	21	38.9%	7	13.0%	4	7.4%	5	9.3%	0	0.0%
d-1-b	3	42	7	16.7%	28	66.7%	0	0.0%	6	14.3%	1	2.4%	0	0.0%
d-1-b	4	32	10	31.3%	16	50.0%	1	3.1%	4	12.5%	1	3.1%	0	0.0%
	Sum	155	44	28.4%	78	50.3%	11	7.1%	14	9.0%	8	5.2%	0	0.0%
	Average	38.8	11	29.1%	19.5	50.9%	2.8	6.8%	3.5	8.5%	2	4.6%	0	0.0%
	StDev	11.9	4.2	8.7%	6.6	11.6%	3.1	6.2%	2.5	6.4%	2	3.1%	0	0.0%
d-1-c	1	23	1	4.3%	3	13.0%	0	0.0%	12	52.2%	7	30.4%	0	0.0%
d-1-c	2	26	1	3.8%	6	23.1%	0	0.0%	5	19.2%	14	53.8%	0	0.0%
	Sum	49	2	4.1%	9	18.4%	0	0.0%	17	34.7%	21	42.9%	0	0.0%
	Average	24.5	1	4.1%	4.5	18.1%	0	0.0%	8.5	35.7%	10.5	42.1%	0	0.0%
	StDev	2.1	0	0.4%	2.1	7.1%	0	0.0%	4.9	23.3%	4.9	16.6%	0	0.0%

Table A-13. Summary of redoximorphic feature by category gathered from sampling location D for three depths. Sample identification is in the format X-Y-Z where X is the sampling point, Y is the replicate number, and Z is the depth (a= 0-15 cm, b= 15-30 cm, c=30-45 cm).

Site, Repetition, Depth	Spot	Total Particles Counted	F/M	% of Total	F	% of Total	S	% of Total	O	% of Total	RC	% of Total	A	% of Total
d-2-a	1	33	21	63.6%	9	27.3%	1	3.0%	2	6.1%	0	0.0%	0	0.0%
d-2-a	2	42	28	66.7%	11	26.2%	0	0.0%	3	7.1%	0	0.0%	0	0.0%
d-2-a	3	49	33	67.3%	14	28.6%	1	2.0%	1	2.0%	0	0.0%	0	0.0%
d-2-a	4	37	24	64.9%	11	29.7%	2	5.4%	0	0.0%	0	0.0%	0	0.0%
d-2-a	5	24	13	54.2%	8	33.3%	3	12.5%	0	0.0%	0	0.0%	0	0.0%
	Sum	185	119	64.3%	53	28.6%	7	3.8%	6	3.2%	0	0.0%	0	0.0%
	Average	37	23.8	63.3%	10.6	29.0%	1.4	4.6%	1.2	3.0%	0	0.0%	0	0.0%
	StDev	9.4	7.5	5.3%	2.3	2.8%	1.1	4.8%	1.3	3.4%	0	0.0%	0	0.0%
d-2-b	1	27	17	63.0%	7	25.9%	0	0.0%	3	11.1%	0	0.0%	0	0.0%
d-2-b	2	34	25	73.5%	6	17.6%	0	0.0%	3	8.8%	0	0.0%	0	0.0%
d-2-b	3	41	30	73.2%	8	19.5%	1	2.4%	2	4.9%	0	0.0%	0	0.0%
d-2-b	4	22	14	63.6%	7	31.8%	0	0.0%	0	0.0%	0	0.0%	1	4.5%
d-2-b	5	27	4	14.8%	22	81.5%	0	0.0%	1	3.7%	0	0.0%	0	0.0%
	Sum	151	90	59.6%	50	33.1%	1	0.7%	9	6.0%	0	0.0%	1	0.7%
	Average	30.2	18	57.6%	10	35.3%	0.2	0.5%	1.8	5.7%	0	0.0%	0.2	0.9%
	StDev	7.4	10.1	24.5%	6.7	26.4%	0.4	1.1%	1.3	4.4%	0	0.0%	0.4	2.0%
d-2-c	1	35	16	45.7%	6	17.1%	11	31.4%	2	5.7%	0	0.0%	0	0.0%
d-2-c	2	29	11	37.9%	11	37.9%	3	10.3%	4	13.8%	0	0.0%	0	0.0%
	Sum	64	27	42.2%	17	26.6%	14	21.9%	6	9.4%	0	0.0%	0	0.0%
	Average	32	13.5	41.8%	8.5	27.5%	7	20.9%	3	9.8%	0	0.0%	0	0.0%
	StDev	4.2	3.5	5.5%	3.5	14.7%	5.7	14.9%	1.4	5.7%	0	0.0%	0	0.0%

Table A-14. Summary of redoximorphic feature by category gathered from sampling location D for three depths. Sample identification is in the format X-Y-Z where X is the sampling point, Y is the replicate number, and Z is the depth (a= 0-15 cm, b= 15-30 cm, c=30-45 cm).

Site, Repetition, Depth	Spot	Total Particles Counted	F/M	% of Total	F	% of Total	S	% of Total	O	% of Total	RC	% of Total	A	% of Total
d-3-a	1	64	25	39.1%	30	46.9%	2	3.1%	7	10.9%	0	0.0%	0	0.0%
d-3-a	2	88	37	42.0%	33	37.5%	11	12.5%	7	8.0%	0	0.0%	0	0.0%
d-3-a	3	64	28	43.8%	22	34.4%	5	7.8%	9	14.1%	0	0.0%	0	0.0%
d-3-a	4	62	32	51.6%	21	33.9%	6	9.7%	3	4.8%	0	0.0%	0	0.0%
d-3-a	5	38	25	65.8%	5	13.2%	1	2.6%	6	15.8%	1	2.6%	0	0.0%
	Sum	316	147	46.5%	111	35.1%	25	7.9%	32	10.1%	1	0.3%	0	0.0%
	Average	63.2	29.4	48.5%	22.2	33.2%	5	7.1%	6.4	10.7%	0.2	0.5%	0	0.0%
	StDev	17.7	5.1	10.7%	10.9	12.3%	3.9	4.2%	2.2	4.4%	0.4	1.2%	0	0.0%
d-3-b	1	34	22	64.7%	7	20.6%	0	0.0%	3	8.8%	2	5.9%	0	0.0%
d-3-b	2	43	25	58.1%	10	23.3%	2	4.7%	5	11.6%	1	2.3%	0	0.0%
d-3-b	3	34	29	85.3%	2	5.9%	0	0.0%	3	8.8%	0	0.0%	0	0.0%
d-3-b	4	41	28	68.3%	7	17.1%	1	2.4%	3	7.3%	2	4.9%	0	0.0%
	Sum	152	104	68.4%	26	17.1%	3	2.0%	14	9.2%	5	3.3%	0	0.0%
	Average	38	26	69.1%	6.5	16.7%	0.8	1.8%	3.5	9.1%	1.3	3.3%	0	0.0%
	StDev	4.7	3.2	11.6%	3.3	7.6%	1	2.2%	1	1.8%	1	2.6%	0	0.0%
d-3-c	1	38	6	15.8%	9	23.7%	0	0.0%	16	42.1%	3	7.9%	4	10.5%
d-3-c	2	47	9	19.1%	17	36.2%	0	0.0%	18	38.3%	1	2.1%	2	4.3%
d-3-c	3	31	12	38.7%	6	19.4%	0	0.0%	10	32.3%	2	6.5%	1	3.2%
d-3-c	4	26	5	19.2%	1	3.8%	0	0.0%	16	61.5%	3	11.5%	1	3.8%
	Sum	142	32	22.5%	33	23.2%	0	0.0%	60	42.3%	9	6.3%	8	5.6%
	Average	35.5	8	23.2%	8.3	20.8%	0	0.0%	15	43.5%	2.3	7.0%	2	5.5%
	StDev	9.1	3.2	10.5%	6.7	13.3%	0	0.0%	3.5	12.7%	1	3.9%	1.4	3.4%

Table A-15. Counts, averages, and standard deviations of Fe and Fe/Mn-cemented redoximorphic features collected from samples collected at three depths (0-15, 15-30, 30-45 cm) at points A, B, and D along the sampling transect in Black Rock Slough. The % column refers to the percentage of each category as compared to the sum of features counted.

Sample	Feature Count	F/M	%	F	%	S	%	O	%	RC	%	A	%
0 – 15 cm													
Sum	2399	1395	58.1%	762	31.8%	79	3.3%	128	5.3%	26	1.1%	9	0.4%
Average	266.6	155.0		84.7		8.8		14.2		2.9		1	
StDev	63.3	64.4		28.2		8.5		9.1		2.0		1.1	
Repetition Average	53.3	31.0		16.9		1.8		2.8		0.6		0.2	
Repetition StDev	16.3	14.9		7.3		2.2		2.4		0.7		0.4	
15 – 30 cm													
Sum	1623	928	57.2%	341	21.0%	78	4.8%	163	10.0%	25	1.5%	88	5.4%
Average	180.3	103.1		37.9		8.7		18.1		2.8		9.8	
StDev	53.1	52.4		21.9		17.0		8.5		2.6		16.8	
Repetition Average	40.6	23.2		8.5		2.0		4.1		0.6		2.2	
Repetition StDev	11.0	10.4		6.2		3.6		3.4		1.0		4.2	
30 – 45 cm													
Sum	915	258	28.2%	93	10.2%	16	1.7%	404	44.2%	35	3.8%	109	11.9%
Average	101.7	28.7		10.3		1.8		44.9		3.9		12.1	
StDev	58.8	19.1		10.4		4.6		50.6		7.1		19.6	
Repetition Average	33.9	9.6		3.4		0.6		15.0		1.3		4.0	
Repetition StDev	8.3	5.3		4.0		2.2		11.0		3.0		6.3	
Overall													
Overall Sum	4937	2581	52.3%	1196	24.2%	173	3.5%	695	14.1%	86	1.7%	206	4.2%
Overall StDev	742.3	571.5		338.2		36.1		150.3		5.5		52.7	

Table A-16. Counts, averages, and standard deviations of Fe and Fe/Mn-cemented redoximorphic features collected from samples collected at three points (A, B, and D) at three depths (0-15, 15-30, 30-45 cm) along the sampling transect in Black Rock Slough. The % column refers to the percentage of each category as compared to the sum of features counted.

Sample	Feature Count	F/M	%	F	%	S	%	O	%	RC	%	A	%
Point A													
Sum	1613	832	51.6%	351	21.8%	78	4.8%	144	8.9%	23	1.4%	185	11.5%
Average	179.2	92.4		39.0		8.7		16.0		2.6		20.6	
StDev	75.2	58.2		27.0		16.9		8.5		1.4		21.3	
Repetition Average	42.4	21.9		9.2		2.1		3.8		0.6		4.9	
Repetition StDev	12.7	10.9		5.7		3.6		3.4		0.7		6.2	
Point B													
Sum	1866	1125	60.3%	334	17.9%	13	0.7%	368	19.7%	14	0.8%	12	0.6%
Average	207.3	125.0		37.1		1.4		40.9		1.6		1.3	
StDev	17.1	18.0		8.6		0.6		11.3		0.7		0.6	
Repetition Average	49.1	29.6		8.8		0.3		9.7		0.4		0.3	
Repetition StDev	17.1	18.0		8.6		0.6		11.3		0.7		0.6	
Point D													
Sum	1458	624	42.8%	511	35.0%	82	5.6%	183	12.6%	49	3.4%	9	0.6%
Average	162.0	69.3		56.8		9.1		20.3		5.4		1.0	
StDev	82.2	48.2		43.0		9.3		17.2		6.8		2.6	
Repetition Average	40.5	17.3		14.2		2.3		5.1		1.4		0.3	
Repetition StDev	14.1	9.8		9.3		3.0		4.6		2.7		0.8	
Overall													
Overall Sum	4937	2581	52.3%	1196	24.2%	173	3.5%	695	14.1%	86	1.7%	206	4.2%
Overall StDev	206.0	251.7		97.7		38.7		119.7		18.2		100.8	

Table A-17. Fe and Fe/Mn-cemented redoximorphic feature and other collected particle selected elemental concentrations from ICP-AES analysis listed by category. Elements are presented in ppm (mg/kg).

Sample Name		As	Cd	Fe	Mn	P	Pb	S	Zn
O-a		95.9	51.3	97,500	9,780	3,620	13,720	1,110	1,790
O-b		109	50.3	97,030	9,730	3,950	13,700	1,190	1,900
	Average	102	50.8	97,280	9,760	3,780	13,720	1,150	1,840
	StDev	9.10	0.7	358	33.9	229	8.0	52.7	78.2
RC-a		178	25.5	141,000	3,280	2,160	9,410	1,160	1,080
RC-b		187	26.2	137,000	3,180	2,110	9,140	1,100	1,050
RC-c		180	26.7	138,000	3,230	2,130	9,180	1,100	1,060
	Average	182	26.1	138,000	3,230	2,130	9,240	1,120	1,060
	StDev	4.8	0.6	2,020	49.4	26.6	148	35.8	18.3
S-a		65.4	16.1	42,900	3,770	1,230	6,670	1,030	1,360
S-b		62.6	16.3	43,400	3,980	1,280	6,990	994	1,350
	Average	64.0	16.2	43,200	3,880	1,250	6,830	1,010	1,350
	StDev	2.0	0.1	304	149	32.8	226	22.1	10.9
Ag1		43.0	44.7	38,800	29,200	1,220	15,700	598	1,160
Ag2		41.6	43.7	38,900	29,000	1,230	17,000	583	1,120
	Average	37.6	43.9	39,400	29,500	1,250	16,800	604	1,130
	StDev	8.1	0.7	903	675	42.2	983	24.0	24.9
F/M1		52.3	38.4	70,200	36,800	1,400	31,900	1,210	1,420
F/M2		65.9	37.6	66,800	26,900	1,380	24,200	1,230	1,440
F/M3		59.4	38.5	74,800	40,300	1,350	24,300	1,250	1,430
	Average	59.2	38.2	70,600	34,600	1,370	26,800	1,230	1,430
	StDev	6.8	0.5	4,015	6,980	25.0	4,380	20.8	9.2
F1		148	24.1	117,000	5,490	795	10,200	1,310	2,000
F2		140	23.2	109,000	5,030	732	9,600	1,230	1,880
F3		156	24.1	116,000	5,320	813	9,290	1,310	1,970
	Average	148	23.8	113,700	5,280	780	9,710	1,280	1,950
	StDev	7.5	0.5	4,330	231	42.6	485	43.6	65.7
SRM 2711 ^a		108%	91.0%	92.5%	92.2%	95.8%	99.6%	132%	100%
SRM 2711 ^a		107%	92.7%	91.2%	94.7%	94.7%	97.8%	132%	97.9%
SRM 2711 ^b		86.0%	93.0%	91.1%	102%	167%	95.7%	108%	98.4%
SRM 2711 ^b		96.7%	84.6%	94.4%	105%	96.3%	98.8%	109%	99.7%

A-1.1 Description of Enrichment Calculation

Enrichment ratio is derived by dividing the averaged metal concentration of the matrix soil into the metal concentration of the Fe and/or Fe/Mn-cemented features. The features were acquired from a three replicate intact soil cores collected at three depths (0-15, 15-30, and 30-45 cm) at points A, B, C, and D along the sampling transect in Black Rock Slough. Matrix soil was composited from the upper 7.5 cm of one replicate of intact soil cores collected at three depths (0-15, 15-30, and 30-45 cm) at points A, B, C, and D along the sampling transect in Black Rock Slough. All feature and soil samples were acid digested and analyzed at ACME Analytical Laboratories Ltd., Vancouver, British Columbia.

Table A-9. Enrichment factor of Fe and/or Fe/Mn-cemented redoximorphic features collected from points A, B, C, and D along the Black Rock Slough sampling transect. Values within parentheses are standard deviation of the average aggregated redoximorphic feature category elemental concentration.

	As	Cd	Fe	Mn	P	Pb	S	Zn
Fe and/or Fe/Mn Redoximorphic Particle (mg/kg)								
Other (O)	102 (9.10)	50.8 (0.70)	97,300 (358)	9,760 (33.9)	3,780 (229)	13,700 (7.9)	1,150 (52.7)	1,840 (78.2)
Root Channel (RC)	182 (4.80)	26.1 (0.6)	138,000 (2,016)	3,230 (49.4)	2,130 (26.6)	9,240 (148)	1,120 (35.8)	1,060 (18.3)
Fine Sand Aggregate (S)	64 (2.00)	16.2 (0.1)	43,153 (304.2)	3,875.5 (149)	1,250 (32.8)	6,830 (226)	1,010 (22.1)	1,350 (11.0)
Coarse Sand Aggregate (A)	37.6 (8.10)	43.9 (0.7)	39,400 (902)	29,500 (675)	1,250 (42.2)	16,800 (983)	604 (24.0)	1,130 (24.9)
Fe/Mn Concretion (F/M)	59.2 (6.80)	38.2 (0.5)	70,600 (4,020)	34,600 (6,980)	1,370 (25.0)	26,800 (4,370)	1,230 (20.8)	1,430 (9.24)
Fe Concretion (F)	148 (7.50)	23.8 (0.5)	113,700 (4,330)	5,280 (231)	780 (42.6)	9,710 (485)	1,280 (43.6)	1,950 (65.7)
Matrix Soil (mg/kg)								
Comp A	156	15.7	92,900	3,500	720	4,840	n/a	2,350
Comp B	140	8.00	93,500	1,180	860	7,230	n/a	2,350
Comp C	169	9.10	77,900	1,200	930	4,980	n/a	1,820
Comp D	103	5.50	55,900	1,040	1,040	4,250	n/a	1,190
Average	142	9.60	80,050	1,730	888	5,330	n/a	1,920
StDev	28.6	4.40	17,600	1,180	134	1,310	n/a	549
Enrichment Factor (unitless)								
Other (O)	0.72	5.31	1.22	5.64	4.26	2.58	n/a	0.96
Root Channel (RC)	1.28	2.73	1.73	1.87	2.40	1.74	n/a	0.55
Fine Sand Aggregate (S)	0.45	1.69	0.54	2.24	1.41	1.28	n/a	0.70
Coarse Sand Aggregates (A)	0.26	4.58	0.49	17.04	1.41	3.16	n/a	0.59
Fe/Mn Concretions (F/M)	0.42	3.99	0.88	20.03	1.55	5.03	n/a	0.74
Fe Concretions (F)	1.05	2.49	1.42	3.05	0.88	1.82	n/a	1.01

Appendix B: Digital Photographs of Cemented Redoximorphic Features

Images of aggregated redoximorphic feature categories are contained on an attached CD Rom disk. The files on the CD ROM are listed by sample (X-#-XX-##.jpg) in which X is the collection site designator (e.g. A, B, or D), # is the replicate number (e.g. 1, 2, or 3), XX is the depth of sample (a = 0 – 15cm, b = 15 – 30 cm, and c = 30 – 45 cm), and ## is the sample categorization and counting point. Collection, separation and counting methods are described in Chapter 1.

Table B-1. File names of aggregated redoximorphic feature photographs on attached CD – ROM.

a-1-a-1.jpg	a-3-a-3.jpg	b-2-c-2.jpg	d-2-a-1.jpg
a-1-a-2.jpg	a-3-a-4.jpg	b-2-c-3.jpg	d-2-a-2.jpg
a-1-a-3.jpg	a-3-a-5.jpg	b-2-c-4.jpg	d-2-a-3.jpg
a-1-a-4.jpg	a-3-b-1.jpg	b-3-a-1.jpg	d-2-a-4.jpg
a-1-a-5.jpg	a-3-b-2.jpg	b-3-a-2.jpg	d-2-a-5.jpg
a-1-b-1.jpg	a-3-b-3.jpg	b-3-a-3.jpg	d-2-b-1.jpg
a-1-b-2.jpg	a-3-b-4.jpg	b-3-a-4.jpg	d-2-b-2.jpg
a-1-b-3.jpg	a-3-c-1.jpg	b-3-a-5.jpg	d-2-b-3.jpg
a-1-b-4.jpg	a-3-c-2.jpg	b-3-b-1.jpg	d-2-b-4.jpg
a-1-b-5.jpg	b-1-a-1.jpg	b-3-b-2.jpg	d-2-b-5.jpg
a-1-c-1.jpg	b-1-a-2.jpg	b-3-b-3.jpg	d-2-c-1.jpg
a-1-c-2.jpg	b-1-a-3.jpg	b-3-b-4.jpg	d-2-c-2.jpg
a-1-c-3.jpg	b-1-a-4.jpg	b-3-b-5.jpg	d-3-a-1.jpg
a-1-c-4.jpg	b-1-a-5.jpg	b-3-c-1.jpg	d-3-a-2.jpg
a-2-a-1.jpg	b-1-b-1.jpg	b-3-c-2.jpg	d-3-a-3.jpg
a-2-a-2.jpg	b-1-b-2.jpg	b-3-c-3.jpg	d-3-a-4.jpg
a-2-a-3.jpg	b-1-b-3.jpg	b-3-c-4.jpg	d-3-a-5.jpg
a-2-a-4.jpg	b-1-b-4.jpg	b-3-c-5.jpg	d-3-b-1.jpg
a-2-a-5.jpg	b-1-b-5.jpg	d-1-a-1.jpg	d-3-b-2.jpg
a-2-b-1.jpg	b-1-c-1.jpg	d-1-a-2.jpg	d-3-b-3.jpg
a-2-b-2.jpg	b-2-a-1.jpg	d-1-a-3.jpg	d-3-b-4.jpg
a-2-b-3.jpg	b-2-a-2.jpg	d-1-a-4.jpg	d-3-c-1.jpg
a-2-b-4.jpg	b-2-a-3.jpg	d-1-a-5.jpg	d-3-c-2.jpg
a-2-b-5.jpg	b-2-a-4.jpg	d-1-b-1.jpg	d-3-c-3.jpg
a-2-c-1.jpg	b-2-a-5.jpg	d-1-b-2.jpg	d-3-c-4.jpg
a-2-c-2.jpg	b-2-b-1.jpg	d-1-b-3.jpg	d-3-c-5.jpg
a-2-c-3.jpg	b-2-b-2.jpg	d-1-b-4.jpg	
a-3-a-1.jpg	b-2-b-3.jpg	d-1-c-1.jpg	
a-3-a-2.jpg	b-2-c-1.jpg	d-1-c-2.jpg	

Appendix C: Na-Hexametaphosphate-Wash Chelation Experiment

Initial observations of within the Black Rock Slough site showed that Fe/Mn-cemented aggregates were 2 mm or less in size. Proper characterization of the Fe/Mn-cemented aggregates involved visual identification thus making it important that the observed particles were free of non-cemented soil. In previous studies nodules and concretions have been extracted from soil through various means. For example, Cescas et al. (1970) used wet sieving, D'Amore et al. (2004) used a Na-hexametaphosphate wash and wet sieving, and Gasparatos et al. (2005) dispersed the soil in Na_2CO_3 and collected the nodules using a wet-sieve.

The use of Na-hexametaphosphate chelates Ca^{2+} ions and promotes the adsorption of Na^+ , which has a large hydrated ionic radius, onto particle surfaces enabling dispersion in soils (Jackson 1956). The chelating properties of Na-hexametaphosphate were investigated by Plouffe et al. (2001) in a Geological Survey of Canada particle size dispersion procedure. A 0.5% Na-hexametaphosphate solution was used to wash glacial sediment samples and then was analyzed for several metals including Zn, Fe, and Mn. The results were compared to the results of an aqua regia digestion and a 1 M Na-acetate leach. It was discovered that the Na-hexametaphosphate solution elemental concentrations were insignificant when compared to that of the aqua regia digest. The Na-hexametaphosphate solution contained 68% of Hg that was found in the Na-acetate leach. Approximately 7% of Cr was lost to the wash solution from the

clay-sized fraction. In our experiment we measured element loss from Fe/Mn-cemented redoximorphic features sieved from Black Rock Slough soil samples using a 5% Na-hexametaphosphate solution wash. The goal of this investigation was to test the effectiveness of dispersing non-concreted soil particles from the surface of Fe/Mn-cemented aggregates with a Na-hexametaphosphate solution. The experiment also was designed to measure the release of metals from the Fe/Mn-cemented aggregates to the wash solution. Again, reorganize this information with the previous section; provide clear justification of what you are doing and logical order of ideas.

Soil collected from sampling location B was wet-sieved through a 1mm standard mesh-size sieve to collect ~21 g of particles. The particles were allowed to air-dry. Three subsamples weighing approximately one gram were collected as a representative non-treated reference and sent to ACME Analytical Laboratories Ltd., Vancouver, British Columbia for acid digestion and subsequent elemental analysis. Six subsamples weighing approximately 1.5 grams each were placed into individual 125 mL Erlenmeyer flasks. 100 mL of 5% Na-hexametaphosphate solution was added to the Erlenmeyer flasks. The flasks were placed on a shaker-table and agitated for approximately 24 hours at 175 RPM. The speed was selected such that the wash solution was allowed to mix while the Fe/Mn-cemented aggregates remained motionless.

Fifty milliliters of Na-hexametaphosphate solution from each of the six Erlenmeyer flasks was pipetted into a new disposable 50 mL centrifuge tube. The remaining Na-hexametaphosphate was decanted with care to avoid loss of any particles. The redoximorphic particles were carefully rinsed three times with triple-

distilled water to remove residual dispersant. The redoximorphic particles were then allowed to air-dry overnight.

The Na-hexametaphosphate solution pH was measured prior to addition to the Erlenmeyer flask containing the redoximorphic feature samples and immediately after shaking was completed. In both measurements the pH of the solution was 6.70.

Three of the six redoximorphic feature samples were randomly selected and ground to a fine powder using an agate pestle and mortar in preparation for elemental analysis. An ICP-MS analysis following an aqua regia and HF digest was provided by ACME Analytical Laboratories Ltd., Vancouver, British Columbia. The six post-dispersant solution samples were passed through a 0.22 μm filter, diluted to a 1:10 ratio with triple-distilled water, and analyzed using an ICP-AES for As, Ca, Cd, Fe, Mn, P Pb, S, and Zn.

In an experiment conducted on glacial till using a Na-hexametaphosphate solution wash, Plouffe et al. (2001) discovered insignificant losses as compared to that of a conventional aqua regia digestion. However, the Plouffe et al. (2001) study employed a 0.5% Na-hexametaphosphate solution and did not include analysis for As, Pb, Cd, or S. The analysis data of the Na-hexametaphosphate used in preparing the redoximorphic features for visual identification and categorization (Table C-1) showed a larger loss of elements than the Plouffe et al. (2001) investigation.

Approximately 20% of Zn and Cd associated with the water-sieved redoximorphic features were released to the Na-hexametaphosphate wash. This may be attributed to the adsorption of Na^+ ions on the soil surface which in turn desorbs Zn or Cd. According to Hickey and Kittrick (1984), 83% of total Cd in four

trace-metal enriched soils was associated with the exchangeable, carbonate, and Fe/Mn oxides fractions. In the Hickey and Kittrick (1984) study, Zn in a soil, sample TRI-I, downwind of a Washington smelting operation was associated with the exchangeable phase.

Soluble zinc and cadmium, once desorbed from the particles surface, may easily pass through most filters. Plouffe et al. (2001) employed 0.45 μm filters while our experiment used 0.22 μm filters. Lead and sulfur was lost from the original redoximorphic features at 11.9% and 36.4% respectively. Both Pb and S preferentially adsorb to organic matter, whose molecular size may be small enough to pass through a 0.22 μm filter. The moderate percentage of As (7.1%) released may also be attributed to colloid-size particles. In a recent publication by Thorai et al. (2005) the presence of nano-aggregated As(III) and Fe(III) complexes were discovered. These complexes were derived from reduced iron (Fe(II)) and As (III) and may illustrate a more mobile species of arsenic in redox environments such a hydric soils. Manganese and iron had the smallest percentage losses due to the wash at 1.1% and 4.6% respectfully which may be attributed to the near neutral pH of the Na-hexametaphosphate wash. The loss of certain elemental concentrations from redoximorphic features washed with Na-hexametaphosphate may prove this technique unsuitable as an initial step for elemental analysis. The loss of high percentages of Cd, Zn, and S indicate that this procedure may interfere with soil organic matter analysis of redoximorphic features.

The loss of selected elemental concentrations from aggregated redoximorphic features washed with a 5% Na-hexametaphosphate solution was

less than 10% for As, Fe, and Mn. Losses of approximately 22%, 11.9%, 36.4%, and 19.2% were associated with Cd, Pb, S, and Zn respectively.

Table C- 1. Averaged results from elemental analysis of digested redoximorphic features after being washed for 24 hours in a 5% Na-hexametaphosphate solution. Values are presented in ppm (mg/kg). Standard deviation of the sample averages are in parentheses.

Sample	As	Cd	Fe	Mn	P	Pb	S	Zn
Pre-wash (1)	54.0	43.7	105,000	60,000	1,590	42,700	900	2,460
Pre-wash (2)	53.0	49.0	100,000	57,900	1,700	39,700	100	2,430
Pre-wash (3)	62.0	39.4	104,000	51,300	1,900	37,400	100	2,250
Average	56.3	44.0	103,000	56,400	1,730	39,900	367	2,380
Standard Deviation	4.90	4.80	2,000	4,540	157	2,660	462	116
Post-wash (1)	60.0	36.3	103,000	54,600	5,440	33,600	300	1,990
Post-wash (2)	45.0	33.8	93,700	54,200	5,260	35,700	200	1,830
Post-wash (3)	52.0	33.0	98,200	58,500	5,600	36,200	200	1,940
Average	52.3	34.4	98,000	55,800	5,430	35,200	233	1,920
Standard Deviation	7.50	1.70	5,000	2,380	170	1,380	57.7	80.5
Percent Difference	7.10%	22.0%	4.62%	1.12%	-214%	11.9%	36.4%	19.2%

Appendix D: X-Ray Diffraction Analysis

Introduction:

The objective of this set of experiments was to characterize the mineralogy of soils collected from the Black Rock Slough research site described in chapter 1. Samples were collected from a sampling site near point B along the transect and separated by particle size. Qualitative XRD analysis of samples was conducted by treating the samples with citrate bicarbonate dithionite (CBD), ethylene glycol, Mg and K saturating cations, and heating to 550° C.

Methods and Materials:

Sampling within the Black Rock Slough study site approximately 15 meters east of the Black Rock Slough sampling transect was conducted at 4 depths; 0 - 10, 10 - 30, 30 - 60, and 60 - 80 centimeters. The soil at the study site is developed from sediment and mine tailings deposited during flood events.

Soil samples were prepared for particle size separation by removing organic matter and checking for the presence of calcium carbonates (McDaniel 2004 a). Application of one to two drops of 1.0 N HCl acid resulted in no noticeable effervescence and is indicative of the lack of calcium carbonates. Particle size separation was performed on the samples as outlined in McDaniel (2004 b). The sand fraction was further separated into very coarse, coarse, medium, fine, and very fine sand sizes using sieves.

Each of the 4 clay samples was divided into 2 separate samples to allow for a control and CBD treatment. The soils in the lower CdA River floodplains have been shown to have appreciable amounts of Fe (hydr) oxides present (EPA 2003). The use of the CBD treatment allows for the dissolution of well crystallized and poorly-crystalline Fe (hydr) oxides such as goethite and ferrihydrite. The control and CBD-treated clay samples were treated with Mg, Mg-glycol, and K solutions. An air-dried K-treated clay sample was heated to 550° C overnight. The treated clay samples were wet-mounted onto microscope slides and dried in preparation for analysis. The untreated silt and very-fine sand samples were powder-mounted for XRD analysis.

An initial XRD scan analysis using a Siemens Diffraktometer D5000 XRD instrument at the Department of Geology, University of Idaho of the 0-5 cm control and CBD samples allowed for determination to whether poorly-crystalline Fe (hydr) oxide presence obstructed key mineral peaks.

Initially, the control and CBD-treated samples were analyzed between 2° θ and 34° θ using a step size of 0.020° with a scan time of 0.5 seconds (Figure D-1). This step was conducted to determine to what extent of poorly-crystalline Fe (hydr)oxides would affect the ability to identify mineralogy present. The CBD treated sample provided diffraction patterns with clearly defined peaks. The Mg-saturated and CBD treated samples were used for identification and analyzed between 2° θ and 34° θ using a step size of 0.020° with a scan time of 0.5 seconds. The Mg-glycol and K treated CBD samples were analyzed to further identify soil mineralogy between 2° θ and 15° θ using a step size of 0.020° with a scan time of 0.5 seconds.

The 0 – 5 and 33 – 46 cm silt and very-fine sand samples were analyzed to identify primary mineral changes between the upper and lower depths of the profile. The silt and very-fine sand sized particles were analyzed between $15^\circ \theta$ and $45^\circ \theta$ using a step size of 0.020° and were 0.6 seconds per step.

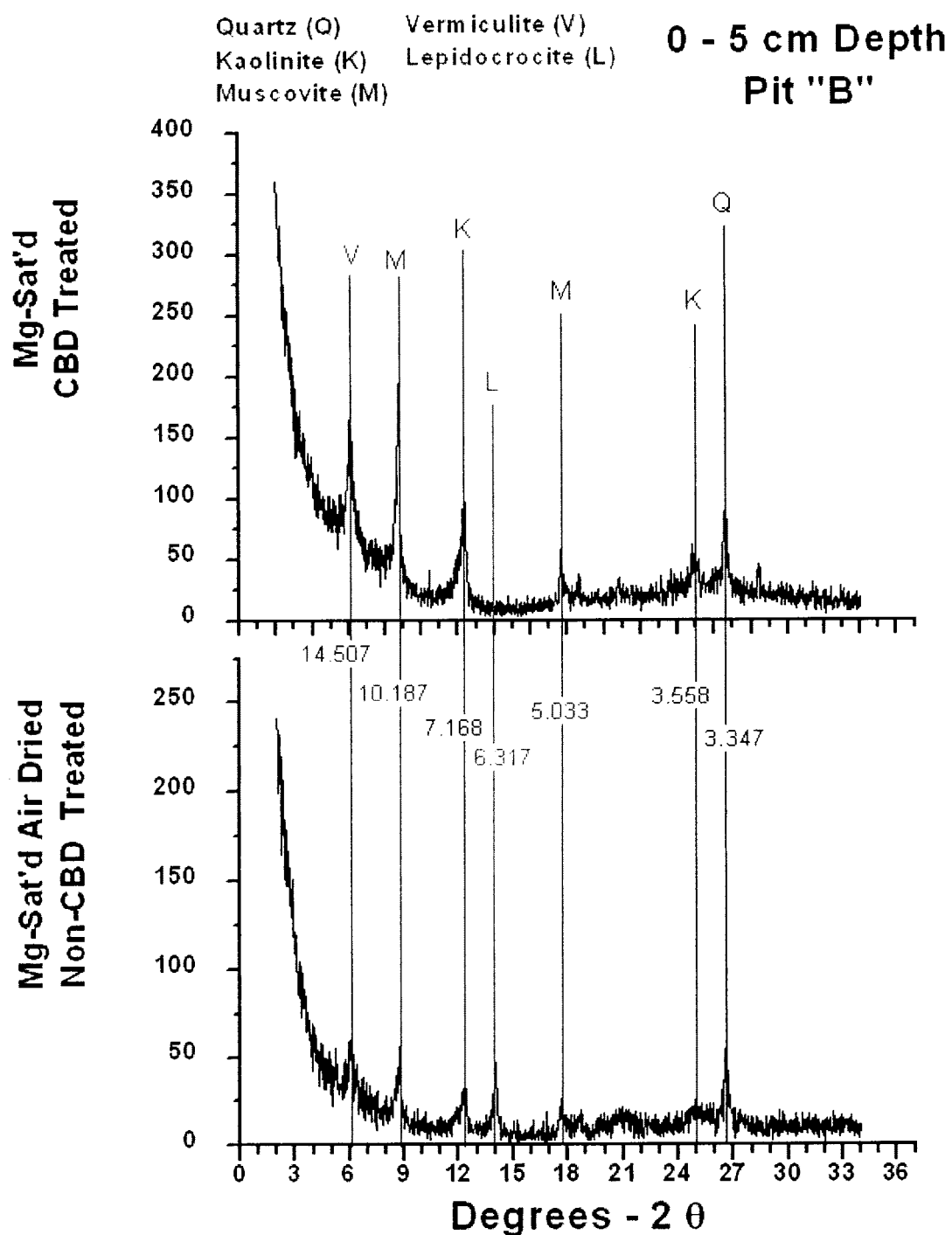


Figure D- 1. Diffraction patterns from clay-sized soil particles taken at the 0-5 cm depth near sampling point B. Vermiculite, muscovite, kaolinite, lepidocrocite, and quartz are the predominate minerals identified

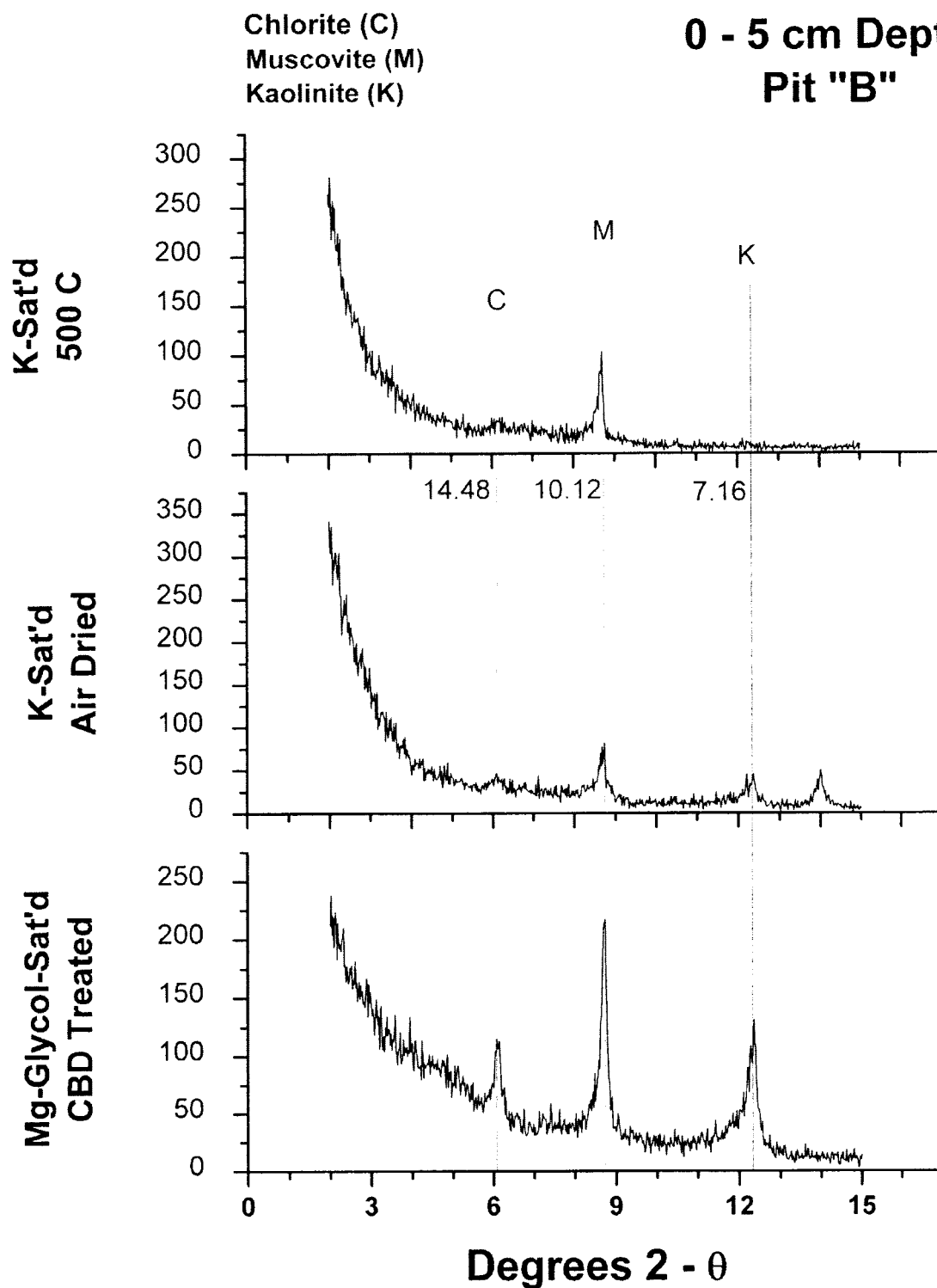


Figure D-2. Diffraction patterns for Mg-glycol and K treated clay-sized soil particles taken at the 0-5 cm depth near sampling point B. Chlorite, muscovite, and kaolinite are the predominate minerals identified.

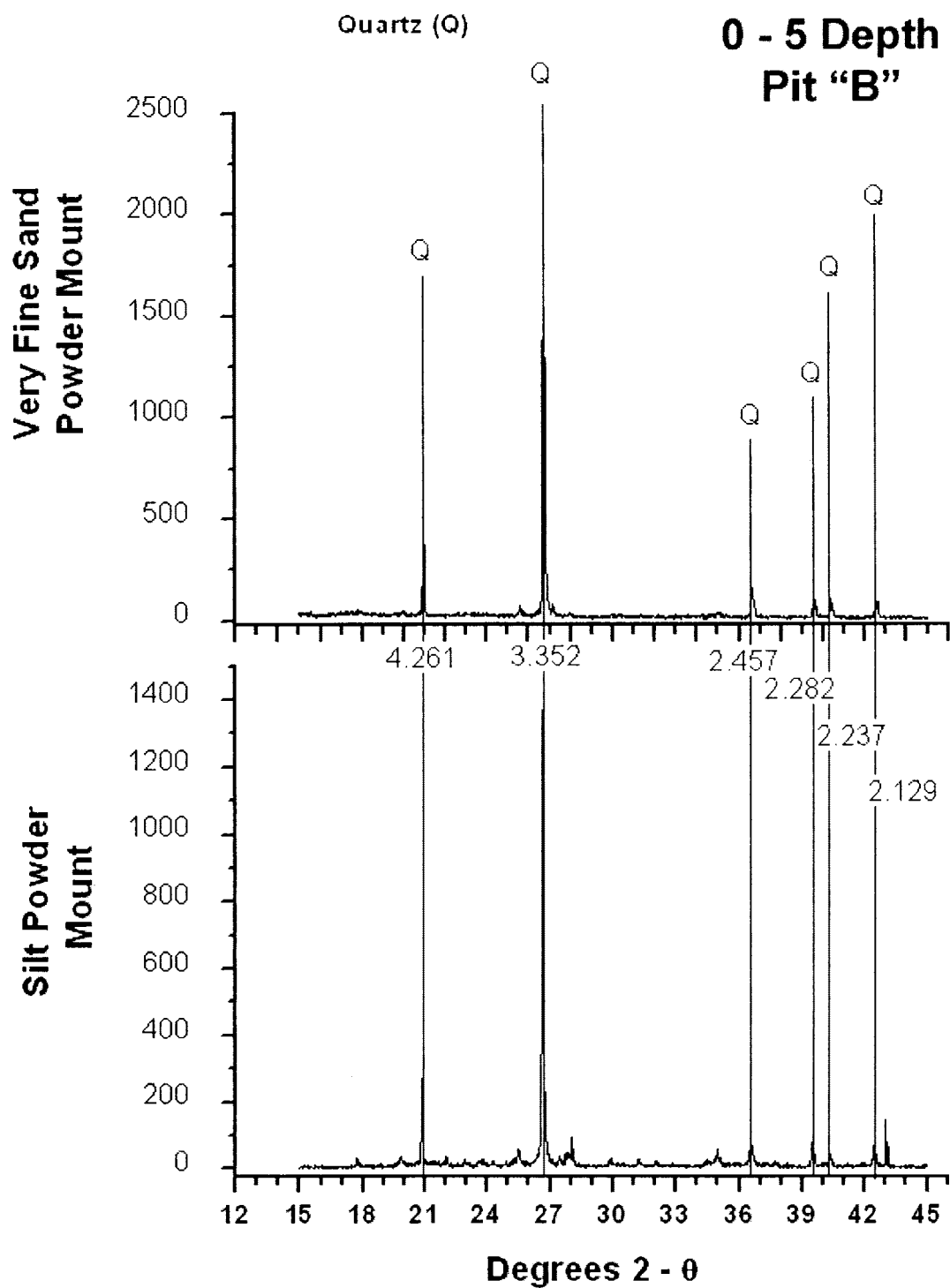


Figure D-3. X-ray diffraction patterns for very fine sand and silt powder mounts of soil sampled at the 0 - 5 cm depth.

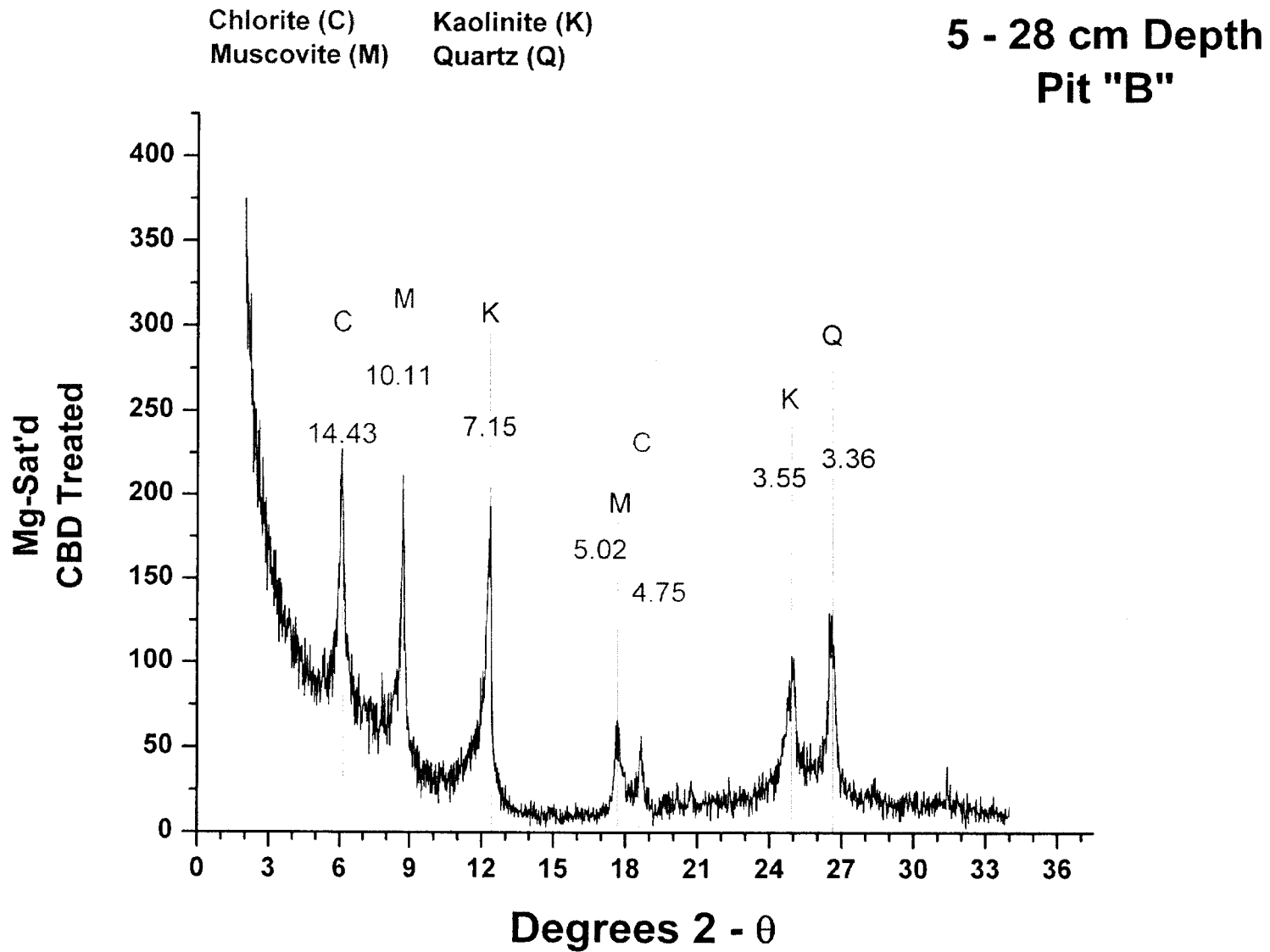


Figure D-4. X-ray diffraction patterns for clay-sized soil particles indicating the presence of quartz, chlorite, kaolinite, and muscovite at the 5-28 cm depth.

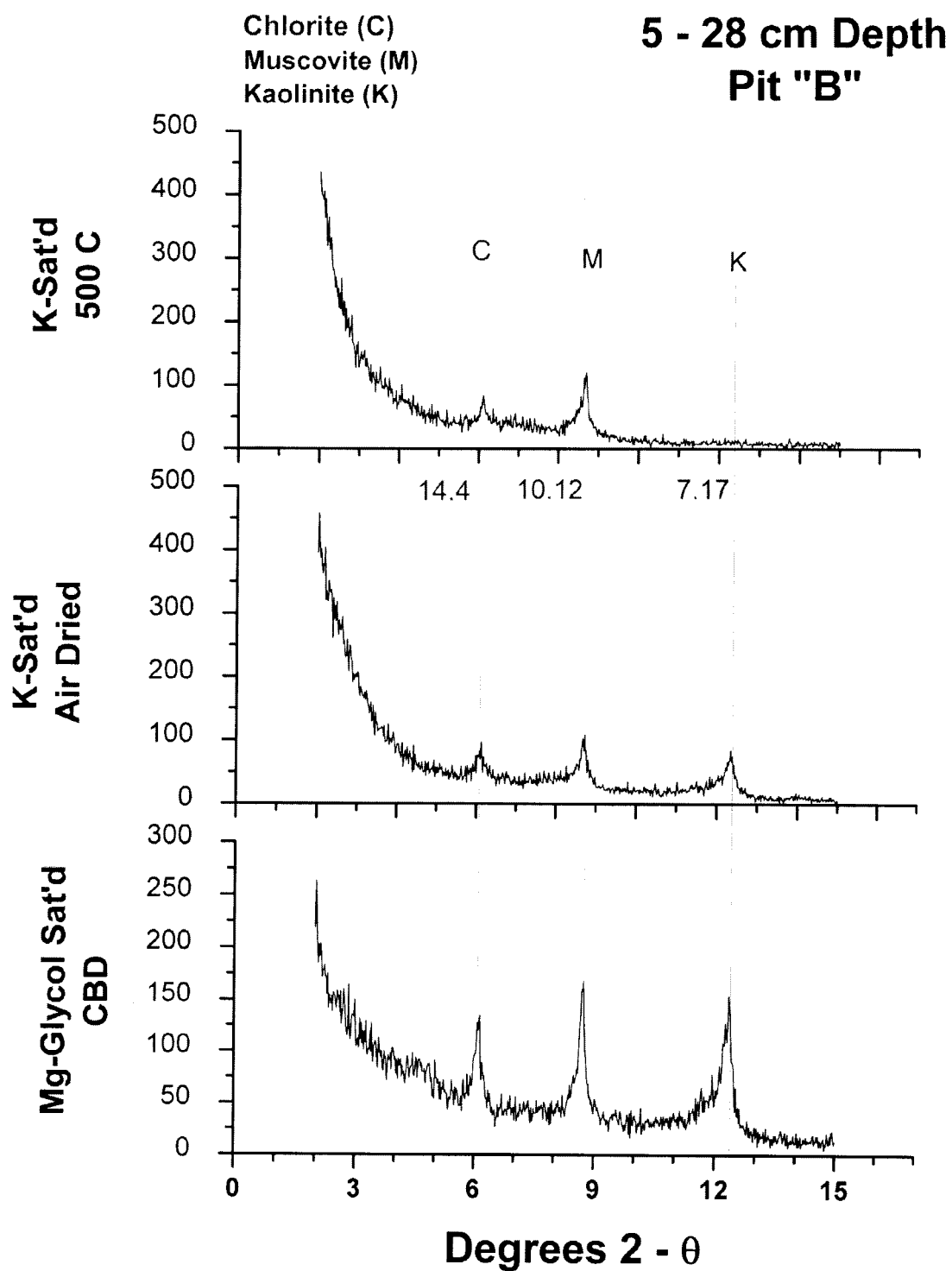


Figure D-5. X-ray diffraction patterns for clay-sized soil particles indicating the presence of chlorite, kaolinite, and muscovite at the 5-28 cm depth.

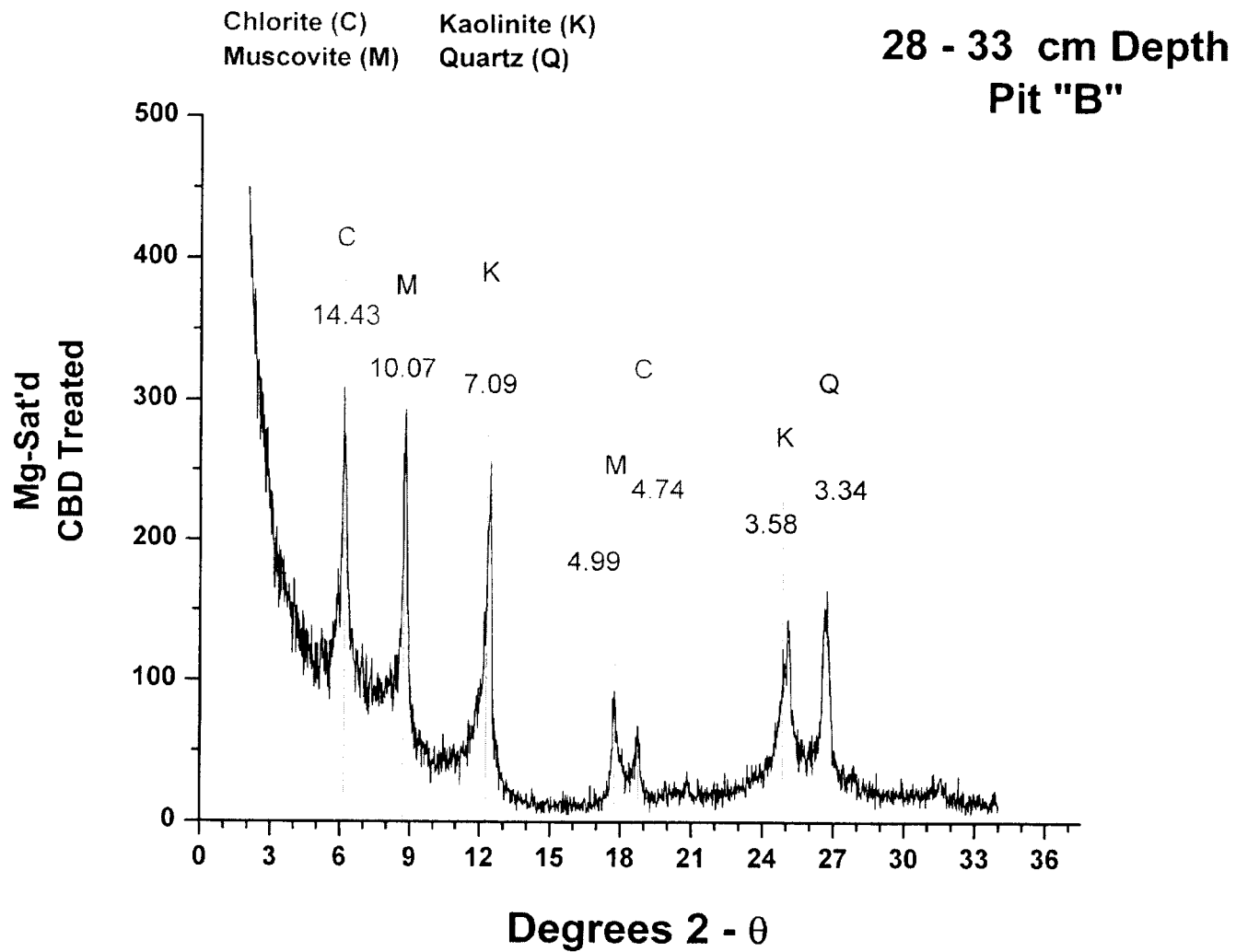


Figure D-6. X-ray diffraction patterns for clay-sized soil particles indicating the presence of quartz, chlorite, kaolinite, and muscovite at the 28-33 cm depth.

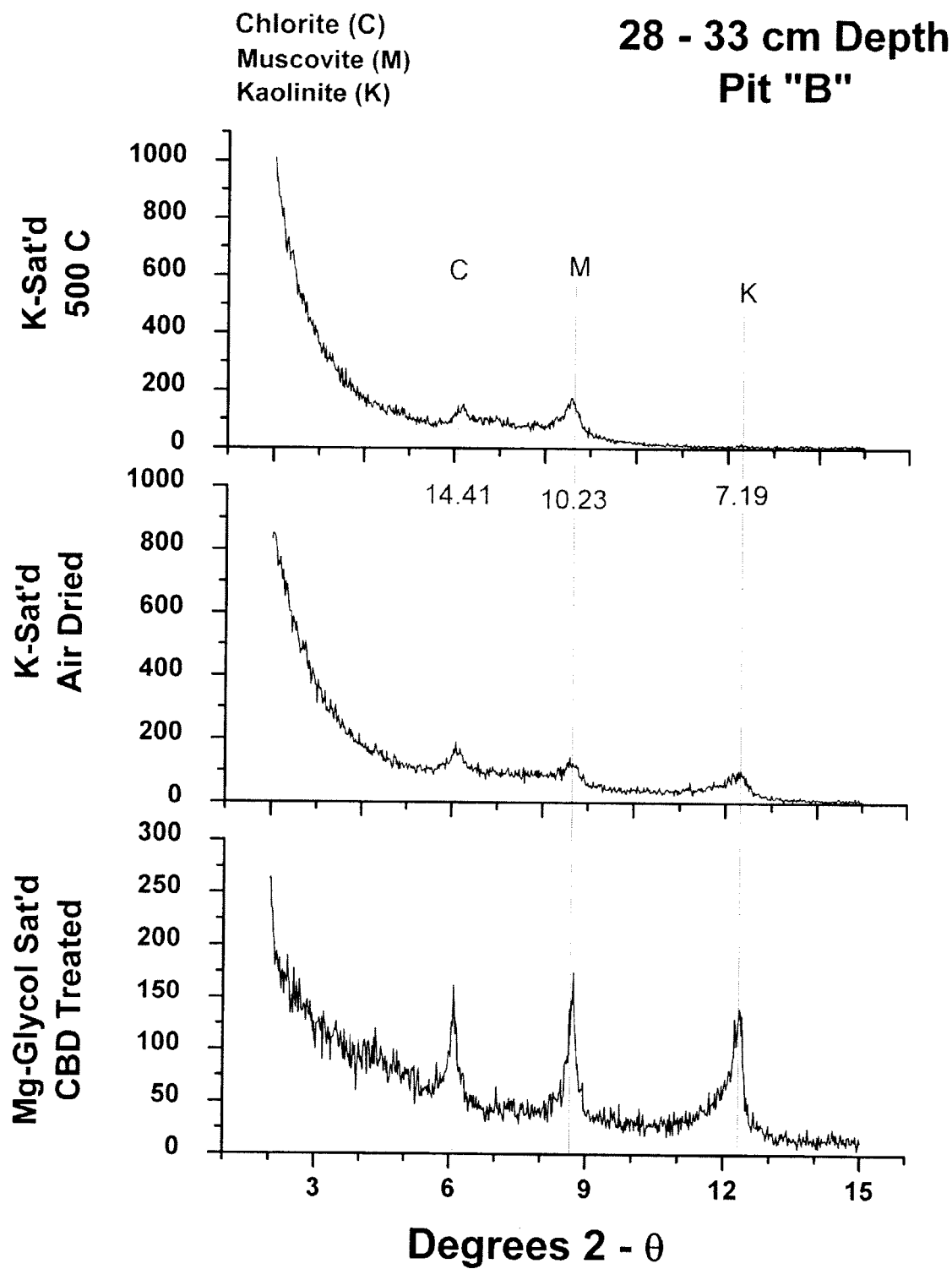


Figure D-7. X-ray diffraction patterns for clay-sized soil particles indicating the presence of chlorite, kaolinite, and muscovite at 28-33 cm depth.

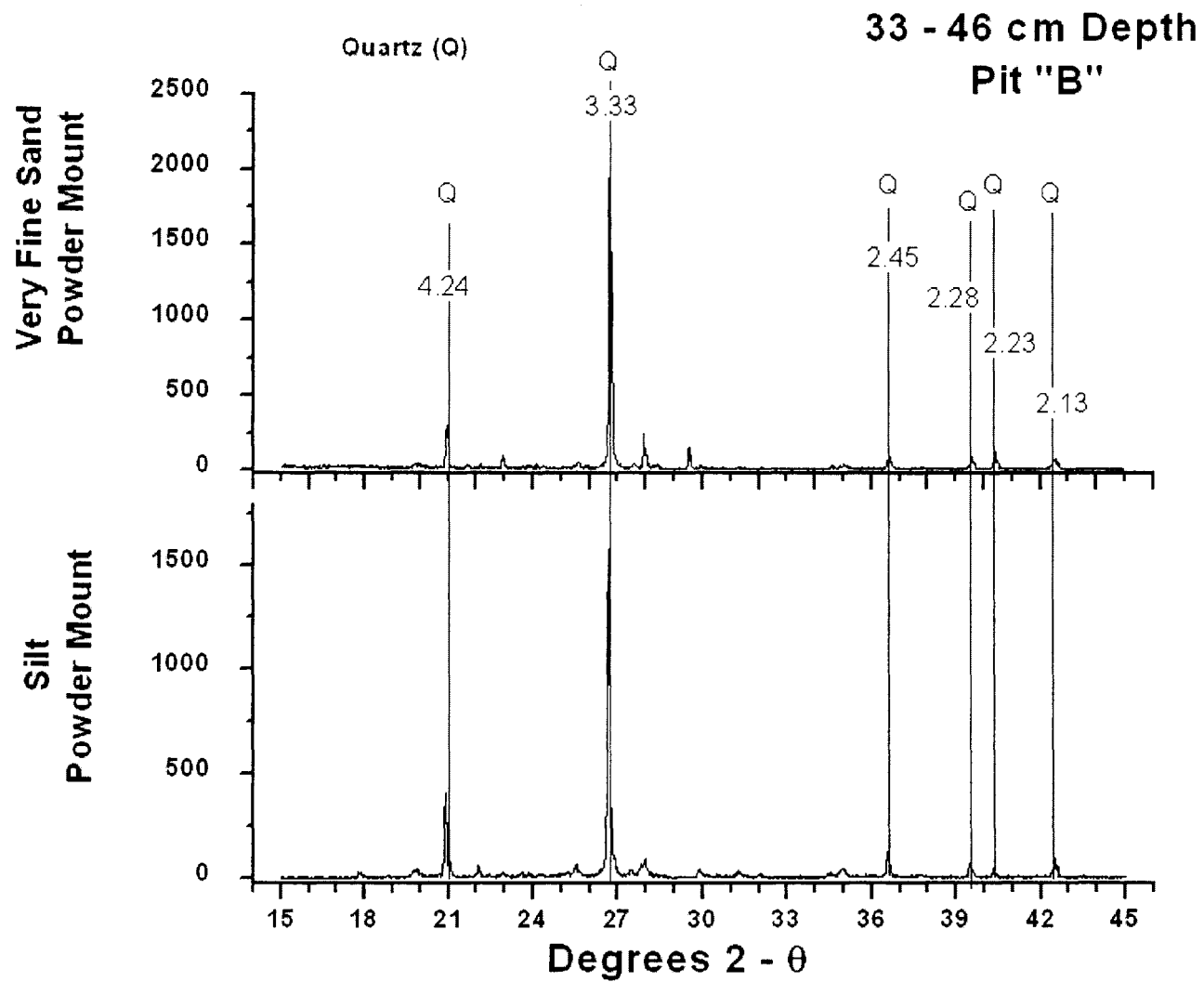


Figure D-8. X-ray diffraction patterns for silt and very-fine sand sized particles indicating the presence of quartz at 33-46 cm depth.

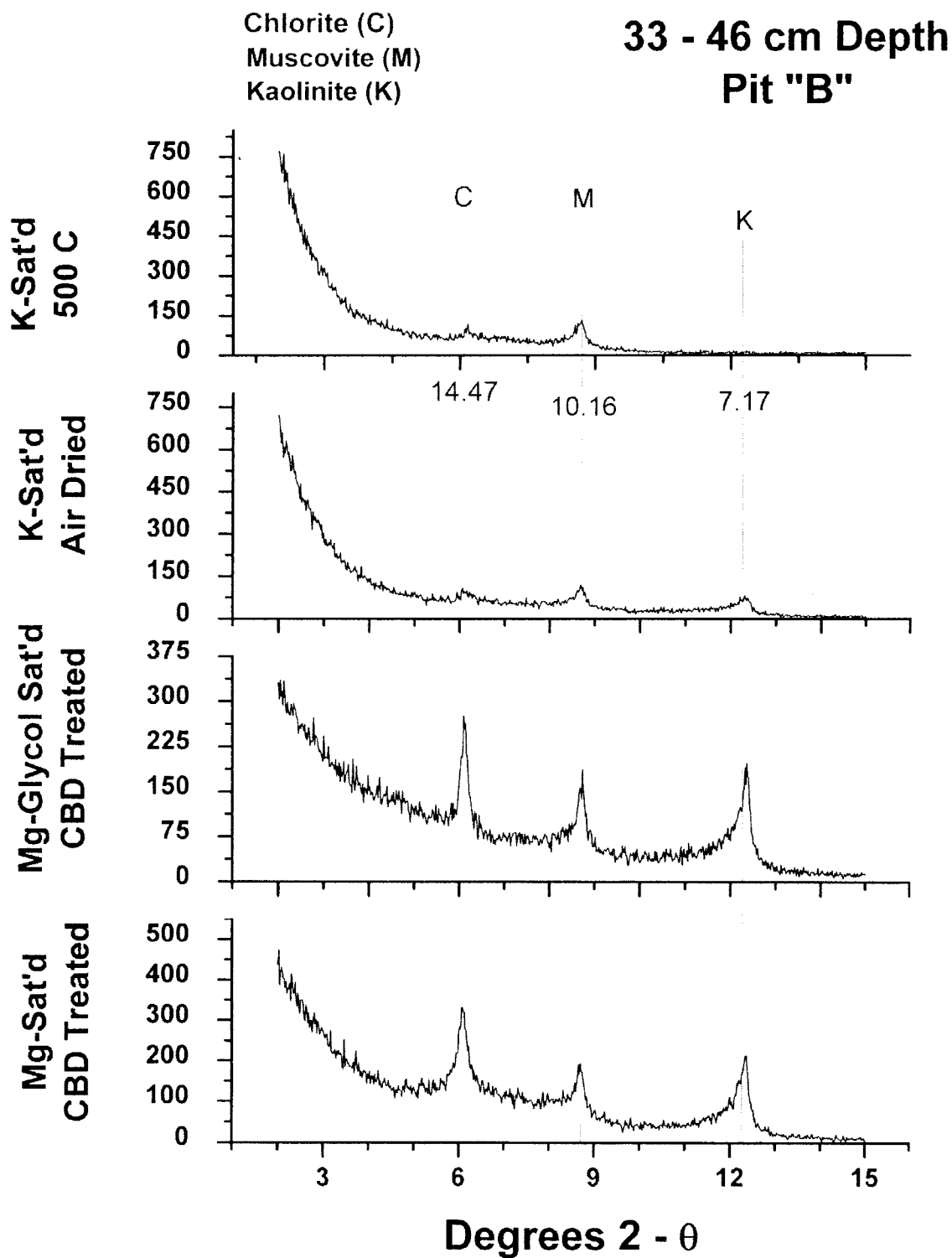


Figure D-9. X-ray diffraction patterns for clay-sized soil particles indicating the presence of chlorite, muscovite, and kaolinite 33-46 cm depth.

References

- EPA. (2003). "Region 10 Superfund: Bunker Hill / Coeur d'Alene Basin - Record of Decision (ROD)." Retrieved 3/21/2004, 2004, from [http://yosemite.epa.gov/R10/CLEANUP.NSF/basin/Record+of+Decision+\(ROD\)](http://yosemite.epa.gov/R10/CLEANUP.NSF/basin/Record+of+Decision+(ROD)).
- McDaniel, P. A. (2004 b). "Particle size distribution - centrifuge." Retrieved 2/16/2004, 2004, from <http://soils.ag.uidaho.edu/pedology/Analyses/Psdcent2.pdf>.
- McDaniel, P. A., Falen, A. (2004 a). "Sample Preparation." Retrieved 2/16/2004, 2004, from <http://soils.ag.uidaho.edu/pedology/Analyses/Psdprep.pdf>.

Appendix E. Fe/Mn-Cemented Aggregate Element Concentration Comparison

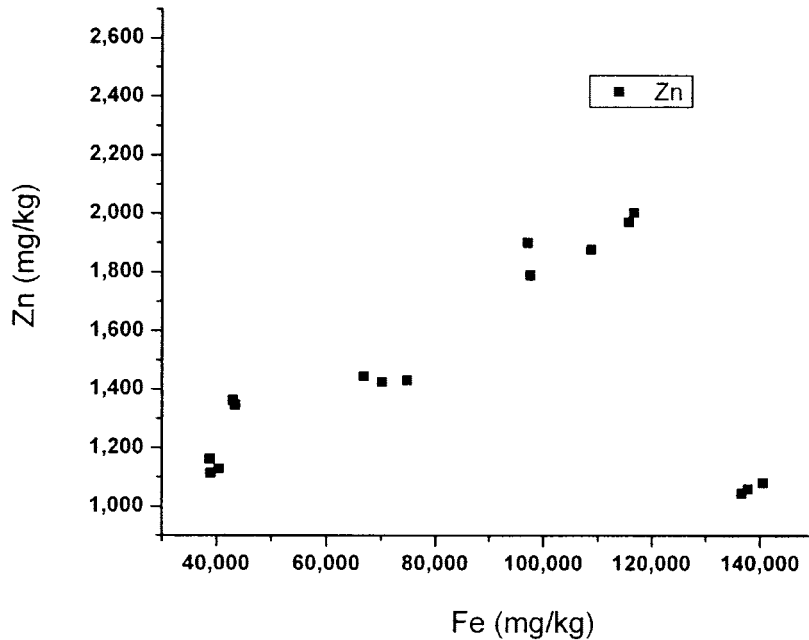


Figure E-1. Comparison of category averaged Fe and Zn concentrations from Fe/Mn-cemented aggregates collected at points A, B, and D within the Black Rock Slough sampling transect.

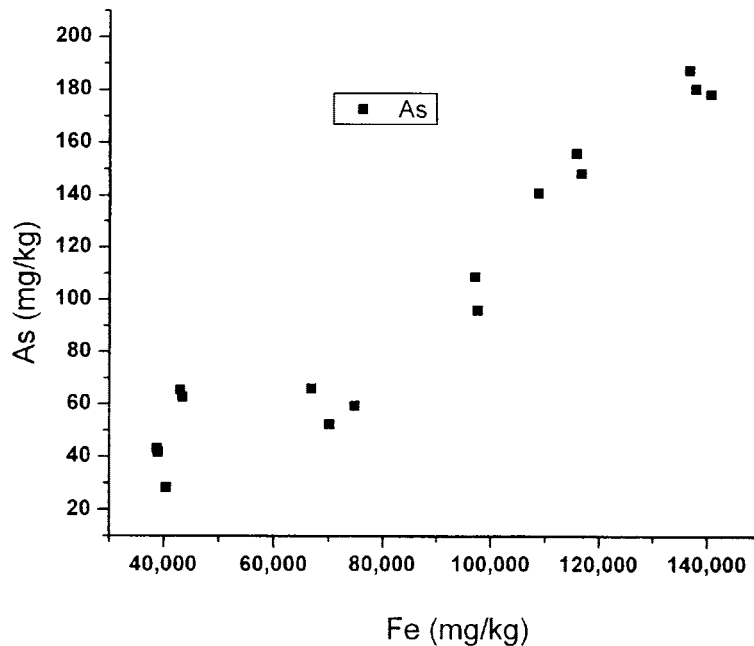


Figure E-2. Comparison of category averaged Fe and As concentrations from Fe/Mn-cemented aggregates collected at points A, B, and D within the Black Rock Slough sampling transect.

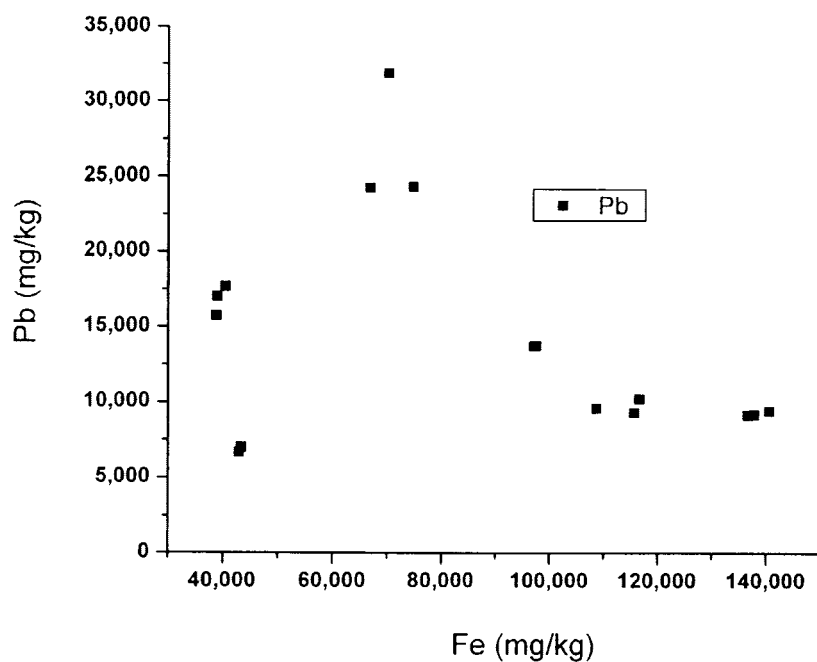


Figure E-3. Comparison of category averaged Fe and Pb concentrations from Fe/Mn-cemented aggregates collected at points A, B, and D within the Black Rock Slough sampling transect.

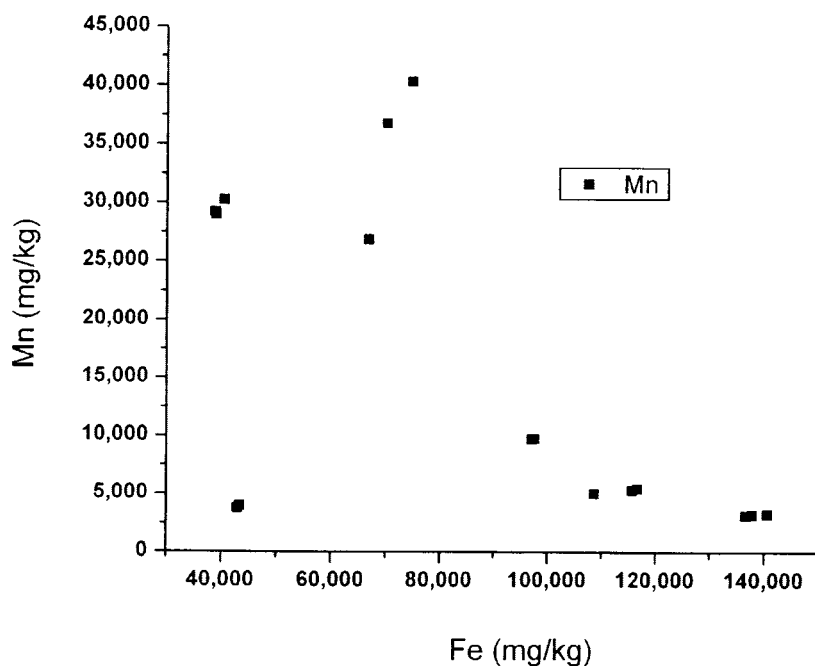


Figure E-4. Comparison of category averaged Fe and Mn concentrations from Fe/Mn-cemented aggregates collected at points A, B, and D within the Black Rock Slough sampling transect.

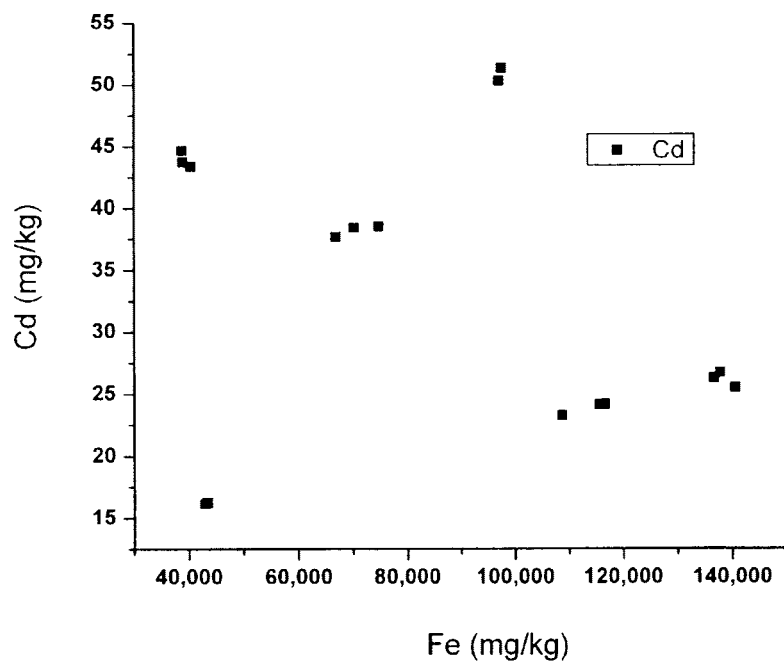


Figure E-5. Comparison of category averaged Fe and Cd concentrations from Fe/Mn-cemented aggregates collected at points A, B, and D within the Black Rock Slough sampling transect.

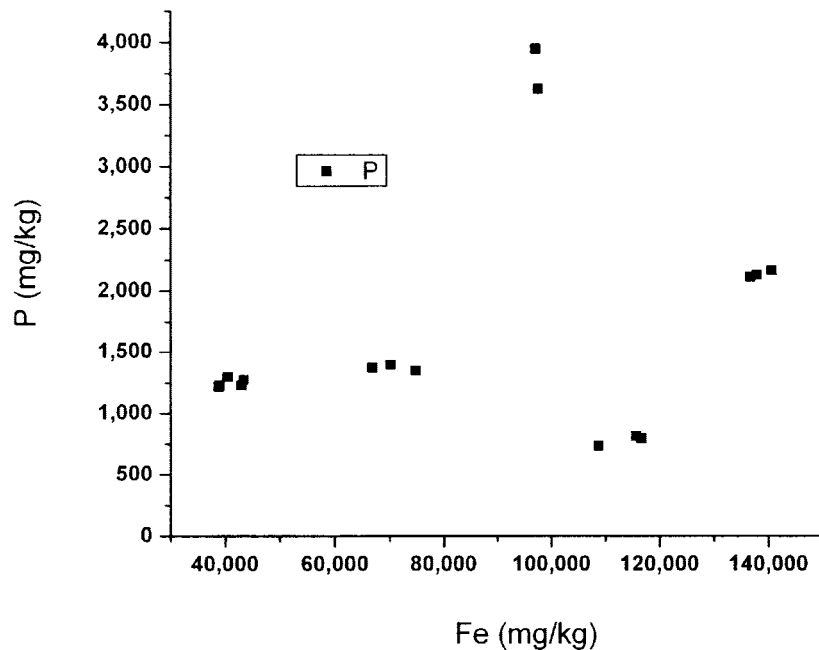


Figure E-6. Comparison of category averaged Fe and P concentrations from Fe/Mn-cemented aggregates collected at points A, B, and D within the Black Rock Slough sampling transect.

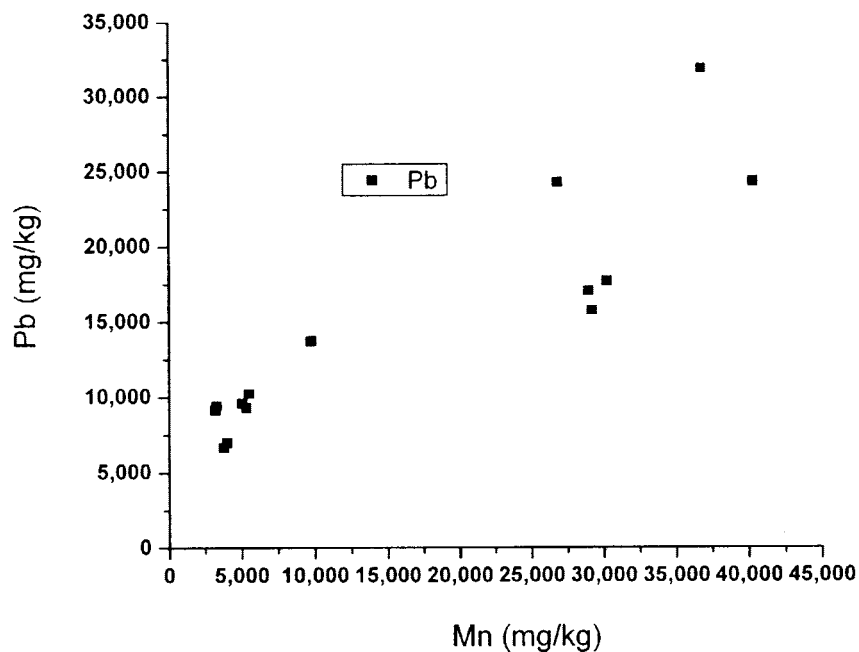


Figure E-7. Comparison of category averaged Mn and Pb concentrations from Fe/Mn-cemented aggregates collected at points A, B, and D within the Black Rock Slough sampling transect.

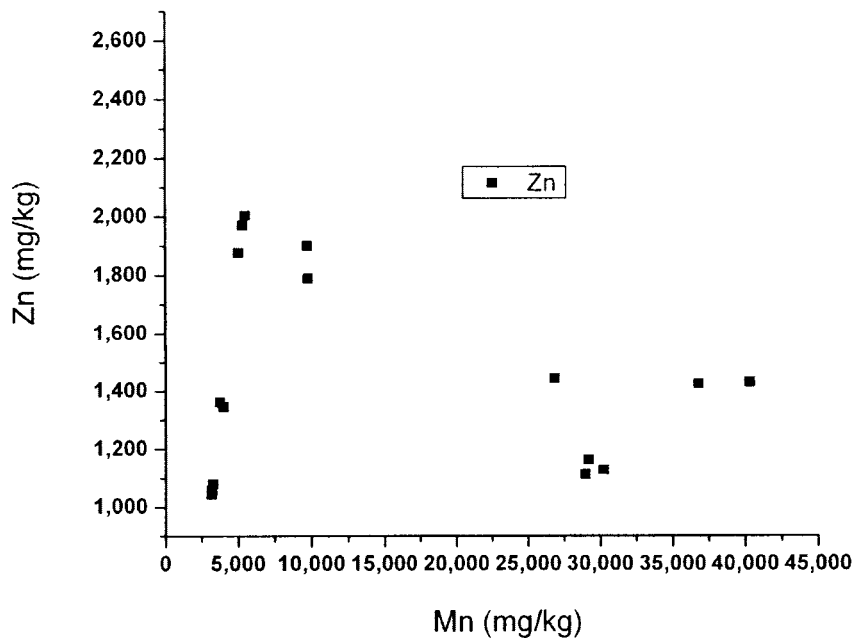


Figure E-8. Comparison of category averaged Mn and Zn concentrations from Fe/Mn-cemented aggregates collected at points A, B, and D within the Black Rock Slough sampling transect.

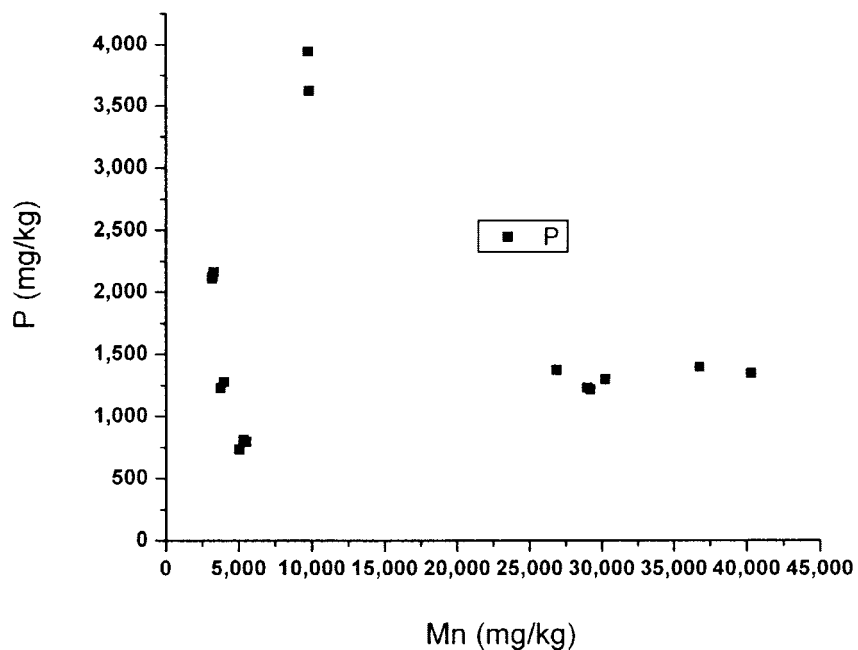


Figure E-9. Comparison of category averaged Mn and P concentrations from Fe/Mn-cemented aggregates collected at points A, B, and D within the Black Rock Slough sampling transect.

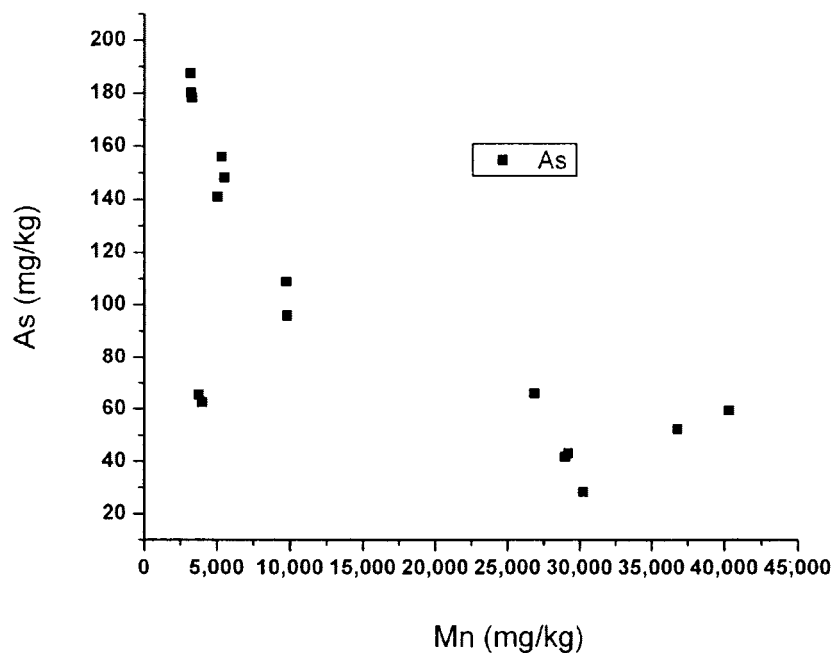


Figure 10. Comparison of category averaged Mn and As concentrations from Fe/Mn-cemented aggregates collected at points A, B, and D within the Black Rock Slough sampling transect.

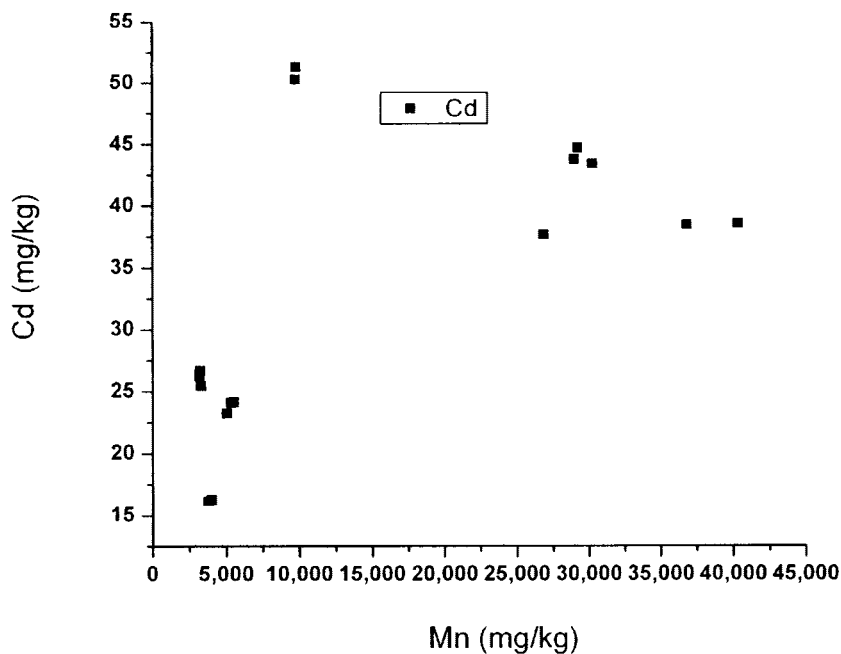


Figure E-11. Comparison of category averaged Mn and Cd concentrations from Fe/Mn-cemented aggregates collected at points A, B, and D within the Black Rock Slough sampling transect.

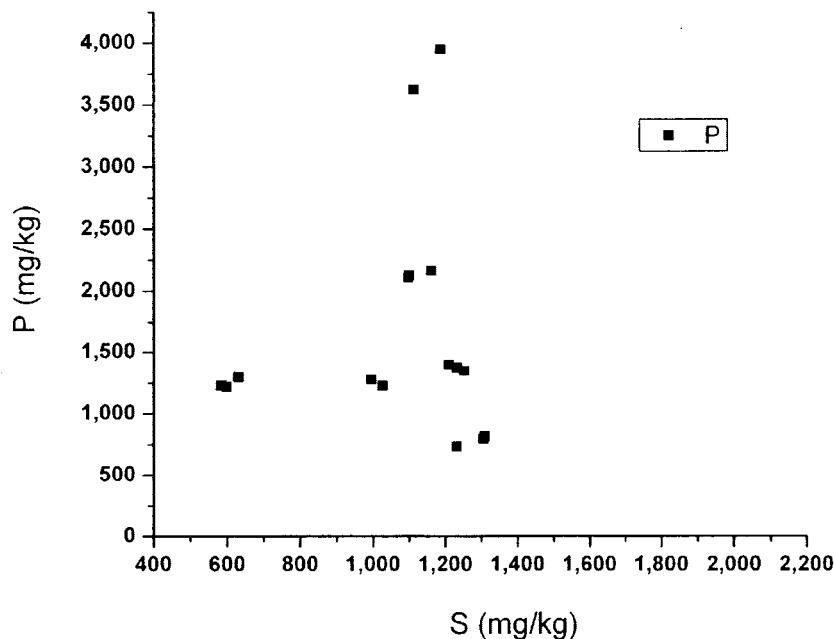


Figure E-12. Comparison of category averaged S and P concentrations from Fe/Mn-cemented aggregates collected at points A, B, and D within the Black Rock Slough sampling transect.

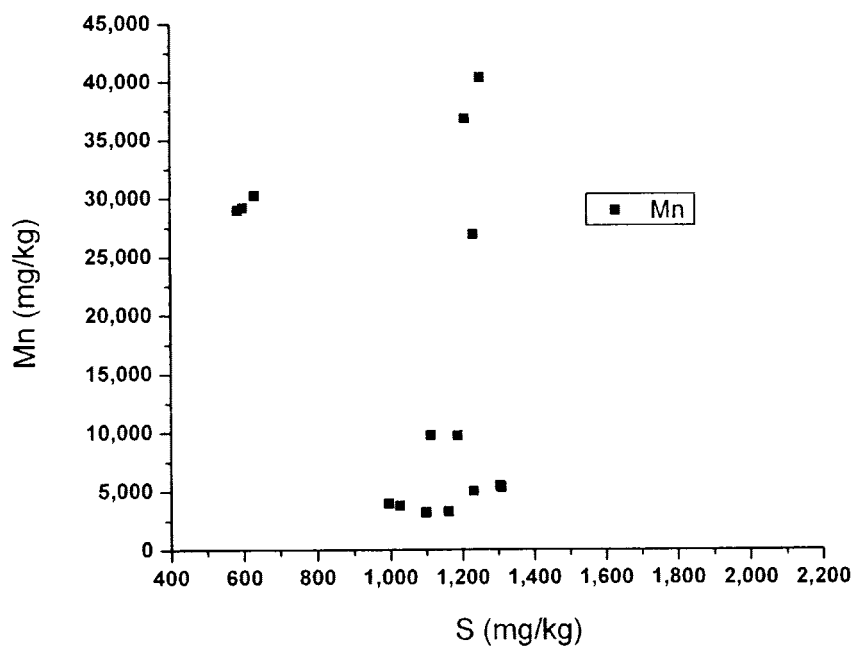


Figure E-13. Comparison of category averaged S and Mn concentrations from Fe/Mn-cemented aggregates collected at points A, B, and D within the Black Rock Slough sampling transect.

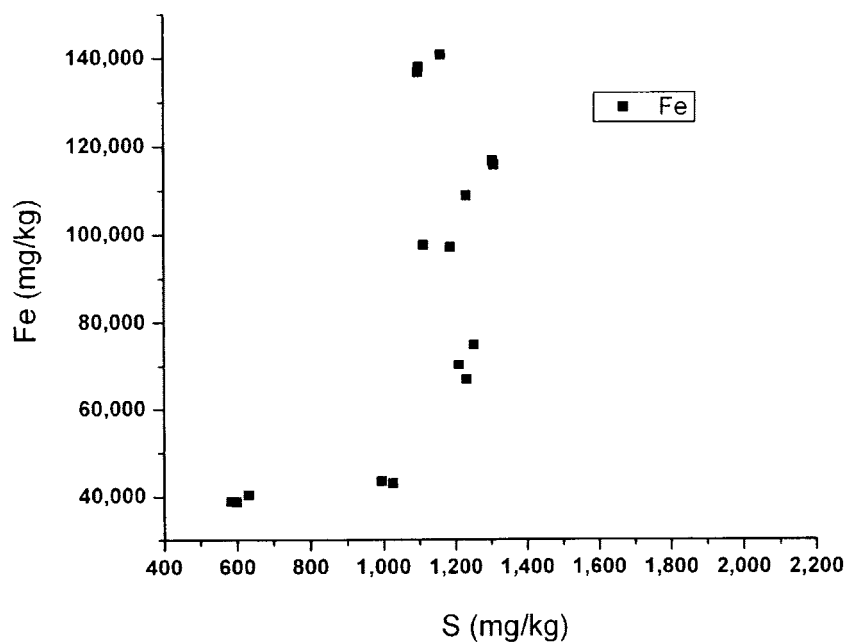


Figure E-14. Comparison of category averaged S and Fe concentrations from Fe/Mn-cemented aggregates collected at points A, B, and D within the Black Rock Slough sampling transect.

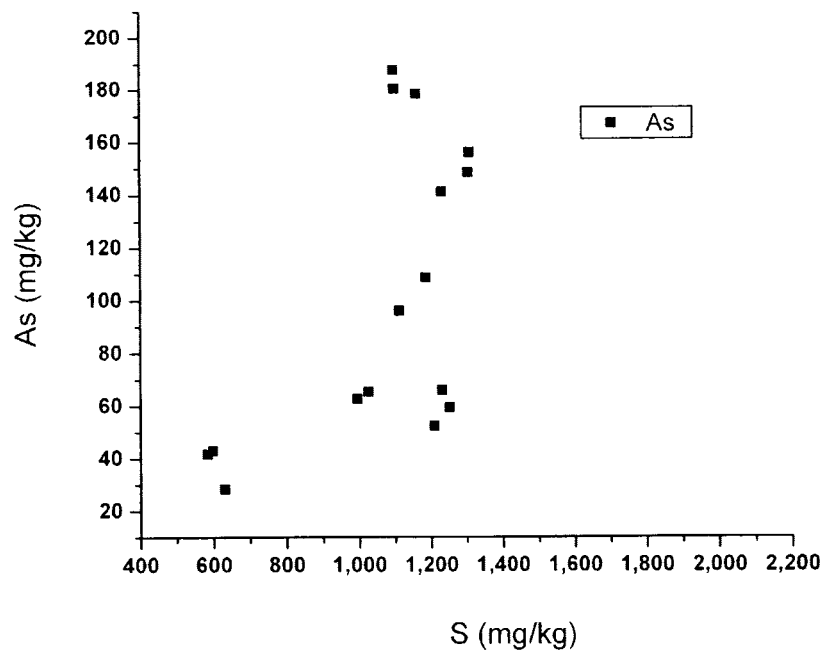


Figure E-15. Comparison of category averaged S and As concentrations from Fe/Mn-cemented aggregates collected at points A, B, and D within the Black Rock Slough sampling transect.

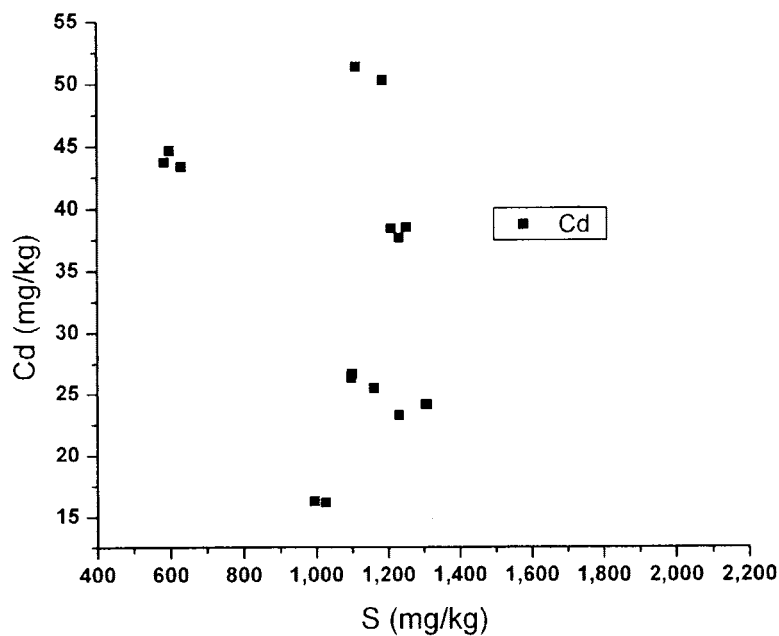


Figure E-16. Comparison of category averaged S and Cd concentrations from Fe/Mn-cemented aggregates collected at points A, B, and D within the Black Rock Slough sampling transect.

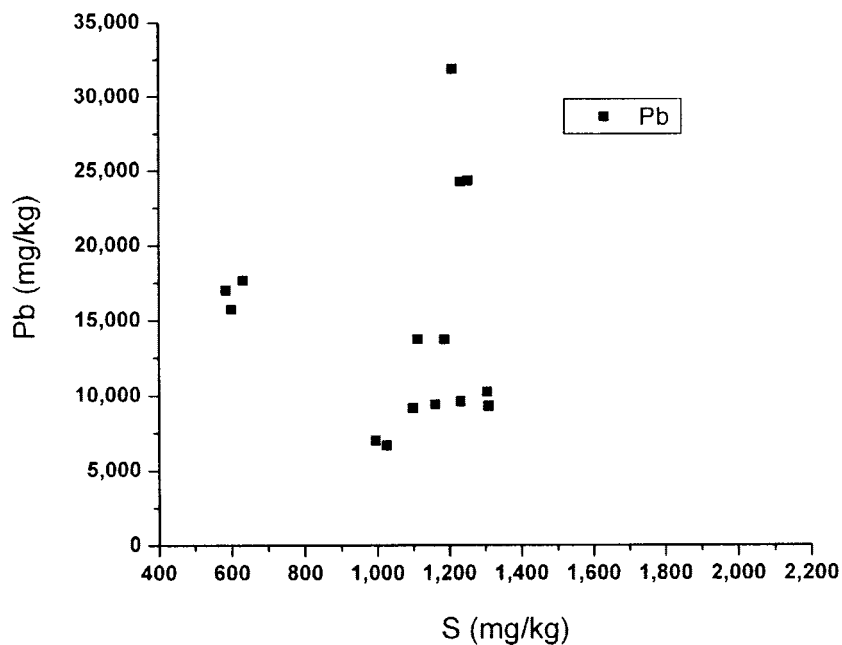


Figure E-17. Comparison of category averaged S and Pb concentrations from Fe/Mn-cemented aggregates collected at points A, B, and D within the Black Rock Slough sampling transect.

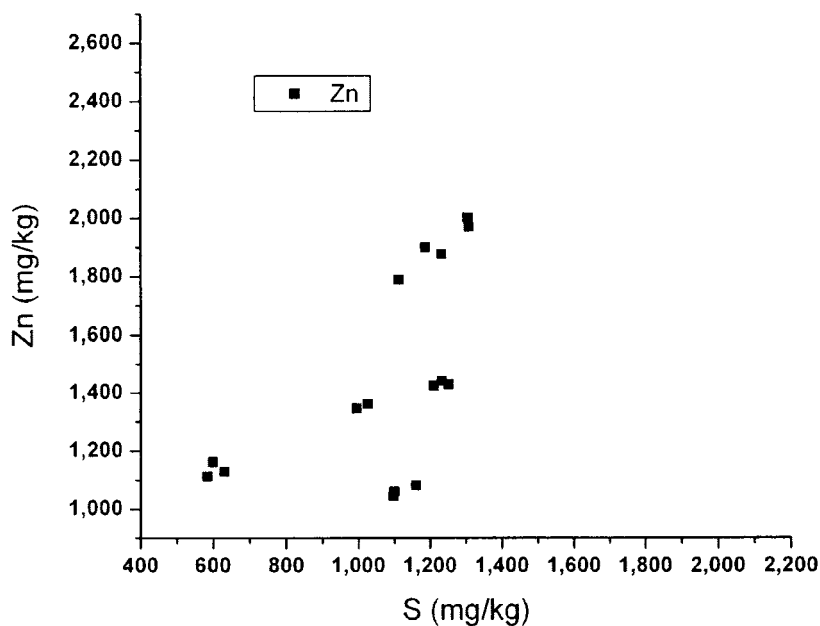


Figure E-18. Comparison of category averaged S and Zn concentrations from Fe/Mn-cemented aggregates collected at points A, B, and D within the Black Rock Slough sampling transect.

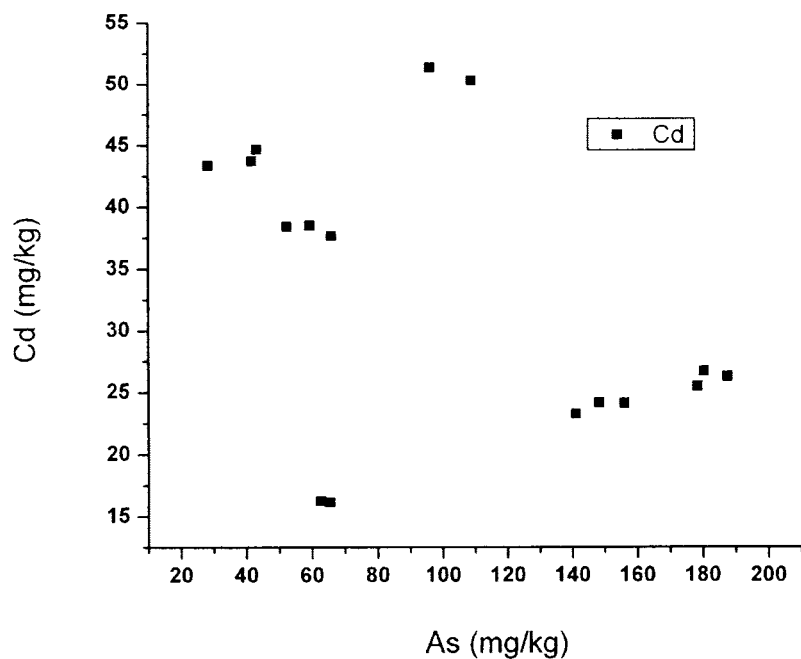


Figure E-19. Comparison of category averaged As and Cd concentrations from Fe/Mn-cemented aggregates collected at points A, B, and D within the Black Rock Slough sampling transect.

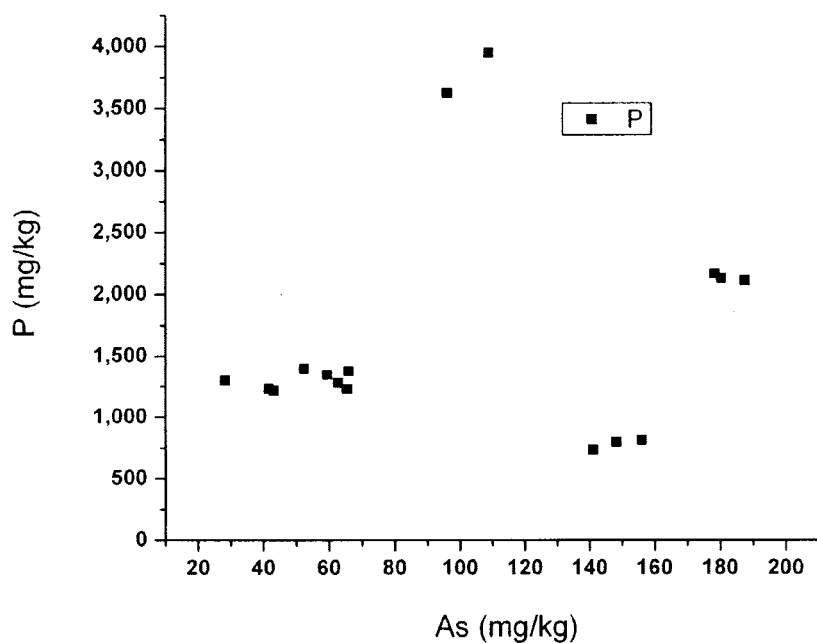


Figure E-20. Comparison of category averaged As and P concentrations from Fe/Mn-cemented aggregates collected at points A, B, and D within the Black Rock Slough sampling transect.

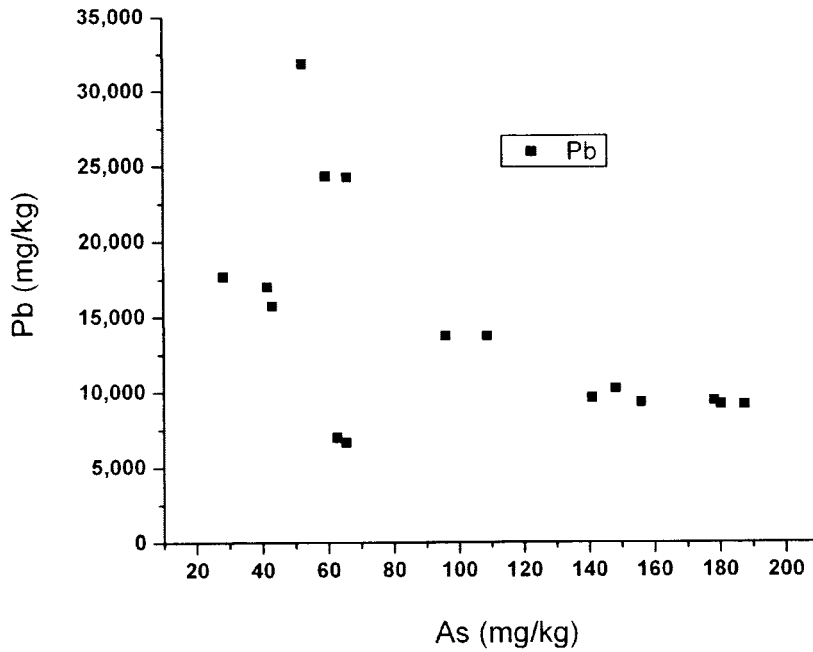


Figure E-21. Comparison of category averaged As and Pb concentrations from Fe/Mn-cemented aggregates collected at points A, B, and D within the Black Rock Slough sampling transect.

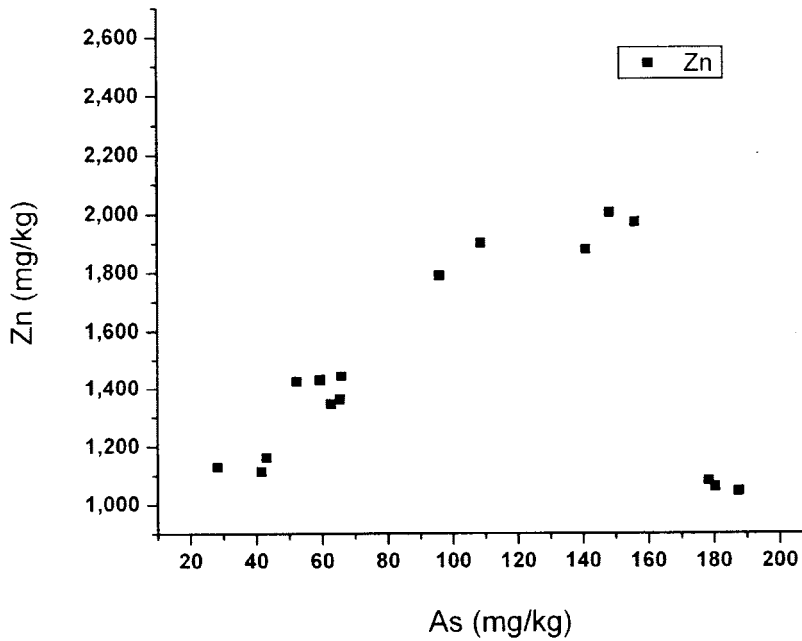


Figure E-22. Comparison of category averaged As and Zn concentrations from Fe/Mn-cemented aggregates collected at points A, B, and D within the Black Rock Slough sampling transect.

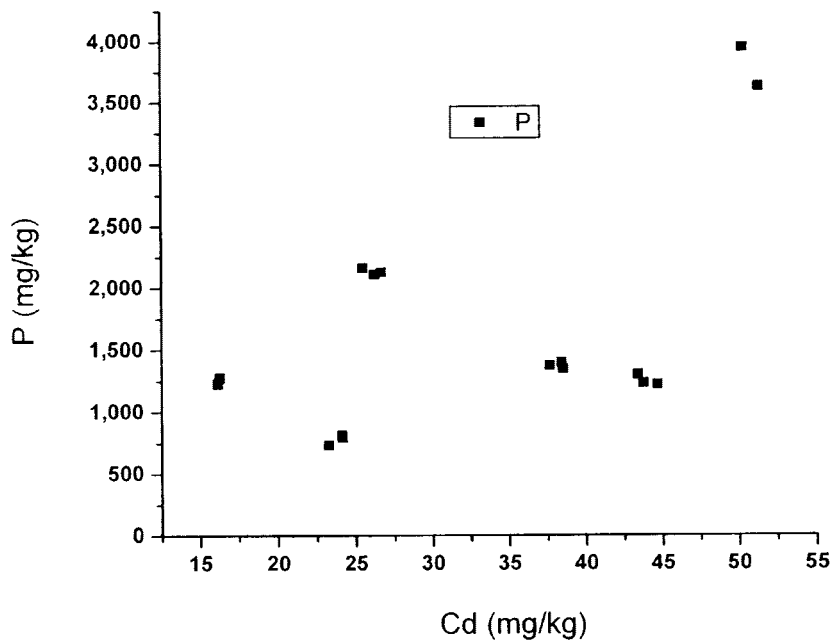


Figure E-23. Comparison of category averaged Cd and P concentrations from Fe/Mn-cemented aggregates collected at points A, B, and D within the Black Rock Slough sampling transect.

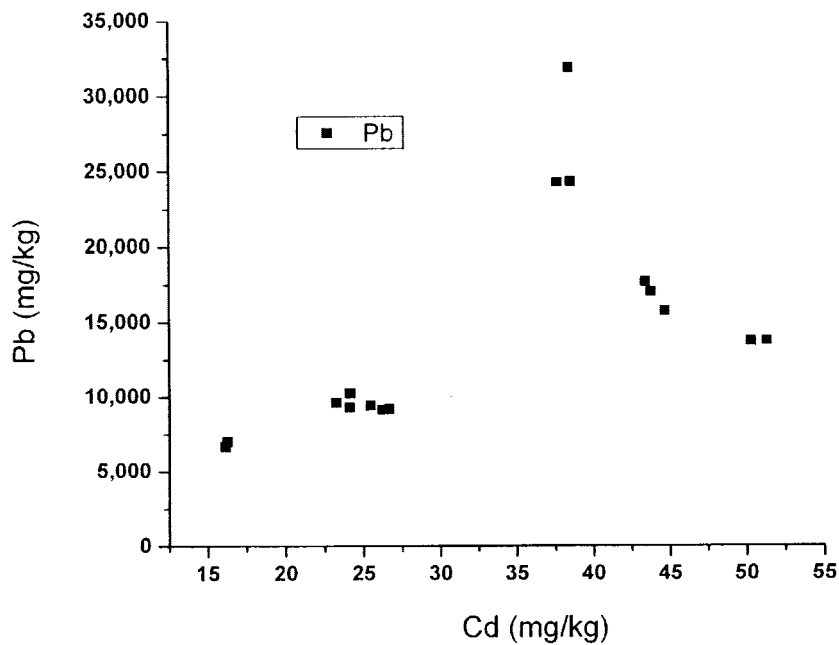


Figure E-24. Comparison of category averaged Cd and Pb concentrations from Fe/Mn-cemented aggregates collected at points A, B, and D within the Black Rock Slough sampling transect.

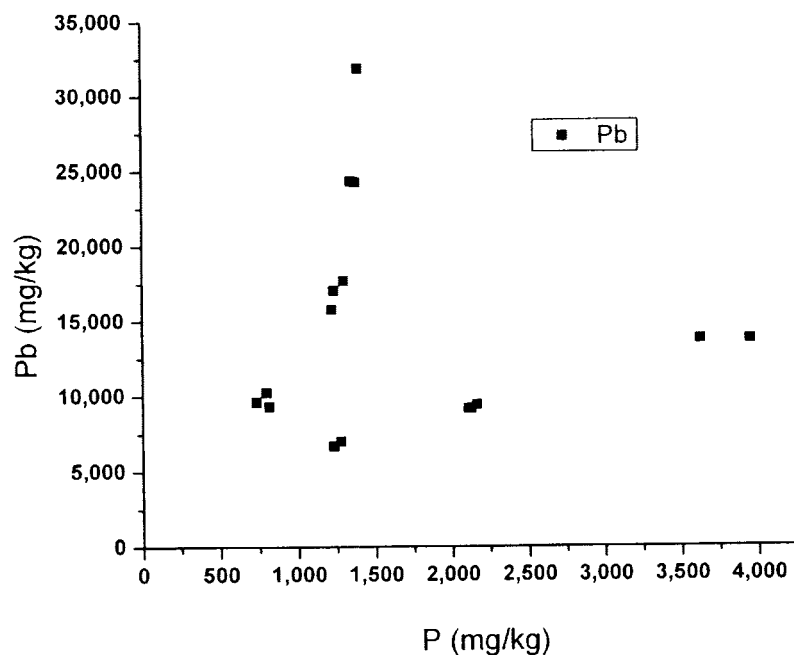


Figure E-25. Comparison of category averaged P and Pb concentrations from Fe/Mn-cemented aggregates collected at points A, B, and D within the Black Rock Slough sampling transect.

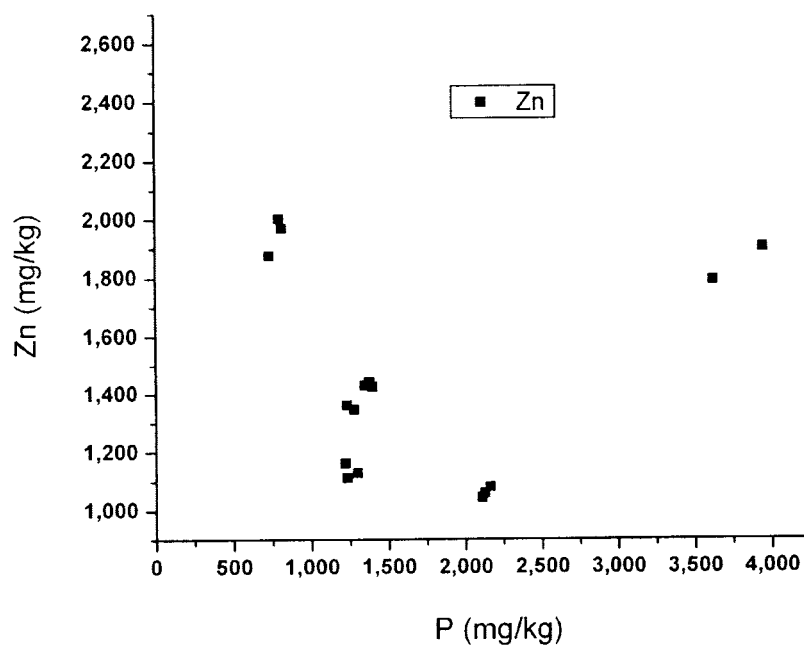


Figure E-26. Comparison of category averaged P and Zn concentrations from Fe/Mn-cemented aggregates collected at points A, B, and D within the Black Rock Slough sampling transect.

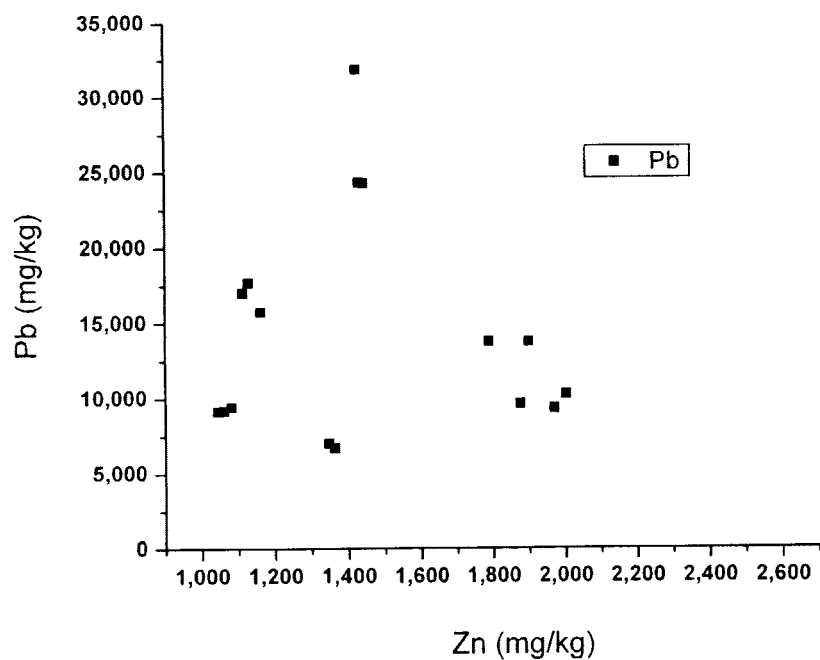


Figure E-27. Comparison of category averaged Zn and Pb concentrations from Fe/Mn-cemented aggregates collected at points A, B, and D within the Black Rock Slough sampling transect.

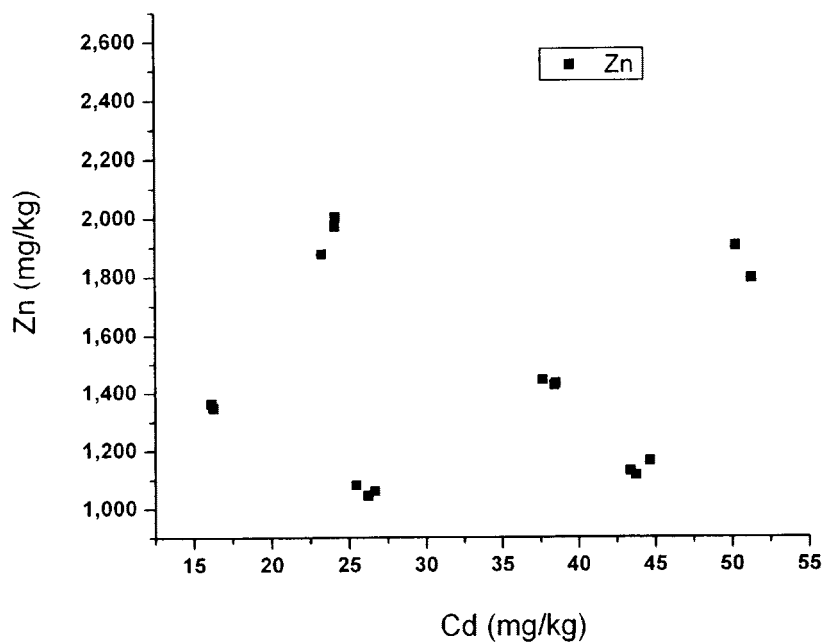


Figure E-28. Comparison of category averaged Cd and Zn concentrations from Fe/Mn-cemented aggregates collected at points A, B, and D within the Black Rock Slough sampling transect.